ABSTRACT

MECHANISMS OF IONIC CURRENT CHANGES UNDERLYING RHYTHMIC ACTIVITY RECOVERY AFTER DECENTRALIZATION

by
Olga E. Khorkova Sherman

Neuronal networks capable of generating rhythmic output in the absence of patterned sensory or central inputs are widely represented in the nervous system where they support a variety of functions, from learning and memory to rhythmic motor activity such as breathing. To perfectly function in a living organism, rhythm-generating networks have to combine the capability of producing a stable output with the plasticity needed to adapt to the changing demands of the organism and environment. This dissertation used the pyloric network of the crab *Cancer borealis* to identify potential mechanisms that ensure stability and adaptation of rhythm generation by neuronal networks under changing environmental conditions, in particular after the removal of neuromodulatory input to this network (decentralization). For this purpose, changes in ionic currents during the process of network activity recovery after decentralization were studied. The previously unreported phenomenon of coordinated expression of ionic currents within and between network neurons under normal physiological conditions was described. Detailed time course of alterations in current levels and in the coordination of ionic currents during the process of activity recovery after decentralization was determined for pacemaker and follower neurons. During the investigation of the molecular mechanisms underlying the post-decentralization changes, a novel role of central neuromodulators and of the cell-to-cell communication within the network in maintaining ionic current levels and their coordinations was demonstrated. Finally, the involvement of the two mechanisms of

network plasticity, namely extrinsic (activity-dependent) and intrinsic (neuromodulator-dependent) regulation, in the recovery process after decentralization was shown. A thorough understanding of the mechanisms that are responsible for the stability and plasticity of neuronal circuits is an important step in learning how to manipulate such networks to cure diseases, enhance performance, build advanced robotic systems, create a functioning computer model of a living organism, etc. The discovery of a novel mechanism of ionic current regulation, i.e. the inter-dependent coordination of different ionic currents, will potentially contribute to this process.

MECHANISMS OF IONIC CURRENT CHANGES UNDERLYING RHYTHMIC ACTIVITY RECOVERY AFTER DECENTRALIZATION

by
Olga E. Khorkova Sherman

A Dissertation
Submitted to the Faculty of
New Jersey Institute of Technology and
Rutgers, The State University of New Jersey - Newark
in Partial Fulfillment of the Requirements for the Degree of
Doctor of Philosophy in Biology

Federated Biological Sciences Department

January 2008

APPROVAL PAGE

MECHANISMS OF IONIC CURRENT CHANGES UNDERLYING RHYTHMIC ACTIVITY RECOVERY AFTER DECENTRALIZATION

Olga E. Khorkova Sherman

Dr. Jörge Golowasch, Dissertation Advisor — Date
Associate Professor, Department of Mathematical Sciences, NJIT and
Department of Biological Sciences, Rutgers University - Newark

---

Dr. Farzan ~~Nadim~~, Committee Member — Date
Interim Chair, Department of Biological Sciences, NJIT
Professor, Department of Mathematical Sciences, NJIT and
Department of Biological Sciences, Rutgers University - Newark

---

Dr. Nihal Altan-Bonnet, Committee Member — Date
Assistant Professor, Department of Biological Sciences,
Rutgers University - Newark

Dr. Victor Matveev, Committee Member — Date
Assistant Professor, Department of Mathematical Sciences, NJIT

Dr. Alfredo Kirkwood, Committee Member — Date
Associate Professor, Johns Hopkins University Mind/Brain Institute

BIOGRAPHICAL SKETCH

Author: Olga E. Khorkova Sherman

Degree: Doctor of Philosophy

Date: January 2008

Undergraduate and Graduate Education:

- Doctor of Philosophy in Biology,
  New Jersey Institute of Technology, Newark, NJ, and
  Rutgers, The State University of New Jersey – Newark, NJ, 2008

- Master of Science in Biology and English,
  Moscow State Pedagogical University, Moscow, Russia, 1983

- Bachelor of Science in Biology and English,
  Moscow State Pedagogical University, Moscow, Russia, 1981

Major: Biology

Presentations and Publications Related to the Topic of the Dissertation:

Khorkova OE and Golowasch J (2006) Ionic current changes during pyloric rhythm recovery after decentralization in crab STG. The 32nd Annual East Coast Nerve Net, Woods Hole, MA.

Khorkova Sherman OE and Golowasch J (2006) Decentralization alters coregulation of ionic currents. Society for Neuroscience 36th Annual Meeting, Atlanta, GA 2006.

Khorkova OE and Golowasch J (2007) Long-term effect of neuromodulatory input on ionic current interactions. The 33rd Annual East Coast Nerve Net, Woods Hole, MA.

Zhang Y, Rodriguez R, Khorkova OE and Golowasch J (2007) Recovery of rhythmic activity depends on both neuromodulator and activity. The 33rd Annual East Coast Nerve Net, Woods Hole, MA.

Khorkova OE and Golowasch J (2007) Long-term effect of neuromodulatory input on ionic current interactions. Frontiers in Applied and Computational Mathematics, Newark, NJ.

Zhang Y, Rodriguez R, Khorkova OE and Golowasch J (2007) Recovery of rhythmic activity depends on both neuromodulators and activity. Frontiers in Applied and Computational Mathematics, Newark, NJ, May 2007.

Khorkova OE and Golowasch J (2007) Neuromodulators, not activity, control coordinated expression of ionic currents. J Neurosci. 27(32):8709-18.

Khorkova OE and Golowasch J (2007) Neuromodulators, not activity, control coordinated expression of ionic currents. Center for Applied Mathematics and Statistics Technical Reports. 0607: 17.

To my mother

ACKNOWLEDGMENT

I would like to express my deepest gratitude to Dr. Jorge Golowasch, my research advisor, who provided guidance and valuable insight. Special thanks are given to Dr. Farzan Nadim who helped greatly by sharing his immense expertise in the field.

I thank Dr. Nihal Altan-Bonnet, Dr. Victor Matveev and Dr. Alfredo Kirkwood for their input and for actively participating in my committee.

I would like to also thank all members of Dr. Golowasch's and Dr. Nadim's labs for their moral support and guidance, especially Shunbing Zhao and Bob LoMauro who had to answer most of my never ending questions. I am very grateful to Yili Zhang who helped me understand a little about modeling neurons.

I thank Drs. Bruce Johnson and David Schulz for their valuable suggestions concerning my research and Drs. Eve Marder and Pierre Meyrand for critically reading the manuscript of the paper. I would also like to acknowledge the advice on statistical analysis from Dr. Kaushik Ghosh.

Special thanks go to Amy Trimarco and Shandel Rivera for their unfailing support throughout my stay in Rutgers and NJIT.

I am very grateful to my family for their patience and optimism.

TABLE OF CONTENTS

Chapter	Page
1 INTRODUCTION	1
1.1 Objectives	1
1.2 Significance	2
1.3 Background	5
1.3.1 Pyloric Network of the Crustacean Stomatogastric Nervous System as an Experimental Model	5
1.3.2 Pyloric Network Decentralization Model	7
1.3.3 Ionic Currents Affecting the Output of the Crustacean Pyloric Network	10
1.3.4 Central Modulators of the Pyloric Network: Proctolin	13
1.3.5 Central Modulators of the Pyloric Network: GABA	14
1.3.6 Glutamatergic Synapses in the Pyloric Network	17
2 MATERIALS AND METHODS	19
2.1 Animal Model	19
2.2 Electrophysiology	20
2.3 Activity-Modifying Pretreatments of the STG	23
2.4 Statistical Analysis	24
3 NEUROMODULATORS, NOT ACTIVITY, CONTROL COORDINATED EXPRESSION OF IONIC CURRENTS	25
3.1 Abstract	25
3.2 Introduction	26

TABLE OF CONTENTS
(continued)

Chapter	Page
3.3 Results	27
3.3.1 Decentralization Modifies Pyloric Network Activity	27
3.3.2 Decentralization Modifies Voltage-Dependent Ionic Current Levels	29
3.3.3 Coregulation of Ionic Current Pairs Depends on Neuromodulatory Input	31
3.3.4 Proctolin Prevents Ionic Current Changes and Loss of Co-Regulation Due to Decentralization	33
3.4 Discussion	38
4 COORDINATED EXPRESSION OF IONIC CURRENTS WITHIN NEURONS AND ACROSS NEURONAL TYPES IN A RHYTHM-GENERATING NETWORK	51
4.1 Abstract	51
4.2 Introduction	52
4.3 Results	55
4.3.1 Pyloric Network of the Crustacean STNS as an Experimental Model	55
4.3.2 Current Levels in the Two PD Neurons Are Closely Coordinated	57
4.3.3 IA and IHTK, but not Ih Levels Are Coordinated between LP and PD Neurons	60
4.3.4 LP and PD Exhibit Complementary Current Changes after Decentralization	61
4.3.5 Disruption of Neuromodulator Supply Correlates with Changes in INTER-cellular Coordination of I_h	63

TABLE OF CONTENTS
(continued)

Chapter **Page**

4.3.6 I_{HTK} and I_A, but not I_h, Coordination between Neurons Is PTX-Sensitive..... 64

4.3.7 PTX-Sensitive Chloride Channel Is Involved in Setting Current Levels of STG Neurons..... 69

4.3.8 GABA Participates in Coordinating I_h Levels between the Cells..... 72

4.4 Discussion..... 75

4.4.1 INTER-cellular Correlations..... 75

4.4.2 Mechanisms of INTER-cellular Coordinations..... 76

4.4.3 Mechanisms of Intracellular Coordinations..... 80

4.4.4 Mechanisms Controlling the Process of Recovery after Decentralization..... 81

4.4.5 Functional Implications..... 83

5 ACTIVITY AND NEUROMODULATORS CONTROL THE RECOVERY OF RHYTHMIC OUTPUT IN A RHYTHM-GENERATING NEURONAL NETWORK..... 89

5.1 Abstract..... 89

5.2 Introduction..... 90

5.3 Results..... 91

5.3.1 Experimental Protocols..... 92

5.3.2 Activity Suppression by Hyperpolarization or Low Sodium Advances Recovery after Decentralization..... 94

5.3.3 Pretreatment with GABA affects Both Time to First Bout and Time of Activity Turnoff..... 95

TABLE OF CONTENTS
(continued)

Chapter		Page
5.3.4	Metabotropic $GABA_B$ Receptor Agonist only Increases Time to Rhythm Turnoff	98
5.3.5	Ionotropic $GABA_A$ Receptor Agonist Only Reduces Time to First Bout	98
5.3.6	An Activity- and Neuromodulator-Dependent Hypothesis of the Recovery Process Regulation is Supported by Proctolin-Pretreatment Experiments	100
5.4	Discussion	101
6	CONCLUSION	110
6.1	Summary of Results	110
6.1.1	Discovery of Ionic Current Coordination within and between Cells	111
6.1.2	Novel Functions of Neuromodulators in Rhythm Generating Networks	112
6.1.3	Novel Function of Glutamatergic Synaptic Communications in Rhythm Generating Networks	112
6.1.4	Mechanisms Involved in INTRA-cellular Current Coregulation	112
6.1.5	Mechanisms Involved in Intercellular Current Coordination	113
6.1.6	Mechanisms Involved in Setting Ionic Current Levels	114
6.1.7	Post-decentralization Changes Occur during a Critical Window	115
6.1.8	Decentralization Leads to Restructuring of Signaling Pathways	116
6.1.9	Recovery after Decentralization is Controlled by Activity-and Neuromodulator-Dependent Mechanisms	116
6.1.10	Current Coregulations Contribute to Stability and Plasticity of the Network	117

TABLE OF CONTENTS
(continued)

Chapter **Page**

6.2 Implications of the Results in the Context of Rhythm Generating Network Biology..... 118

REFERENCES..... 121

LIST OF TABLES

Table		Page
3.1	Input Resistance (in MΩ) Changes during Organ Culture and Decentralization	42
3.2	Linear Regression Analysis of Iionic Current Density Coordinated Regulation	42
4.1	Parameters of the Linear Regression Analysis of Current Coordinations between the Two PD Cells of the Pyloric Network	85
4.2	Parameters of the Linear Regression Analysis of Current Coordinations between the PD and LP Cells of the Pyloric Network	86
4.3	Parameters of the Linear Regression Analysis of Intracellular Pairwise Current Coordinations in the LP Cells of the Pyloric Network	87
4.4	Parameters of the Linear Regression Analysis of Intracellular Pairwise Current Coordinations in the PD Cells of the Pyloric Network	88
5.1	Parameters of the Recovery Process in Controls and Preparations with Different Pretreatments before Decentralization	109

LIST OF FIGURES

Figure		Page
1.1	Stomatogastric nervous system of crab *Cancer borealis*	6
1.2	Pyloric network output of crab *Cancer borealis*	7
3.1	Effects of decentralization on pyloric network activity	28
3.2	Decentralization affects most ionic current densities in PD neurons	43
3.3	Co-regulation of voltage-gated currents depends on continuous neuromodulatory input	44
3.4	Effect of proctolin on pyloric rhythm activity	45
3.5	Neuromodulator prevents current density changes due to decentralization	46
3.6	Exogenous neuromodulator bath application prevents the loss of current density co-regulation in decentralized preparations	47
3.7	Effect of tetrodotoxin on proctolin-induced pyloric rhythm	48
3.8	Neuromodulator applied past a critical window after decentralization does not restore control current densities	49
3.9	Effect of neuromodulators on the co-regulation of ionic currents after long-term decentralization	50
4.1	Changes in pyloric activity observed in decentralized, PTX-treated and 3MPA-treated preparations after 24 hours in culture	56
4.2	Decentralization evokes complementary changes in PD and LP current densities	58
4.3	Current densities are coordinated between the two PD neurons	65
4.4	Current densities are coordinated between PD and LP neurons	67

LIST OF FIGURES
(continued)

Figure	Page
4.5 Average current density levels in LP and PD neurons from the same ganglion in control conditions	69
4.6 Intracellular current density correlations in LP neurons are altered by decentralization, but not by PTX or 3MPA treatments	70
4.7 Intracellular current density correlations in pd neurons are not affected by PTX or 3MPA treatments	73
4.8 INTERcellular current density correlations between PD and LP neurons.	77
4.9 Intracellular current density correlations in PD and LP neurons	83
5.1 Pyloric rhythm frequency changes recorded via *lvn* after decentralization	93
5.2 Examples of post-decentralization changes in pyloric rhythm frequency in different pre-inhibited preparations	97
5.3 Examples of post-decentralization changes in pyloric rhythm frequency in different neuromodulator pre-treated preparations	99
5.4 Schematic diagram of intracellular activity- and neuromodulator dependent regulation model	108
5.5 The recovery process after decentralization in the proctolin pre-treated preparation	109

LIST OF ABBREVIATIONS

CPG	Central Pattern Generator
STNS	Stomatogastric Nervous System
STG	Stomatogastric Ganglion
AB	Anterior Burster Neuron
PD	Pyloric Dilator Neuron
LP	Lateral Pyloric Neuron
PY	Pyloric Constrictor Neuron
CoG	Commissural Ganglion
OG	Oesophageal Ganglion
stn	Stomatogastric Nerve
lvn	Lateral Ventricular Nerve
PTX	Picrotoxin
TTX	Tetrodotoxin
3MPA	3-Mercaptopropionic Acid

CHAPTER 1

INTRODUCTION

1.1 Objective

The objective of this dissertation is to identify potential mechanisms that ensure stability together with adaptation of rhythm generating neuronal networks under changing environmental conditions.

For this purpose, a model of rhythm generating neuronal network adaptation to changing environmental conditions, in particular the recovery after decentralization of the pyloric network of the crab, *Cancer borealis*, is employed. Since the activity of neurons is to a large extent determined by the characteristics of ionic currents that they express, it is expected that the characteristics of ionic currents will change during the process of restoring the rhythmic output of the network. To elucidate the mechanisms that control the adaptation of the neuronal network to the changing environmental conditions, the changes in ionic current levels at the time of significant perturbations in the activity of a rhythm generating neuronal network, and particularly during the functional recovery of the network, are investigated. Previously published data indicate that ionic current levels within and between network neurons could be correlated. If such correlations exist, they could be involved in the maintenance of stable network output and thus could change during environmental perturbations. To confirm or disprove this expectation, coordinated expression of currents within and between network neurons under normal physiological conditions is investigated. To understand the molecular underpinnings of the observed current level and coordination dynamics, the role of neuromodulators in the maintenance

of current levels and their coordinations is explored. Next, the role of cell to cell communication within the network in maintaining ionic current levels and their coordinations is studied. Finally, the question of the involvement of the two very important mechanisms of network plasticity, activity-dependent vs neuromodulator-dependent regulation, in the recovery process after decentralization is addressed.

1.2 Significance

Neuronal networks capable of generating rhythmic output in the absence of patterned sensory or central inputs are widely represented in the nervous system where they support a variety of functions, including learning (Singer 1993, Lisman 1997), memory formation (Klimesch 1999) and rhythmic motor activity such as breathing (Von Euler 1983). Disturbances in the stable activity of rhythm-generating networks can have pathological effects. For example, abnormal synchronization of the oscillations among cortical neurons leads to epileptic seizures (Wong et al. 1986). However, to perfectly function in a living organism, rhythm-generating networks have to combine stability with the plasticity needed to adapt to the changing demands of the organism and environment (Marder and Bucher 2007). Finding the molecules that are responsible for the stability and plasticity of neuronal circuits will be the first step in learning how to manipulate such networks to cure diseases, enhance performance, build advanced robotic systems, create a functioning computer model of a living organism and achieve other goals.

Activity of ionic current-conducting channels is generally regarded as a major mechanism producing membrane potential changes that comprise neuronal output. Studying the modulation and coordination of ionic current expression within and between

the network neurons can provide significant insights into the mechanisms underlying stability and plasticity of the network output. In spite of the potential importance of coordinated current expression for maintaining the stability and plasticity of rhythm generating networks, and in spite of multiple indications that such current coordination might exist (Turrigiano et al. 1995, Szucs et al. 2003, LeMasson et al. 1993, Franklin et al. 1992, Fengler and Lnenicka 2001, Haedo and Golowasch 2006, Ueda and Wu 2006, Wierenga et al. 2005, Coleman et al. 1995, DiCaprio and Fourtner 1988, Ramirez and Pearson 1990, Weaver and Hooper 2003, Schulz et al 2006, Zhang et al. 2003a, Golowasch et al. 1999b), there have been few direct studies of current coordination (MacLean et al. 2003, 2005, Schulz et al. 2006).

Many rhythm generating networks, although normally dependent on activity and neuromodulator inputs from other neurons, can also recover their functions after this input is interrupted. In some cases such network function recovery leads to the recovery of the physiological function controlled by the network. An example of function recovery after removal of the external input to the network (deafferentation) is observed in the case of vestibular nerve damage in mammals. Vestibular nerve connects to the vestibular nucleus complex (VNC), which controls balance. The neurons in the VNC typically display a spontaneous output that initially disappears after deafferentation, but reappears after a certain time allowing a partial recovery of balance control (Darlington et al. 2002).

However, studying rhythm-generating networks in mammalian systems is extremely difficult due to the large number and small size of the neurons in these networks. Mammalian networks are also difficult and costly to maintain in culture. Invertebrate systems have long served as a solution to these problems in neuroscience,

one example being the pioneering work of Hodgkin and Huxley (1952). The stomatogastric nervous system (STNS) of decapod crustaceans was historically a system that provided an invaluable input to understanding the function of rhythm-generating networks (Maynard 1972, Marder 1985, Marder et al. 2005, Marder and Bucher 2001, Marder and Bucher 2007, Stein 1997). The pyloric rhythm generating network, a part of the STNS, contains 11-14 neurons (depending on the species) about 50-100 μm in diameter receiving a limited number of central inputs through a single nerve. The network can be easily dissected and maintained in organ culture in a saline solution for many days while consistently producing neuronal output closely resembling the one recorded in vivo (Rezer and Moulins 1983, Clemens et al. 1998, Heinzel et al. 1993). Over the last 35 years the architecture and neuroregulatory inputs of the crustacean pyloric network have been thoroughly investigated providing an extensive background for studying the network response to environmental changes (reviewed in Marder and Bucher 2007). Multiple computer models of the network have been developed which significantly facilitates the understanding of the relationships between ionic currents and network activity.

This dissertation takes advantage of the pyloric network model system to investigate the molecular mechanisms involved in the recovery of the stable rhythmic network output after environmental perturbations not unlike those encountered in cases of trauma or axonal degeneration. One such case, in particular the loss of central modulatory input (decentralization) of the pyloric network, was the focus of this dissertation. The results presented in this dissertation will potentially have wide implications in understanding the mechanisms involved in maintaining both stability and plasticity in

rhythm generating networks, and in understanding how recovery of function can be optimized.

1.3 Background

1.3.1 Pyloric Network of the Crustacean Stomatogasric Nervous System as an Experimental Model

The crustacean STNS is a widely used model (Selverston and Moulins 1987; Harris-Warrick and Marder 1991, Harris-Warrick 1992; Abbott and Marder 1998) in which neuronal identities and connections are well understood. It was first employed as an experimental preparation in 1972 (Maynard 1972). The STNS comprises a set of ganglia (Figure 1.1A) that control the movements of the crustacean foregut. One of these ganglia, the stomatogastric ganglion (STG) contains the neurons of the pyloric rhythm-generating network (Figure 1.1B) that controls the filtering of the food. When the STNS is dissected and maintained in organ culture, the pyloric network expresses a steady rhythm almost identical to the one observed *in vivo* (Rezer and Moulins 1983, Clemens et al. 1998, Heinzel et al. 1993). The pyloric rhythm (Figure 2) recorded from the lateral ventricular nerve (*lvn*) consists of a burst of action potentials in the pyloric dilator (PD) neurons, followed by a burst in the lateral pyloric (LP) and then the pyloric constrictor (PY) neurons (Harris-Warrick et al. 1992).

There are two PD neurons in pyloric network. Together with the anterior burster (AB) neuron they constitute the pacemaker kernel of the network (Figure 1.1B). The neurons in the pacemaker kernel are electrically coupled and can maintain oscillations in the absence of an external rhythmic input. AB is an interneuron that projects to the

commissural ganglia (CoG) through the stomatogastric nerve (*stn*). LP neuron is a part of the group of follower neurons that need the rhythmic input from the pacemaker kernel to maintain rhythmic activity (Eisen and Marder 1982, Marder and Eisen 1984, Miller and Selverston 1982). Neurons in the pacemaker kernel inhibit the LP neuron, causing it to fire in alternation with the PD neurons.

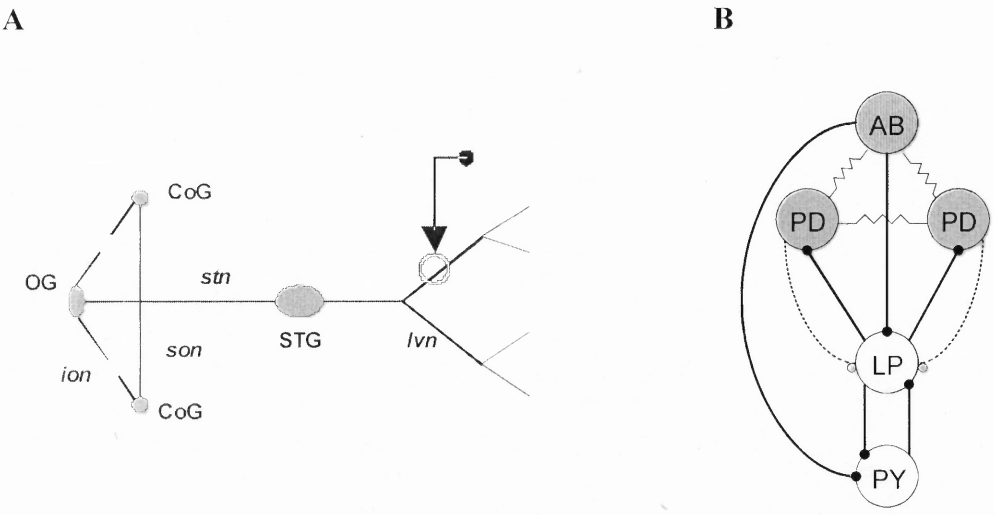

Figure 1.1 Stomatogastric nervous system of crab *Cancer borealis*. A, Schematic diagram of the stomatogastric nervous system preparation. Grey circles represent ganglia, lines represent nerves, a circle with an arrow represents a Vaseline well used for extracellular recordings. OG, oesophageal ganglion; CoG, commissural ganglion; STG, stomatogastric ganglion; *stn*, stomatogastric nerve; *lvn*, lateral ventricular nerve; *ion*, inferior oesophageal nerve, *son*, supraoesophageal nerve. B, Simplified synaptic connectivity diagram of the crab pyloric network. AB, anterior burster neuron; PD, pyloric dilator neuron; LP, lateral pyloric neuron; PY, pyloric burster neuron. Large grey circles represent neurons of the pacemaker kernel, large white circles represent follower neurons. Lines with black circles at the ends represent glutamatergic synapses, lines with grey circles represent cholinergic synapses, zigzag lines represent electrical coupling.

The LP neuron, which is studied in detail in this dissertation, receives a glutamatergic synapse from the AB neuron and is the only neuron in the pyloric network that feeds back onto the pacemaker kernel, through a glutamatergic synapse to PD (Maynard 1972, Selverston et al. 1976, Miller and Selverston 1982, Marder and

Paupardine-Tritsch 1978) (Figure 1.1B). In lobster, feedback from the LP neuron slows the pacemaker in a certain range of frequencies (Weaver and Hooper 2002). Thus, the LP neuron appears to be an important network activity regulating partner in the pyloric network.

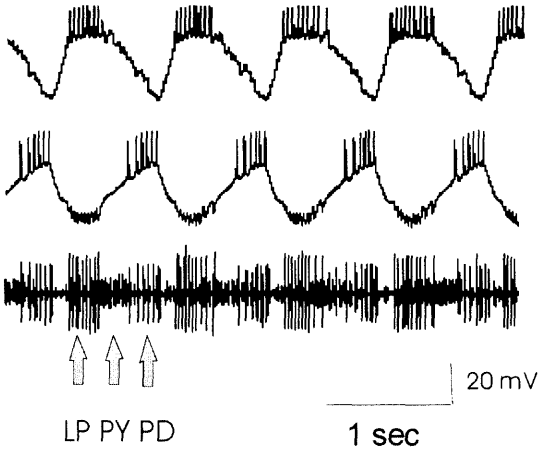

Figure 1.2 Pyloric network output of crab *Cancer borealis*. Simultaneous recordings from LP neuron (top trace), PD neuron (middle trace) and *lvn* (bottom trace). Note inhibitory postsynaptic potentials from LP on PD trace.

1.3.2 Pyloric Network Decentralization Model

Neurons in the STG receive neuromodulatory inputs from the other three ganglia of the STNS: the paired CoGs and the single OG (Fig 1.1A). In *C. borealis* there are about 20 pairs of neurons projecting to the STG (Coleman et al. 1992). Most of the descending projection neurons produce multiple neuromodulators (Nusbaum et al. 2001). More than 20 of the neuromodulators released by the descending axons from the modulatory projection neurons have been identified (Katz 1985, Nusbaum et al. 2001, Marder and Bucher 2001, Nusbaum and Beenhakker 2002). Some of the central neuromodulators are

not synthesized by the STG neurons, including GABA (Ducret et al 2007, Swensen et al. 2000) and proctolin (Nusbaum and Marder 1989a, b).

When the neuromodulatory input is discontinued, the normal pyloric activity temporarily ceases, only to reappear again 30 to 100 h later (Rezer and Moulins 1992, Thoby-Brisson and Simmers 1998, 2000a, 2002, Golowasch et al. 1999b, Luther et al. 2003). This phenomenon resembles that of deafferentation observed in mammals, including the vestibular nerve damage case described above. Because of this ability of the pyloric network to spontaneously recover its lost activity, it is expected that studying the pyloric network decentralization model will contribute to understanding of general mechanisms involved in maintaining both stability and plasticity of the rhythm generating networks.

In the pyloric network, rhythm recovery after decentralization proceeds through a period of unstable activity, termed the bouting period (Luther et al. 2003). It is characterized by bouts of normal pyloric rhythm interspersed by periods of irregular activity or complete inactivity. Rhythm recovery in the pyloric network decentralization model has been suggested not to depend on the preparation's activity since it occurs both in preparations maintained in a chronically active state by elevated extracellular K^+ or by muscarinic agonist oxotremorine, and in TTX, which stops all action potential generation (Thoby-Brisson and Simmers 1998). Also, photoinactivation of the pacemaker AB neuron did not alter the recovery process. If a PD neuron was isolated from all its network connections by photoablating the AB neuron and the second PD neuron, and blocking the LP to PD synapse with PTX, it still exhibited the same behavior before and after decentralization as it did in the intact network: normal bursting with

neuromodulatory inputs intact, initial cessation of bursting upon decentralization and rhythm recovery after 5 days in culture (Thoby-Brisson and Simmers 2002). On the other hand, modeling studies have shown that an activity-dependent mechanism is sufficient to explain the timing of the recovery as well as the dynamical properties during the bouting period (Golowasch et al. 1999b, Zhang and Golowasch 2007). This apparent discrepancy concerning the nature of the mechanism driving the recovery of activity after decentralization is addressed in Chapter 5.

The recovered network obviously exhibits significantly changed architecture compared to control network. In recovered preparations, in contrast to the neuromodulator-intact ones, the follower LP and PY neurons continued to oscillate when isolated from all their network contacts (Thoby-Brisson and Simmers 2002). These findings indicate that the essential processes underlying the recovery of the pyloric rhythm occur at the single cell level, and that these processes lead to changes in the oscillatory properties of the neurons and of the network as a whole.

After decentralization, the efficacy of cholinergic synapses between PD and PY and PD and LP neurons and glutamatergic synapses between LP and PD neurons decreased, while the strength of electrical coupling between the two PD cells remained unchanged (Thoby-Brisson and Simmers 1998). One possible explanation for these observations is that decentralization eliminates modulatory inputs that normally increase synaptic strength. For example aminergic up-modulation of synaptic strength has been shown in vertebrates (Knapp and Dowling 1987) and invertebrates, the pyloric network of lobsters in particular (Johnson and Harris-Warrick 1990). The reduction in synaptic strength can also arise from the reduction in ionic currents involved in the release of

synaptic neurotransmitters or in the responsiveness of the post-synaptic receptors.

It has been shown that levels of several currents in the preparations recovered after decentralization are changed, in particular the TEA-sensitive potassium current was decreased and I_h was increased in PD neurons in lobster (Thoby-Brisson and Simmers 2002). The observed changes in the measured current levels may be caused not only by the changes in mRNA copy number and translational regulation, but also by channel redistribution among the neuronal segments, or regulation of their activation state. Immunocytochemical studies show that the distribution of staining for shal ionic channels carrying the A-type current, changes after decentralization, with more shal channels seen in the neuronal somata (Mizrahi et al. 2001).

The existence of transcription-dependent changes during recovery after decentralization is confirmed by the fact that the rhythm recovery is blocked by the inhibitors of RNA synthesis acting in a short window of up to 2 h after decentralization (Thoby-Brisson and Simmers 2000a).

Modeling studies confirm that in the STG decentralization model significant changes in ionic current expression are expected as the ganglion resumes its rhythmic activity (Liu et al. 1998, Golowasch et al. 1999b).

1.3.3 Ionic Currents Affecting the Output of the Crustacean Pyloric Network

Several ionic currents are known to play crucial roles in generating oscillatory behavior, including I_{Kd}, I_{KCa}, I_h, I_A and I_{Ca} (Calabrese 1998).

The hyperpolarization activated inward current (I_h) is a mixed cation current carried by PAIH channel in lobster (Gisselmann et al. 2003, Zhang et al. 2003a) or IH

channel in crab (Schulz et al. 2006). I_h in *C. borealis* activates at voltages below –50 to –60 mV, has slow kinetics and shows no inactivation. Its reversal potential was shown to be about –20 to –30 mV (Golowasch and Marder 1992a). I_h is reversibly blocked by bath application of 5 mM Cs^+. When I_h current was increased by injecting PAIH RNA into a bursting PD neuron, the cell membrane potential was depolarized, the oscillation amplitude as well as time to the first spike were decreased, and duty cycle and number of action potentials per burst were increased (Zhang et al. 2003a). Blockade of I_h current in isolated respiratory network of mice by Cs^+ or ZD7288 increased respiratory frequency and the amplitude of integrated population activity (Thoby-Brisson et al. 2000b). Postinhibitory rebound in STG neurons is shaped by the interaction of I_h and the transient A-type current (I_A) (Harris-Warrick et al. 1995).

I_A in *C. borealis* LP neuron was described by Golowasch and Marder (1992a). I_A de-inactivates at holding potentials below –60 mV. I_A activation steeply increased during pulses to voltages between –40 and +20 mV, after which it leveled off. I_A reached its peak amplitude more rapidly as the voltage was increased. I_A in crab was partially and irreversibly blocked by 4-aminopyridine (4-AP) but was not affected by Ca^{2+}. Its maximum conductance was approximately equal to I_{Kd}, and was two fold lower than that of I_{KCa} in crab LP neurons (Golowasch and Marder 1992a). I_A was completely inactivated at holding voltages equal or higher than –40 mV, i.e. when voltage pulses were applied from the holding potential of –40 mV, only I_{Kd} and I_{KCa} could be activated. This property is used to isolate I_A from other outward currents. In crustacean STG both I_A and I_h play important roles in determining when a follower neuron recovers from inhibition (Hooper 1997, Harris-Warrick et al. 1995, Tierney and Harris-Warrick 1992). I_A sets the bursting

rate in oscillatory neurons, contributes to the timing of action potentials in the spike trains and the duration of postinhibitory rebound (Graubard and Hartline 1991, Golowasch and Marder 1992a, Tierney and Harris-Warrick 1992). Shal channel carrying the A-current has been cloned from lobster (Baro et al.1996) and crab (Schulz et al. 2006).

The other two currents studied in this dissertation that are also essential for the rhythmic activity of the neurons are the delayed rectifier (I_{Kd}) and the calcium-dependent potassium current (I_{KCa}). Channels carrying I_{Kd} (shab) and I_{KCa} (BK-KCa) from lobster and crab (Schulz et al. 2006) have been cloned. I_{KCa} shows significant Ca^{2+} dependence. In crab I_{KCa} was activated at voltages higher than –30 mV and its maximum conductance is about two fold higher than that of I_{Kd} in LP neurons (Golowasch and Marder 1992a). I_{KCa} was almost completely blocked by TEA. I_{KCa} could be separated from I_{Kd} by subtracting currents measured in saline containing Cd^{2+} or Mn^{2+} from the currents measured in normal saline (Golowasch and Marder 1992a). Cd^{2+} and Mn^{2+} block the Ca^{2+} channels, which eliminates Ca^{2+} influx into the cell and inhibits I_{KCa}. Because of the long-term potential toxic effects of the blockers, in this dissertation these two currents were normally not separated and a high threshold potassium current (I_{HTK}), which comprises I_{Kd} and I_{KCa}, was measured instead.

The calcium current (I_{Ca}) affects the intracellular concentration of calcium and through it I_{KCa} and multiple other cellular processes. I_{Ca} in crab STG neurons was described by Golowasch and Marder (1992a). Its pharmacological and kinetic characteristics were significantly different from those of known vertebrate calcium currents. I_{Ca} was activated at voltages above –30mV. I_{Ca} in crab could be blocked by 200 μM Cd^{2+} or 10 mM Mn^{2+} (Golowasch and Marder 1992a). Ba^{2+} permeates Ca^{2+} channels

better than Ca^{2+}, thus Ba^{2+} currents are larger in amplitude, and I_{KCa} in Ba^{2+} saline is inhibited due to the lack of Ca^{2+} influx. For these reasons I_{Ba} was measured in this dissertation in lieu of I_{Ca}.

1.3.4 Central Modulators of the Pyloric Network: Proctolin

Proctolin is a pentapeptide (Arg-Tyr-Leu-Pro-Thr) that was first isolated from insect tissues (Starratt and Brown 1975) and later found in Crustacea (Marder et al. 1986). Using immunohistochemical methods Marder et al. (1986) have shown that proctolin is located in neuronal somata and axons of CoG and OG neurons but not of STG neurons, and acts as a modulator of pyloric activity. The modulatory proctolin-containing neurons were later identified (Nusbaum and Marder 1989a, b) and the distinct motor patterns they elicit from STG neurons were studied (Blitz et al. 1999). It was shown that the effects of bath-applied proctolin are roughly equivalent to some of the effects of descending terminal-released proctolin, (Nusbaum and Marder 1989a, b), but not others (Blitz et al. 1999).

Drosophila genes encoding preproctolin and proctolin receptor have been cloned (Egerod et al. 2003, Taylor et al. 2004). It is generally agreed that the proctolin receptor is G-protein coupled and that its activation leads to an increase in intracellular levels of calcium through an IP3-mediated mechanism and through promoting the entry of extracellular calcium into the cell. Desensitizing proctolin receptor involves translocation of beta-arrestin to the plasma membrane and its binding to the receptor (Johnson et al. 2003). At the crustacean neuromuscular junction, application of PKC activator mimicked the effects of proctolin, which also could be inhibited by the PKC inhibitor BIM1, but not

a PKA inhibitor H89 (Philipp et al. 2006). Proctolin did not change the intracellular concentration of cAMP, but reduced the concentration of cGMP. The reduction in cGMP concentration was not observed in the presence of BIM1 (Philipp et al. 2006). In insects at least two proctolin receptor subtypes have been identified (Baines et al. 1996).

In many crab STG neurons proctolin evokes an inward current with a peak at approximately –50 mV and reversal potential of ~0 mV. The current is believed to be carried mostly by Na^+, and partially by K^+ and Cl^-. Low Ca^{++}/high Mg^{++} saline increases the amplitude of proctolin current and linearizes its current-voltage relationship (Golowasch and Marder 1992b). A calmodulin inhibitor increased the amplitude and altered the voltage dependence of the "proctolin" current (Swensen and Marder 2000). The so called “proctolin current” is also activated by several other neuromodulatory substances in the STG (Swensen and Marder 2000) and is thus better named “neuromodulator-activated current”.

1.3.5 Central Modulators of the Pyloric Network: GABA

In *C. borealis* GABA is synthesized in the three pairs of projection neurons in the CoGs and is delivered to the STG via the stn (Blitz et al. 1999, Swensen et al. 2000, Ducret et al. 2007). Stimulation of these neurons causes strong excitation of the pyloric rhythm. In contrast, when bath-applied to the STNS preparation, or separately to the STG or CoGs+OG, GABA causes an immediate shut down of the pyloric rhythm (Swensen et al. 2000, Ducret et al. 2007) presumably due to the inhibitory effect it has on the pacemaker kernel neurons (Swensen et al. 2000).

All pyloric neurons respond to GABA and presumably have GABA receptors,

however, the pharmacological profiles of these receptors are different from their vertebrate counterparts. There could also be several subtypes of ionotropic GABA receptors in crustaceans. In projection neurons dissociated from lobster brain, a GABA-evoked, Cl-mediated current was described (Zhainazarov et al. 1997). The current characteristics in a single channel patch were identical to the whole-cell current. The channel was partially blocked by picrotoxin (PTX), insensitive to bicuculline (competitive vertebrate $GABA_A$ antagonist) and activated by $GABA_A$ vertebrate receptor agonists in the following order: TACA>muscimol>GABA>isoguacine>CACA, as well as, surprisingly, by $GABA_C$ receptor antagonists THIP, 3APS, I-4AA, but with lesser potency than GABA (Zhainazarov et al. 1997). $GABA_B$ receptor agonists baclofen and 3APA were not effective in activating the crustacean GABA-activated channel. TBPS, a potent ligand to vertebrate PTX binding site, did not have much effect on the lobster channel, i.e., lobster GABA receptor was different from both vertebrate B and C receptors (Zhainazarov et al. 1997). Similarly, most vertebrate GABA antagonists were ineffective on the GABA-activated channel from the lobster STG, including bicuculline, phaclofen, 2-hydroxysaclofen and some of the agonists showed little or no response including baclofen and 3-aminopropanesulphonic acid (Swensen et al. 2000). $GABA_B$-like receptors were reported in the lobster (Gutovitz et al. 2001, Miwa et al. 1990) and crab *Eriphia spinifrons* (Rathmayer and Djokaj 2000) neuromuscular junction. Metabotropic $GABA_B$-type receptors were also described in other crustacea (Marder and Paupardin-Tritsch 1978). A functional chloride channel subunit activated by GABA and inhibited by PTX has been cloned from *Homarus americanus* (Hollins and McClintock 2000).

If GABA is applied individually to the LP, PY or VD neurons it causes large depolarizations that often elicit firing. When applied locally to AB, PD or IC neurons, GABA caused a slight hyperpolarization and inhibition of bursting activity (Swensen et al. 2000). These differences could be explained by the presence of different GABA-activated channels in different pyloric cell types. For example, the reversal potential of GABA-evoked currents in LP changed from –50 in normal saline to –75 mV in PTX. The amplitude of the currents evoked at more hyperpolarized holding potentials decreased in PTX, indicating that, in the LP neuron, GABA activated at least two different currents, and that PTX partially blocked the one with a more depolarized reversal potential. Muscimol (a $GABA_A$ agonist) evoked a large partially Na-dependent inward current (reversal potential >–35 mV) that was blocked by PTX. β-guanidinopropionic acid (β-GP) preferentially activated the other one of the two GABA-evoked currents, with a K^+ and a Cl^- components (Swensen et al. 2000). This second current resembles a $GABA_B$-evoked current. In PD cells GABA may induce a current active in PTX (Swensen et al. 2000) and reminiscent of bicarbonate responses to GABA seen in other systems (Kaila and Voipio 1987). PTX produced little change in the reversal potential of GABA response of the PD cell (Swensen et al. 2000). Muscimol and β-GP induced an outward current similar to the one induced by GABA and unaffected by PTX (Swensen et al. 2000).

GABA seems to regulate gap junction coupling in lobster STG. When GABA synthesis was inhibited by 3MPA, the number of neurons dye-coupled to PD in the adult preparations increased from approximately 8 to 20, same as the number of coupled neurons in the embryonic network (Ducret et al. 2007). Bath application of GABA

decreased the number of neurons dye coupled to PD, to four, and the coupling coefficient between the two PD cells measured using simultaneous dual electrode intracellular recordings decreased by more than 50% (Ducret et al. 2007).

1.3.6 Glutamatergic Synapses in the Pyloric Network

Glutamatergic synaptic transmission is a major building block of oscillatory neuronal networks (Marder and Paupardin-Tritsch 1978). In cultured lobster STG neurons glutamate evoked an outward current with two kinetically distinct components and a reversal potential of about −50 mV. Glutamate-evoked conductance increase was primarily mediated by chloride with a small potassium component (Cleland and Selverston 1995). In intact STG the reversal potential of glutamate response was −70 mV (Marder and Eisen 1984).

Although crustacean neurons readily respond to glutamate, the pharmacology of their receptors significantly differs from those of vertebrate species. Ibotenic acid binds the same receptors as glutamate, while the agonists NMDA, AMPA, kainate or quisqualate failed to induce a response. PTX, at 100 μM, completely blocked glutamate response, while niflumic acid blocked it partially (Cleland and Selverston 1995). An ionotropic glutamate receptor from cultured lobster neurons mediated recurrent synaptic inhibition in the STG; it was neither cross-activated nor cross-desensitized by GABA, and the observed GABA-evoked chloride current was distinct, i.e. the glutamate and GABA activated chloride channels were different (Cleland and Selverston 1998). The ionotropic glutamate receptor was weakly blocked by the chloride channel blocker furosemide and glutamate receptor antagonist CNQX, but not by the vertebrate $GABA_A$

receptor antagonist bicuculline, or glycine receptor antagonist strychnine (Cleland and Selverston 1998).

Besides ionotropic Cl^- and K^+ mediated effects, glutamate can elicit modulatory influences in lobster STG that are apparently mediated by metabotropic, G-protein/PLC/IP3-dependent glutamate receptors (Levi and Selverston 2006). Activation of mGluRs in crustacean STG led to acceleration of the gastric rhythm, and increases in spike frequency and burst duration (Krenz et al. 2000). mGluR agonist L-quisqualic acid induced a current similar to the proctolin current. In contrast to vertebrate receptors, internal Ca^{++} stores did not participate in the invertebrate mGluR response, i.e. G-proteins could be directly interacting with the effector ion channels (Levi and Selverston 2006). Agonists to all three groups of vertebrate mGluR had an effect on the gastric rhythm in lobster STG (Krenz et al. 2000). However, while group I agonists quisqualic acid and 3,5-dihydroxyphenylglycine accelerated the rhythm and were able to reactivate gastric rhythm in silent preparations, group II agonist L-CCG-I and group III agonist AP4 blocked or slowed down the rhythm (Krenz et al. 2000). The action of group II and III agonists was partially reversed by their respective antagonists. NMDA antagonist did not prevent the effects of any of the agonists. PTX did not interfere with group II and III agonists, while PTX effect on group I agonists was not investigated (Krenz et al. 2000).

CHAPTER 2

MATERIALS AND METHODS

In Chapter 2, materials and methods used in all experiments described in this dissertation are presented.

2.1 Animal Model

The stomatogastric nervous system of cold-anesthetized Jonah crabs *Cancer borealis* was dissected as described (Selverston et al. 1976; Harris-Warrick 1992). The animals were obtained from local fishermen and kept in seawater aquaria at ~14°C. The stomatogastric nervous system was pinned onto Sylgard-lined Petri dishes (Sylgard 184, Dow Corning) and superfused with chilled (10-15°C) normal Cancer saline with the following composition (in mM): NaCl - 440, KCl - 11, $CaCl_2$ - 13, $MgCl_2$ - 26, maleic acid - 5, trizma base - 11 (pH 7.4 - 7.5). In the STNS preparation inferior oesophageal nerves were always transected. Organotypic cultures of the isolated stomatogastric nervous system were kept for up to 5 days in an incubator at 4 - 6°C in normal saline supplemented with 1 g/l dextrose, 35 u/ml penicillin and 50 u/ml streptomycin. Mn^{++} (or Ba^{++}) saline was made by substituting 12.9 mM Mn^{++} (or Ba^{++}) for Ca^{++}, always leaving 0.1 mM Ca^{++} in the bath to ensure membrane stability (Golowasch and Marder 1992a). Low concentrations of divalent cations ($\leq$ 200 μM) were added without compensation. Unless otherwise specified all chemicals were obtained from Fisher Scientific (Fairlawn, NJ). Picrotoxin (PTX) and 3-mercaptopropionic acid (3MPA) were obtained from Sigma,

tetrodotoxin (TTX) was obtained from Calbiochem (San Diego, CA) and proctolin from Bachem (San Carlos, CA). Proctolin was bath applied as a 1μM solution in *Cancer* saline. 3MPA was diluted in Ringer's saline and applied into a Vaseline well surrounding desheathed CoGs and OG.

All data reported here are from PD and LP neurons, which are located in the STG. Two PD neurons and the network's pacemaker anterior burster (AB) neuron are members of the pyloric network and electrically coupled. No attempt was made here to isolate each neuron because, although current flow through gap junctions can contribute to ionic currents measured in any of these neurons, the contribution is negligible at the high voltages we have used for our measurements (Rabbah et al. 2005). PD neurons were identified by matching intracellular action potential recordings to their corresponding extracellular recordings on either the lateral ventricular (*lvn*) or pyloric dilator (*pdn*) motor nerves (Selverston et al. 1976, Harris-Warrick 1992).

Most neuromodulatory inputs to the STG originate in adjacent ganglia connected to it via a single nerve, the stomatogastric nerve (*stn*). To remove the neuromodulatory inputs to the STG (decentralization) the *stn* was either transected, or action potential transmission along the nerve was blocked by adding isotonic (750 mM) sucrose + 0.1 μM TTX to a Vaseline well built around the *stn* (Luther et al. 2003). The method of decentralization did not affect the results.

2.2 Electrophysiology

Extracellular recordings were made using stainless steel electrodes placed inside Vaseline wells built around motor nerves. Intracellular recordings from PD neurons were

performed using theta glass electrodes filled with 0.6M K_2SO_4 + 20 mM KCl (15-30 MΩ resistance) inserted into the soma. An Axoclamp 2B (Molecular Devices, Union City, CA) was used for all intracellular recordings and all data were acquired with a Digidata 1200A interface and pClamp 9.2 software (Molecular Devices, Union City, CA).

Unless otherwise stated, all currents were measured in normal saline or normal saline supplemented with 0.1 μM TTX. The presence of TTX during voltage clamp measurements did not affect current amplitudes. TTX washed off completely in approximately 2 hrs. There was no noticeable effect of short term (less than 30 min) TTX applications on the process of activity recovery or current density changes after decentralization. All currents were measured in two electrode voltage clamp as described before (Golowasch and Marder 1992a).

Leak currents generated at the test potentials V_{test}, was subtracted using the P/n methods: n subpulses of amplitude V_{test}/n were applied (n = 4-5) in the opposite direction from the test pulse, and the sum of the currents measured during the subpulses was added to the current measured at V_{test}.

A high threshold potassium current (I_{HTK}) was defined here as the current activated in normal saline by applying 800 msec depolarizing voltage steps from a holding potential of –40 mV, leak subtracted using the P/n method described above. A large fraction of this current is generated by the Ca-dependent K^+ current (I_{KCa}) (Golowasch and Marder 1992a, Haedo and Golowasch 2006). Peak I_{HTK} amplitudes were measured at 30 ms after the test pulse onset. Because I_A is fully inactivated at –40 mV, I_{HTK} estimated using this protocol is not contaminated by I_A. The delayed rectifier current (I_{Kd}) was defined as the current measured in the same way as I_{HTK} but in Mn^{++} containing

saline. I_{KCa} was estimated by subtracting total outward current measured in Mn^{++} saline in response to 800 msec depolarizing voltage steps from a holding potential of –40 mV from the current measured in the same way in normal saline. Steady state I_{HTK}, I_{KCa} or I_{Kd} values were measured at the end of the 800 msec pulse at +40 mV. The A current (I_A) was determined in normal saline taking advantage of its strong voltage-dependence of inactivation, which distinguishes it from I_{HTK}. I_A is known to be completely inactivated in pyloric neurons of *C. borealis* at –40 mV but nearly completely de-inactivated at –80 mV (Golowasch and Marder 1992a). Thus, to estimate I_A total outward current measured by applying 800 msec depolarizing voltage steps from a holding potential of –40 mV was subtracted from the current measured at the same membrane potentials but from a holding voltage of –80 mV. I_A amplitude was measured at 30 ms after the start of the pulse at +40 mV. To confirm that I_A was not contaminated by I_{HTK}, the effects of partially blocking I_{HTK} with Mn^{++} saline or with 10 mM TEA (Golowasch and Marder 1992a) on our measurements of I_A were evaluated. No significant differences from the current measured in the same cells in normal saline were found (I_A in normal saline: 96.1 ± 51.5 nA/nF, in TEA: 87.2 ± 32.0 nA/nF, n = 15, P = 0.4; I_A in normal saline: 109.9 ± 29.6 nA/nF, in Mn^{++}: 105.8 ± 40.0 nA/nF, n= 18, P = 0.5).

The hyperpolarization-activated current (I_h) was activated with hyperpolarizing pulses from a holding potential of –40 mV. Maximum amplitude was measured at the end of an 8 sec pulse at –110 mV after leak-subtraction. To determine the leak current during I_h measurements, a linear fit to the I-V curve at –60 to –40 mV was extrapolated to –110 mV. I_{Ba} corresponds to the current flowing through Ca^{++} channels but carried by Ba ions, and was calculated as a difference between a current measured as described for

I_{HTK}, but in low Ca^{++} saline + 0.1μM TTX + 10 mM TEA + 12.9 mM Ba^{++}, and the same current measured in TTX + TEA + Ba^{++} + 200 μM Cd^{++} at 210 msec from the onset of the test pulse.

The membrane capacitance was determined by integrating the area of the capacitive current for 12 msec long voltage steps from −50 to −60 mV. Current density was estimated by dividing the current amplitude by the membrane capacitance. Examples of raw current traces and I-V curves for all these currents are shown in Fig. 3.2 for PD and 4.2 for LP (first and second columns, respectively). Day 0 measurements correspond to initial control measurements taken in every condition tested. In decentralized preparations, day 0 measurements were taken immediately before decentralization. Measurement of all five different voltage-gated currents was not always possible in the same cell. Therefore, the sample sizes of the correlation graphs may differ.

2.3 Activity-Modifying Pretreatments of the STG

Organotypic cultures of the STNS were recorded continuously for up to 2 days on an electrophysiology setup at 11 - 13°C in normal or modified saline (see below) supplemented with 1 g/l dextrose, 35 u/ml penicillin and 50 u/ml streptomycin. When low external Na^+ solutions were used we replaced 50-60% of the Na^+ in the normal saline with N-methyl-D-Glucamine (Acros Organics, New Jersey). To experimentally modify the activity of the pyloric network we used several pharmacological methods, including low Na^+, GABA, muscimol, baclofen and proctolin bath applications. These substances where dissolved immediately prior to use (GABA) or kept as stock solutions at 100-1000x concentration at 4 °C for up to 2 weeks, then diluted immediately prior to use.

After dissection of the STNS, and desheathing of the STG, the pyloric rhythm was recorded for ~30 minutes in normal crab saline before any treatment was started. The solution was then changed and the preparations were superfused with the substance of choice dissolved in crab saline. To reduce pyloric network activity the injection of hyperpolarizing current (–2 to –5 nA) into the two pyloric dilator (PD) neurons found in the ganglion was used. These two neurons are both strongly electrically coupled to the pacemaker AB neuron (coupling coefficient ~0.2, Rabbah et al. 2005) and their hyperpolarization effectively reduces or eliminates rhythmic activity.

Pyloric frequency was measured cycle by cycle using software developed in our laboratory (Datamaster) on a LabWindows platform, which determines bursts of action potentials from extracellular recordings by detecting threshold crossings by the action potentials. Frequency data for each 5 or 10 minutes of pyloric activity was averaged and plotted as one bar on a frequency bar graph.

2.4 Statistical Analysis

All data are shown as averages ± standard deviation. Statistical significance was determined using linear regression analysis, t-tests, or one-way ANOVAs with Tukey post-hoc tests (SigmaStat 2.03, Aspire Software International, Leesburg, VA). Two-way mixed design ANOVAs, ANCOVAs and multivariate analyses were performed using custom functions (SigmaStat 2.03, Excel, Microsoft).

CHAPTER 3

NEUROMODULATORS, NOT ACTIVITY, CONTROL COORDINATED EXPRESSION OF IONIC CURRENTS

Results presented in Chapter 3 were published in Journal of Neuroscience (Khorkova and Golowasch 2007).

3.1 Abstract

The ionic currents that determine neuronal activity have been shown to express wide neuron-to-neuron amplitude variability. Nevertheless, neuronal electrical activity across individuals is often remarkably similar, and can be stable over long periods. This apparent random variability of individual current amplitudes may obscure mechanisms that globally reduce variability and that contribute to the generation of the same neuronal output. One mechanism that could compensate for this individual variability and may enhance output stability could be the coordinated regulation of expression of ionic currents. In this dissertation, studying identified neurons of the *Cancer borealis* pyloric network it was discovered that the removal of neuromodulatory input to this network (decentralization) was accompanied by the loss of the coordinated regulation of ionic current levels. Additionally, decentralization induced large changes in the absolute levels of several ionic currents. The loss of co-regulation and the changes in current levels were prevented by continuous exogenous application of proctolin, a peptide known to be part of the normal neuromodulatory input to the pyloric network. This peptide does not exert fast regulatory actions on any of the currents affected by decentralization. Hence

neuromodulatory inputs to the pyloric network have a novel role in the regulation of ionic current expression. They can control, over the long-term, the coordinated expression of multiple voltage-gated ionic currents that they do not acutely modulate. These results suggest that the loss of current co-regulation after decentralization may remove constraints on intrinsic plasticity that permit recovery of function.

3.2 Introduction

Neuronal activity is mainly the result of the operation of ion channels, and their conductance levels are known to be highly variable (Liu et al. 1998, Golowasch et al. 1999a, Golowasch et al. 2002, Schulz et al. 2006). In spite of this variability, neurons and neural networks can maintain remarkable functional stability under variable conditions (Davis 2006), can restore their functional levels of activity after perturbations and injury (Thoby-Brisson and Simmers 1998, Luther et al. 2003, Saghatelyan et al. 2005) and sometimes show great similarity of activity patterns across individuals (Bucher et al. 2005). It is therefore important to understand how this conductance variability can result in stable activity. One possibility is that the conductance levels are regulated by activity-dependent feedback mechanisms. This has been shown at the synaptic (Turrigiano 1999, Turrigiano and Nelson 2004), neuronal (Turrigiano et al. 1994, Hong and Lnenicka 1997, Galante et al. 2001, Xu et al. 2005, Davis 2006) and network levels (Thoby-Brisson and Simmers 1998, Golowasch et al. 1999b, Gonzalez-Islas and Wenner 2006).

Other possibilities include activity-independent mechanisms, such as developmentally regulated ion channel expression programs (Linsdell and Moody 1994, Spitzer 2006). Furthermore, it is often found that conductance levels of two or more ionic

currents are simultaneously regulated as a consequence of neuronal activity changes (Linsdell and Moody 1994, Desai et al. 1999, Golowasch et al. 1999a, Gibson et al. 2006). Whether such simultaneous changes actually involve a coordinated regulation between multiple ionic currents is known for only a very small number of cases (McAnelly and Zakon 2000, MacLean et al. 2003), and the coordinating mechanisms are unknown. In lobster stomatogastric ganglion (STG) neurons an activity-independent mechanism seems to coordinate the conductance level of the outward A-current (I_A) with the conductance level of the hyperpolarization-activated inward current (I_h), resulting in the preservation of neuronal and network patterns of activity (MacLean et al. 2003). The coordination between these currents occurs at the transcript level (Schulz et al. 2006).

3.3 Results

3.3.1 Decentralization Modifies Pyloric Network Activity

The pyloric network of the crustacean STG shows a robust form of stabilization of its rhythmic activity. Pyloric activity is temporarily interrupted when central neuromodulatory inputs from other ganglia are removed (decentralization), but can recover to near control levels hours to days later (Thoby-Brisson and Simmers 1998, Golowasch et al. 1999a, Luther et al. 2003). An example of these changes in activity is shown in Figure 3.1. On the left (Control) are extracellular recordings of the main pyloric motor nerve (*lvn*) and intracellular recordings of a PD neuron of a preparation in which the neuromodulatory input nerve is intact, shown at different times in organ culture (days 0, 1 and 4). Only a slight variation in the frequency of the rhythm is observed.

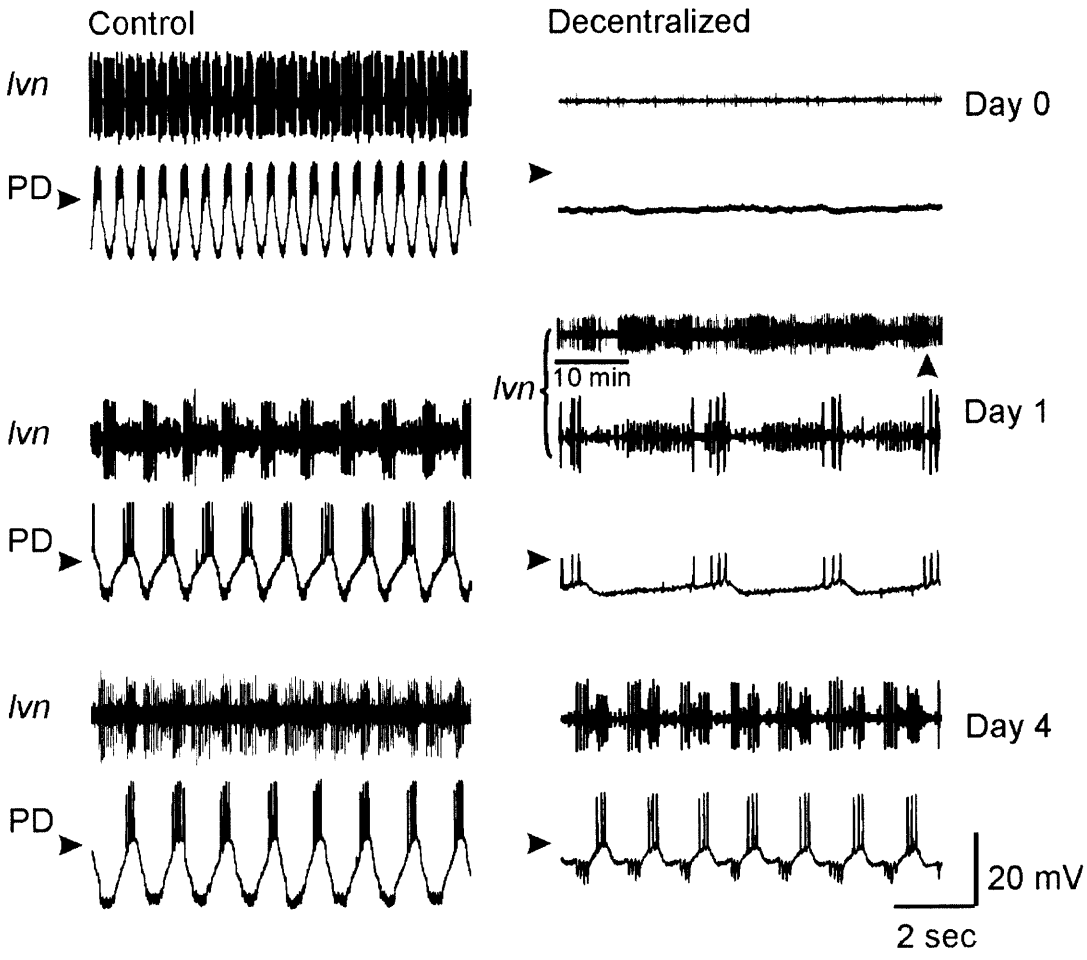

Figure 3.1 Effects of decentralization on pyloric network activity. All extracellular recordings were obtained from the lateral ventricular nerve *lvn* and all intracellular recordings are from the PD neuron, in normal saline. Control (left panels) and decentralized (right panels) preparations were recorded at days 0, 1 and 4 in organ culture. Decentralized day 0 corresponds to activity ~15 minutes after decentralization. On day 1, the decentralized preparations showed bouts of pyloric activity lasting seconds to a few minutes and repeating at irregular intervals of minutes to hours (top *lvn* panel) comprising the so-called "bouting period". During these bouts, pyloric activity was slow and irregular (bottom *lvn* panel and PD trace are expanded recordings at time of vertical arrowhead). Regular pyloric activity recovered after this bouting phase (day 4). Arrowheads point to –40 mV. *lvn* recordings monitor the activity of three different pyloric cells types: LP neuron (largest action potentials), PY neurons (smallest action potentials) and PD neurons (intermediate action potentials).

If the neuromodulator-containing input nerve (*stn*) is severed, the pyloric rhythm ceases in seconds to minutes (Decentralized, day 0). This activity recovers after ≥ 1 day

in organ culture (Decentralized, day 4). During the process of recovery the pyloric rhythm undergoes a period of several hours in which it turns on and off irregularly for a few seconds to minutes at a time, a process termed "bouting" and illustrated in Figure 3.1 (Decentralized, day 1).

3.3.2 Decentralization Modifies Voltage-Dependent Ionic Current Levels

In the lobster *Jasus lalandii*, the recovery of the pyloric rhythm is correlated with an increase in the ionic conductance levels of I_h, and a conductance decrease of the TEA-sensitive K^+ current component in PD neurons four days after decentralization (Thoby-Brisson and Simmers 2002). In *Homarus gammarus* recovery was associated with an increase in I_A four days after decentralization (Mizrahi et al. 2001). This has been argued to be partly consistent with the acquisition of bursting properties not normally expressed by these cells (Thoby-Brisson and Simmers 2002). In lobsters, however, the transitional bouting phase observed in crabs has not been reported. To establish if similar conductance changes are observed in *C. borealis*, several ionic currents were measured during the entire recovery period.

Figure 3.2 (left panels) shows examples of raw current traces of five voltage-gated currents we measured in *C. borealis* PD neurons: I_h, I_A, the high threshold Ba^{++} current (I_{Ba}), the Ca-dependent K^+ current (I_{KCa}), and the delayed rectifier K^+ current (I_{Kd}). Figure 3.2 (center panels) shows examples of current-voltage plots of these currents before decentralization (open symbols/dashed lines) and 24 hours after decentralization (solid symbols/lines). Changes in I_h, I_{Ba} and I_{KCa} (measured at steady state), and in I_A were consistently observed, while I_{Kd} did not change. To determine the time course of these changes, we measured current densities of these voltage-gated currents at 0, 1 and 4

days in organ culture in control preparations (no decentralization) and in preparations decentralized immediately after the day 0 measurements were taken. All data points were normalized to the measurements in the same cell at day 0 (Figure 3.2, right panels). Significant current density changes occurred over 4 days after decentralization relative to the changes observed in control preparations (all comparisons made using two-way mixed design ANOVA): I_h ($P < 0.001$, $n = 39$), I_{Ba} ($P < 0.05$, $n = 26$), I_{KCa} (steady state, $P < 0.05$, $n = 23$) and I_A ($P < 0.001$, $n = 62$) (Figure 3.2, right panels). I_{Kd} (Figure 3.2, bottom) and the peak of I_{KCa} (not shown) were not significantly affected over this period ($P = 0.80$, $n = 22$, $P = 0.28$, $n = 23$, respectively). The largest changes in decentralized preparations compared to controls on the same day occurred 24 hours after decentralization: I_h, I_{Ba} and I_{KCa} (steady state) increased, and I_A decreased (post-hoc Tukey tests: I_h: $P < 0.001$, I_{Ba}: $P = 0.002$, I_{KCa}: $P = 0.025$, I_A: $P = 0.03$). Only the current density of I_h remained significantly elevated in decentralized preparations after 4 days ($P = 0.007$), while the current densities of I_A, I_{Ba} and I_{KCa} all returned to levels indistinguishable from control non-decentralized preparations (Figure 3.2, right panels). Current levels in non-decentralized preparations remained generally stable over time in organ culture except I_h and I_A that significantly decreased by day 4 compared to day 0 ($P < 0.01$ for both). Changes in decentralized preparations were significant with these trends taken into consideration.

Because I_{Kd} showed no tendency to change over time in either non-decentralized (control) or decentralized preparations, and to avoid applications of Ca^{++} current blockers (e.g. Mn^{++}), that could potentially interfere with normal physiological processes, we henceforth used the high threshold potassium current (I_{HTK}) comprising I_{Kd} and I_{KCa} as a

measure of I_{KCa}. The same trends and their significance were observed when I_{HTK} was used for our analyses (two-way mixed design ANOVA $P < 0.05$, $n = 23$) even though the relative level changes were smaller for I_{HTK} than I_{KCa} (ΔI_{HTK} at day 1: 131.1 ± 30.2 %, ΔI_{KCa} at day 1: 222.4 ± 80.3 %).

In a subset of experiments, measurements were made both immediately prior to, and 10-30 minutes after decentralization. No significant current density differences were observed over this brief time span (current densities measured 10-30 min after decentralization expressed as percent of currents measured before decentralization in the same cell were: I_{HTK}: 101 ± 39%, I_A: 98 ± 30%, I_h: 98 ± 31%, all t-test P values were > 0.05, $n = 20$). This indicates that long-term current changes are not the immediate effect of the neuromodulatory input removal.

No effects of decentralization or time in organ culture on neuronal input resistance were observed (Table 3.1). With the exception of I_{Ba}, which sometimes showed a hyperpolarizing shift in its activation curve, we also did not observe significant changes in other conductance parameters (not shown).

3.3.3 Co-regulation of Ionic Current Pairs Depends on Neuromodulatory Input

In the experiments reported in this dissertation current densities of all the currents studied displayed a high level of variability (I_h = −6.0 ± 5.1 nA/nF, I_A = 97.5 ± 21.0 nA/nF, I_{HTK} (steady state) = 105.8 ± 18.9 nA/nF, I_{KCa}=66.2±34.7 nA/nF, I_{Kd} = 53.9 ± 26.4 nA/nF, and I_{Ba} = −1.62 ± 1.92 nA/nF), similar to what has been reported for PD neurons before (Goldman et al. 2000). Surprisingly, it was found that the densities of I_h, I_A and I_{HTK} or

I_{KCa} significantly correlate with each other at all times during organ culture in non-decentralized preparations (Figure 3.3A-C and Table 3.2). No other current density combination proved significantly correlated (not shown). To confirm that correlation of I_A and I_h can not simply be explained by correlation of each of these currents with I_{HTK}, multivariate analysis was performed. If the effect of I_{HTK} was removed, the resulting partial correlation coefficient for the I_A/I_h pair is still significant ($R = 0.50$, $P < 0.001$), which indicates that there is an independent relationship between I_A and I_h. Further, the multiple correlation among the three currents were determined: it can be described as $I_{HTK} = 120.85 + 0.97*I_A + 6.12*I_h$.

The strong correlations between I_A vs I_{HTK} and I_h vs I_{HTK} observed in control preparations, however, disappeared one day after decentralization (Figure 3.3 D and Table 3.2) and the currents remained uncorrelated on day 4 after decentralization (Figure 3.3 E and Table 3.2). In contrast, I_h vs I_A remained strongly correlated at all times after decentralization (Figure 3.3D, E right panels, and Table 3.2) suggesting a mechanism of co-regulation between I_h and I_A that is different from the mechanism that explains the co-regulation of I_{HTK} and both I_A and I_h.

It was hypothesized that the lack of neuromodulator release, and/or the lack of rhythmic activity caused by decentralization, must mediate the changes in ionic current density and ionic current co-dependence shown in Figures 3.2 and 3.3. To test our hypothesis, we examined the effects of proctolin, one of the naturally released neuromodulators that can induce rhythmic activity when bath applied or when released onto the STG by projection neurons (Blitz and Nusbaum 1999), on activity, on ionic current levels and on current co-regulations.

3.3.4 Proctolin Prevents Ionic Current Changes and Loss of Co-Regulation Due to Decentralization

Figure 3.4 illustrates the effects of proctolin on activity in control (non-decentralized, Figure 3.4A) and decentralized preparations (Figure 3.4B). In non-decentralized preparation, after 15 minutes in proctolin (column 2) a slight increase in pyloric rhythm frequency and an increase in PD neuron oscillation amplitude are observed. In preparations decentralized in normal saline, pyloric rhythm is completely shut down 15 min after decentralization (panel B, column 1). However, if a preparation is decentralized in the presence of 10^{-6} M proctolin, pyloric activity is strong and regular (panel B, column 2). In these experiments electrodes were removed after recording in proctolin on day 0 (column 2) and reinserted 24 hours later still in the presence of bath applied proctolin (column 3). Although regular pyloric activity continues uninterrupted during a 24 hour application of proctolin in both control (Figure 3.4A, column 3) and decentralized preparations (Figure 3.4B, column 3) upon re-impalement, we observed a slight decrease in the amplitude of the membrane potential oscillations. This coincided with a slight decrease in the PD neurons' input resistance (R_{in} = 26.3 MΩ on day 0, R_{in} = 21.7 MΩ on day 1 in this preparation). However, on average, input resistances of the preparations examined in this study were statistically indistinguishable at all stages (Table 3.1). A strong decrease in the amplitude of the inhibitory synaptic potentials that PD neurons receive from LP neurons was also sometimes observed (Figure 3.4B, column 3), which is consistent with observations previously reported in lobster (Thoby-Brisson and Simmers, 2002). Finally, upon washout of proctolin, both control and decentralized preparations slowed down and decreased the amplitude of the PD neuron membrane

potential oscillations, consistent with well known effects of proctolin (Hooper and Marder 1987, Nusbaum and Marder 1989a, b).

The acute application of proctolin did not significantly affect the current amplitudes of either I_{HTK}, I_A or I_h. After 15 minutes of 10^{-6} M proctolin bath application in intact preparations current densities were (in % of densities in normal saline in the same cell): I_{HTK}, 114.9 ± 46.7% (P = 0.273), I_A, 95.1 ± 25.0% (P = 0.115), I_h, 114.7 ± 57.8% (P = 0.707). P values are the result of paired t-tests (n = 15). The lack of acute effects of proctolin on these voltage-dependent currents has also been thoroughly documented before (Golowasch and Marder 1992b, Swensen and Marder 2000). In these previous studies proctolin was applied at various times after decentralization. Continuous application of 10^{-6} M proctolin for 24 hours in intact, non-decentralized, preparations produced no significant differences in current densities (in % of densities in the same cell on day 0): I_{HTK}, 110.8 ± 28.8% (P = 0.431), I_A, 91.9 ± 46.1% (P = 0.816), I_h, 110.1 ± 44.2% (P = 0.495). P values are the result of paired t-tests (n = 5). Similar results were obtained in the preparations decentralized and continuously maintained in the presence of proctolin for 24 hr (in % of densities in the same cell on day 0 before decentralization): I_{HTK}, 109.3 ± 30.2% (P = 0.36), I_A, 94.0 ± 27.6% (P = 0.36), I_h, 76.8 ± 26.2% (P = 0.24). P values are the result of paired t-tests, n = 12. Figure 3.5 shows these results (compare grey and white bars). Here hatched bars show the effects of decentralization in normal saline for comparison.

Figure 3.6A shows the effects of the continuous bath application of 1 μM proctolin on ionic current co-regulation. Ionic currents were measured, proctolin was applied, and the preparations were decentralized immediately thereafter. The preparations

were then maintained in proctolin for 18-24 hours, and current densities were measured again. In the presence of proctolin, regular pyloric activity was maintained in spite of decentralization (Figure 3.4D, column 3), and the three current pairs (I_A/I_{HTK}, I_h/I_{HTK} and I_h/I_A) remained highly significantly correlated (Figure 3.6A, and Table 3.2), similar to non-decentralized preparations (Figure 3.3A-C, and Table 3.2) and in contrast with the effects of decentralization alone (Figure 3.3D-E, and Table 3.2). To determine whether the uninterrupted activity or uninterrupted neuromodulator supply accounted for the maintenance of current co-regulation, rhythmic activity was suppressed with 0.1 μM tetrodotoxin (TTX) applied together with 1 μM proctolin 10 minutes before decentralization (Figure 3.7 right, Golowasch and Marder 1992b). Bath-applied TTX not only blocks the generation of action potentials in STG motorneurons, but also blocks the release of endogenous neuromodulators from axon terminals onto the STG, which eliminates subthreshold oscillatory activity. Blockade of action potentials only is not sufficient to block slow subthreshold oscillatory activity in STG neurons (Raper 1979). A similarly strong correlation of ionic currents in the presence of proctolin + TTX was observed (Figure 3.6B, and Table 3.2), again similar to non-decentralized preparations (Table 3.2) or decentralized preparations treated with proctolin alone (Table 3.2). TTX application alone did not preserve the co-regulation of I_A/I_{HTK} and I_h/I_{HTK}, while I_h/I_A co-regulation was again not affected (Figure 3.6C, and Table 3.2), similar to the effects of decentralization alone (Figure 3.3D-E, and Table 3.2). The preservation of co-regulation among these three currents in the presence of proctolin (or proctolin + TTX) was accompanied by the elimination of the current density changes observed after decentralization (no proctolin application) relative to each current's levels at day 0

(Figure 3.5, white and black bars). Together with the complete loss of oscillatory activity in TTX + proctolin, these results indicate that proctolin, and not activity, regulates the coordinated expression of ionic currents in this system.

These results suggest the possibility that the "non-decentralized" ionic current density levels and their co-regulation could be rescued by neuromodulators after the ionic currents have already undergone the decentralization-induced changes in current density and co-regulation we have observed. To address this possibility two sets of experiments were conducted. In the first experiment, a reversible TTX/sucrose block of action potential transmission along the stomatogastric nerve (*stn*) was used rather than *stn* transection (see Methods) to decentralize the preparations. After approximately 24 hours, current densities were measured. At this point the decentralized preparations have entered the so-called bouting stage of irregular pyloric activity, described by Luther et al. (2003) or, in some cases, fully recovered their pyloric rhythmic activity (Figure 3.1, decentralized day1 and 4). The *stn* block was then removed by extensive washing of the sucrose/TTX block with normal saline and the preparation was maintained in organ culture for additional 24 hours, at which point current densities were measured one more time. The effectiveness of the block, and of its removal, was confirmed by stimulating the *stn* (on the side of the Vaseline well used for the block opposite to the STG) with 20 sec long trains of 0.4 msec voltage pulses (1-2 V amplitude) at 10 Hz. The *stn* block was deemed effective if stimulation for 20 seconds was unable to elicit change in pyloric activity, a block was deemed removed if similar stimulation could elicit the pyloric rhythm or change its frequency, at least for the duration of the stimulus. In the second set of experiments, preparations were decentralized by *stn* transection and kept in organ

culture for 24 hours. At this point current densities were measured. The preparations were then incubated in bath-applied 1 μM proctolin for additional 24 hours. Currents were then measured for a second time. The day 2 changes were expressed relative to day 0 using population averages because currents at day 0 were not measured in these preparations to avoid more than two impalements per cell (see Methods). The effect of these treatments on current density levels of I_{HTK}, I_A and I_h are shown in Figure 3.8. The restoration of the full complement of endogenous neuromodulators by the removal of the *stn* block after 24 hours (Decentralization reversed after 24 hrs) or the addition of exogenous proctolin (24 hrs decentralized then proctolin) were not able to restore the control levels of I_{HTK} or I_A densities observed before decentralization (day 0) or the levels of non-decentralized preparations at the same time point. In fact, the levels of I_{HTK} and I_A remained approximately equal to the levels observed in decentralized preparations on the same day in culture (but significantly higher than control in preparations in the case of I_{HTK} and significantly lower than control preparations in the case of I_A, $P < 0.05$ for both). In contrast, the current density of I_h was closer to levels observed in control preparations. These results suggest that the effects of decentralization on ionic current levels are irreversible past a critical window of ≤ 24 hours.

The effect of the two treatments described above on the co-regulation of currents is shown in Figure 3.9 (data combined). Not only was the co-regulation of the pairs I_A/I_{HTK} and I_h/I_{HTK} not recovered by continuous proctolin bath application starting 24 hours after decentralization, or by re-establishing normal action potential transmission along the *stn*, but the robust co-regulation we observed of the I_h/I_A pair was further lost (compare right panels in Figure 3.3 and Figure 3.9). These results suggest that prolonged

removal of neuromodulators causes a restructuring of the signaling pathway connecting the neuromodulator receptors and their ion channel effectors.

3.4 Discussion

The results reported here reveal a hitherto unknown role of neuromodulators, namely that of controlling the co-dependence of ionic currents (in this particular system of I_{HTK}, I_A and I_h). It is shown in this dissertation that this effect is likely to be mediated by neuromodulators (such as proctolin) directly rather than indirectly via electrical activity changes. Proctolin is known to activate a peptide-specific current (Golowasch and Marder 1992b, Swensen and Marder 2000) via a metabotropic receptor (Swensen and Marder 2000). Acute effects of proctolin on other ionic currents have not been previously reported. The results reported in this chapter suggest that proctolin has effects on several other voltage-gated currents expressed by PD neurons that are not acutely apparent and are revealed when neuromodulatory input (including proctolin) to the STG is removed. At this point it is unknown whether the acute effects of proctolin on the peptide-activated current and the long-term effects on the amplitude and co-regulation of other voltage-gated currents are mediated by the same or by distinct signaling pathways linked to proctolin receptor.

An activity-independent mechanism linking I_A and I_h has been shown in PD neurons in lobster (MacLean et al. 2003), apparently acting at the transcription level (Schulz et al. 2006). The results reported in this chapter are consistent with this mechanism since the I_A/I_h co-regulation does not appear to be significantly affected by the loss of rhythmic activity. However, here it is shown that I_A and I_h both co-vary with

I_{HTK}, in a manner that appears to be independent of the co-variation between I_A and I_h and of activity, but controlled by the neuromodulatory input to the pyloric network. Furthermore, the loss of current co-regulation after decentralization can be prevented by exogenous neuromodulators only during a critical window lasting for an as yet undetermined period no longer than 24 hours after decentralization. This period coincides with the critical window after decentralization during which RNA synthesis is required for rhythmic pyloric activity recovery in lobster (Thoby-Brisson and Simmers 2000). Thus, a possible mechanism underlying the co-regulation of currents by neuromodulator could be the simultaneous regulation of the expression of multiple genes (cf. Adams and Dudek 2005) in conjunction with a relatively fast turnover rate of the channels involved. Alternatively, ion channels can also express enzymatic activity, which could regulate inter-ion channel activation directly (Runnels et al. 2001, Cai et al. 2005). The existence of multi-molecular complexes including ion channels, enzymes and cofactors capable of recruiting and activating enzymes (Catterall et al. 2006, Levitan 2006) may provide the molecular framework for the coordinated regulation of multiple channels.

The data reported here show that most ionic currents affected in PD neurons by decentralization show transient current density changes that are maximal at a time during the recovery (day 1) when pyloric rhythm displays a high degree of instability characterized by intermittent bouts of pyloric activity (Luther et al. 2003). Preliminary evidence indicates that this is also true for other neuronal types in the network. These transient changes may in fact be responsible for bouting behavior, as suggested by similar current changes during bouting observed in a conductance-based model of PD neuron decentralization (Zhang and Golowasch 2007).

Sustained rhythmic activity in non-decentralized preparations is in large part driven by an additional inward current activated by neuromodulators (Golowasch et al. 1992b, Swensen and Marder 2000). This neuromodulator-gated current is activated by proctolin and is thought to be inactive in decentralized preparations due to the abolished release of neuromodulators, yet rhythmic activity slowly recovers back to near control levels (Thoby-Brisson and Simmers 1998, Luther et al. 2003). It is in principle possible that the neuromodulator-gated current activated by proctolin after decentralization becomes constitutively active and independent of the peptide, thus reactivating the pyloric rhythm. Alternatively, two effects may compensate for the prolonged removal of neuromodulator-gated currents and help restore rhythmic network activity: 1) A subset of the voltage-gated ionic currents irreversibly change in amplitude relative to control levels during the recovery after decentralization (i.e. I_h), this may be sufficient to restore the neuron's ionic current balance and rhythmic activity. 2) The change in co-regulation of a subset of voltage-gated currents (i.e. I_h, I_A and I_{HTK}) after decentralization may be sufficient to alter the balance of conductances to a state that restores rhythmic activity in key neurons, such as the PD neurons that are strongly coupled to the pacemaker AB neuron. As a consequence the entire network may recover its rhythmic pattern of activity. Data obtained in this dissertation (Chapter 4) indicate that different neurons in the network respond differently to long-term decentralization. Additionally, synaptic changes may also occur as suggested by Thoby-Brisson and Simmers (2002).

Thus, the pyloric network recovery of activity is likely the result of a complex interplay and balance of ionic current and synaptic changes across the entire network. It is possible that the high degree of consistency of pyloric network activity across

individuals (Bucher et al. 2005) is the result of conductance co-regulation set by neuromodulatory input. On the other hand, our data indicate that coordinated expression of ionic currents is not by itself necessary to ensure a stable neuronal output since stable output was restored even in the absence of their coordinated expression. Perhaps it is precisely the loss of co-regulation that, in combination with other synaptic and/or ionic current changes, releases certain constraints imposed on the network under normal conditions to allow the recovery of rhythmic activity to within functional levels. Although a large degree of ionic current variability can theoretically sustain specific types of neuronal activity (Goldman et al. 2001, Prinz et al. 2004), a restriction of the global current variability by co-regulation can help to ensure the maintenance of activity within functional limits (Goldman et al. 2001, MacLean et al. 2003, Burdakov 2005, MacLean et al. 2005) in the intact system. However, the release from the co-regulated condition plus significant current density changes of a subset of ionic currents may be required to ensure the recovery of specific activity patterns, such as the pyloric activity pattern, when one of the ionic currents responsible for rhythm generation is lost (i.e. the neuromodulator-gated current (Swensen and Marder 2000)). Ionic current co-regulation may also play other, as yet unidentified, roles, e.g. gain adjustment (Burdakov 2005). Finally, conductance parameters other than those identified in this work, which could contribute to the restoration of the functional output of the network, may also be subject to co-regulation (e.g. McAnelly and Zakon 2000). These results highlight the complexity of the balance of conductances and their properties in the generation of neuronal activity, and that potentially many important factors regulating neuronal activity remain to be identified.

Table 3.1 Input Resistance (in MΩ) Changes during Organ Culture and Decentralization

	Day 0	*Day 1*	*Day 2*	*Day 4*	*P*
Control	10.7 ± 10.3	9.4 ± 6.1	10.6 ± 13.2	11.9 ± 10.2	
	n = 71	n = 35	n = 71	n = 71	0.819
Decentralized	9.7 ± 9.8	10.6 ± 16.8	12.0 ± 9.0	8.8 ± 7.6	
	n = 206	n = 174	n = 59	n = 43	0.525

Table 3.2 Linear Regression Analysis of Ionic Current Density Coordinated Regulation

	I_A vs I_{HTK}			I_h vs I_{HTK}			I_h vs I_A		
	R^2	P	n	R^2	P	n	R^2	P	n
Control, day 0*	0.48	<0.0001	95	0.37	<0.0001	94	0.4	<0.0001	89
Control, day 1	0.49	0.007	12	0.81	0.002	8	0.54	0.009	11
Control, day 4	0.73	<0.001	22	0.44	0.002	21	0.50	<0.001	28
Decentralized, day 1	**0.06**	**0.07**	52	**0.02**	**0.22**	48	0.55	<0.001	51
Decentralized, day 4	**0.05**	**0.35**	19	**0.01**	**0.76**	19	0.56	0.0002	18
Control + Proctolin, day 1	0.88	0.01	5	0.92	0.02	5	0.89	0.05	5
Decentralized + Proctolin, day 1	0.87	<0.0001	11	0.87	<0.0001	11	0.83	0.0002	10
Decentralized + Proctolin + TTX, day 1	0.73	0.002	9	0.65	0.05	6	0.87	0.0006	8
Control + TTX, day 1	**0.009**	**0.75**	12	**0.05**	**0.500**	10	0.52	0.007	12

Low R^2 values are shown in bold. Notice that these correspond only to decentralized and TTX-treated preparations (TTX effectively decentralizes the STG by blocking action potential transmission along the *stn*). Proctolin was bath applied at 1μM and TTX at 0.1 μM. * Day 0 corresponds to pooled data of preparations measured on day 0 before decentralization for all experiments. Similar correlations and statistical significance were obtained for subsets of day 0 measurements corresponding to each experimental set listed below.

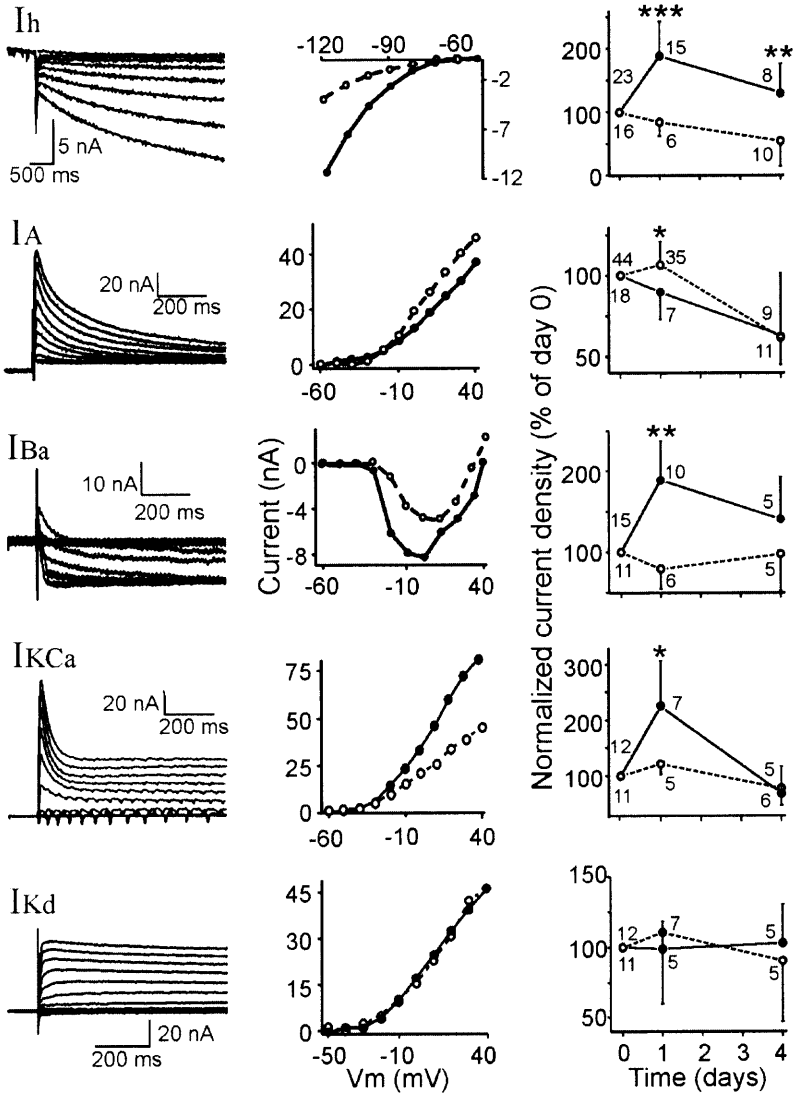

Figure 3.2 Decentralization affects most ionic current densities in PD neurons. Left panels: examples of raw current traces. Currents are (from top to bottom) I_h, I_A, I_{Ba}, I_{KCa} (steady state) and I_{Kd}. Center panels: examples of current-voltage plots of the five currents (I_{KCa} measured at steady state). Open symbols/dashed lines are currents measured before decentralization. Solid symbols/lines are currents measured in the same cell 24 hours after decentralization. Right panels: current densities measured in decentralized (solid symbols/lines) and non-decentralized preparations (open symbols/dashed lines) at days 0, 1 and 4 in organ culture. Current densities on day 1 and 4 are normalized to values measured in the same cell on day 0, no cell was impaled more than twice. A two-way mixed design ANOVA and post-hoc Tukey tests were used to compare data from decentralized and non-decentralized preparations day by day (comparisons for control preparations at different times are discussed in the text) : * $P < 0.05$, ** $P < 0.01$, *** $P < 0.001$. Number of experiments is shown next to each point.

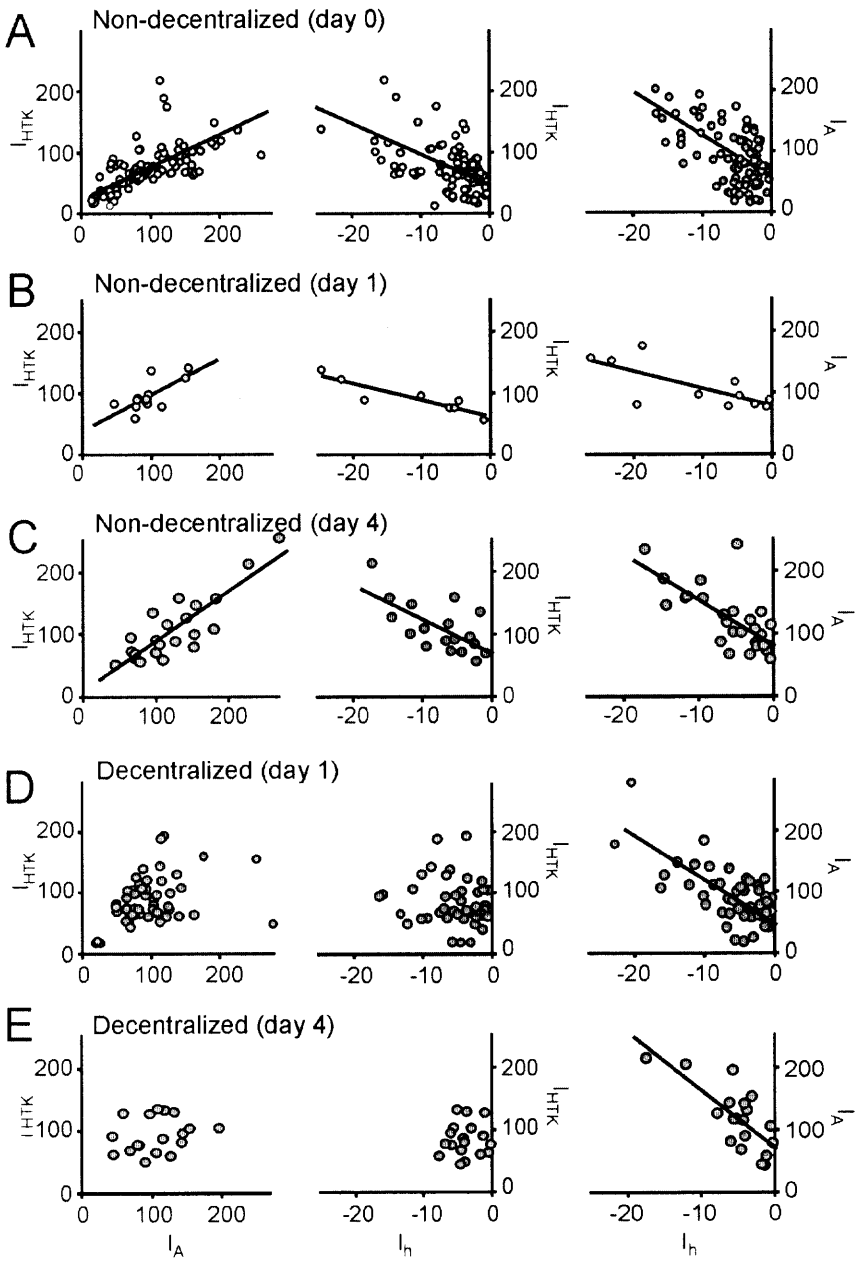

Figure 3.3 Co-regulation of voltage-gated currents depends on continuous neuromodulatory input. Each point corresponds to current densities of the two indicated currents measured in an individual PD neuron. Not all current pairs were always measured in each cell, which resulted in different sample sets for the different current pairs. A, Currents measured on day 0 before decentralization. B, Currents measured after 1 day in organ culture in non-decentralized preparations. C, Currents measured after 4 days in organ culture in non-decentralized preparations. D, Currents measured 1 day after decentralization. E, Currents measured 4 days after decentralization. Lines are the result of linear regression analysis in each case and are plotted only for cases when correlation slopes were statistically significant ($P \leq 0.05$) (R^2 and P values are reported in Table 3.2). All currents densities are expressed in nA/nF.

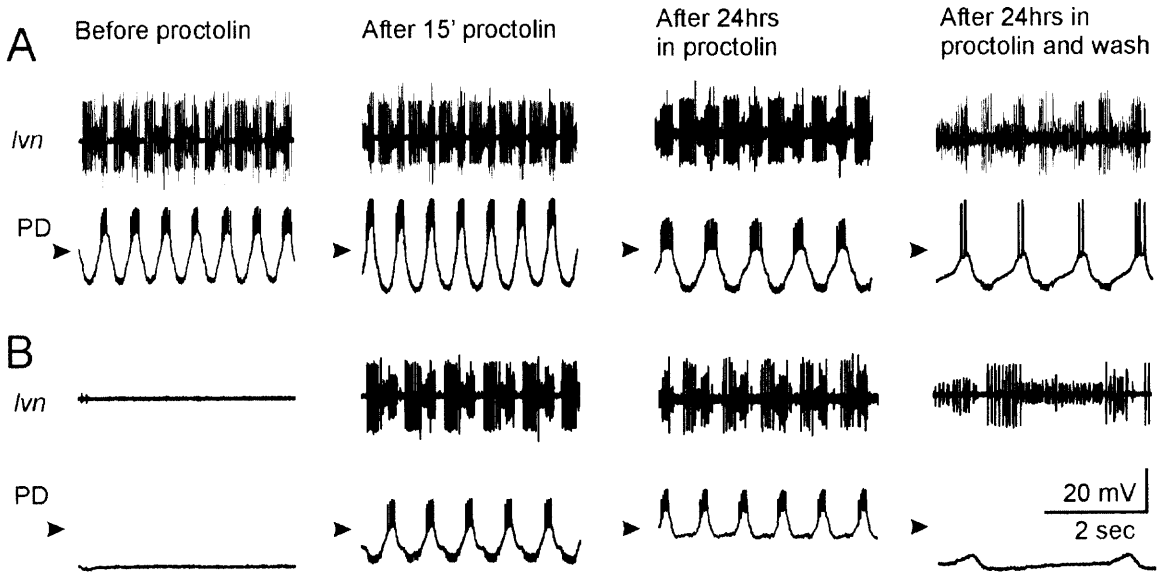

Figure 3.4 Effect of proctolin on pyloric rhythm activity. All extracellular recordings were obtained from the lateral ventricular nerve *lvn* and all intracellular recordings from a PD neuron. A, Non-decentralized preparations. B, Decentralized preparations. Cells were impaled and left to recover until all traces were stable. Recordings were obtained on day 0 before (column 1) and 15 minutes after application of 1 μM proctolin (column 2). The electrodes were removed and proctolin was left continuously in the bath for 24 hours. The PD neurons were then reimpaled and recordings were allowed to stabilize (column 3). Proctolin was then washed out for ~15 minutes before a new recording was made. Arrowheads point to –40 mV.

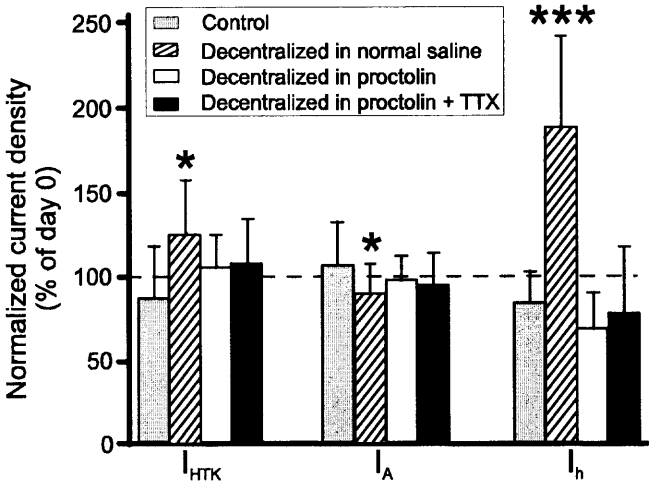

Figure 3.5 Neuromodulator prevents current density changes due to decentralization. Current densities on day 1 normalized to day 0 values are shown for I_{HTK}, I_A and I_h. Control: non-decentralized preparations. Decentralized in normal saline: preparations were decentralized on day 0 in normal saline. Decentralized in proctolin: preparations were decentralized on day 0 in bath-applied 1 μM proctolin. Decentralized in proctolin + TTX: preparations were decentralized on day 0 in bath applied 1 μM proctolin + 0.1 μM TTX. Bars represent average of at least 12 experiments ± SD. Stars indicate statistically significant changes compared to day 0 (two-way mixed design ANOVA, * $P \leq 0.05$).

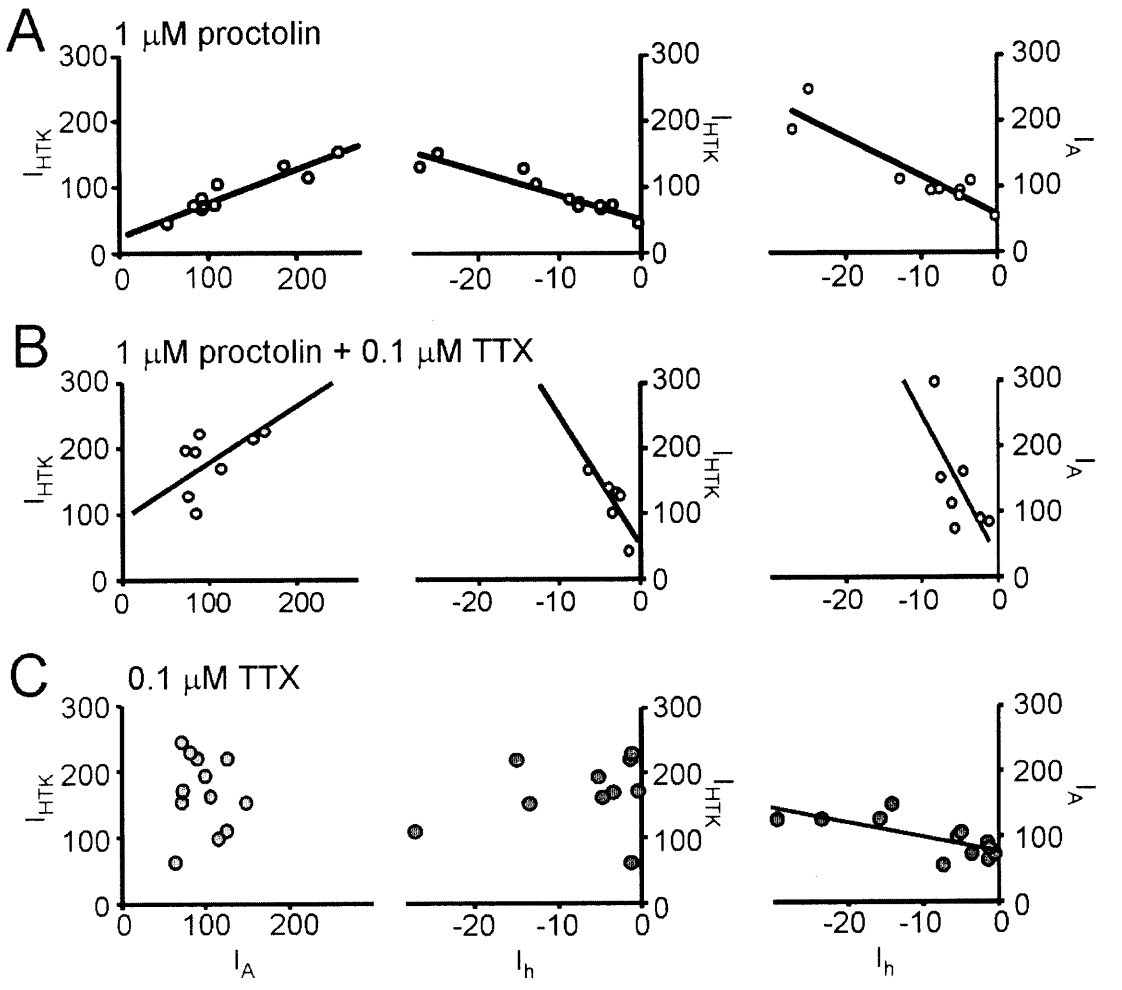

Figure 3.6 Exogenous neuromodulator bath application prevents the loss of current density co-regulation in decentralized preparations. Each point corresponds to current density values of the two indicated currents measured in an individual PD neuron. Not all current pairs were always measured in each cell, which resulted in different sample sets for the different current pairs. A, Decentralization in continuously bath applied 1 μM proctolin. B, Decentralization in continuously bath applied 1 μM proctolin + 0.1 μM TTX. C, Non-decentralized preparations in continuously bath applied 0.1 μM TTX. Proctolin and TTX bath application were maintained for 18-24 hours and measurements were made thereafter. Lines are the result of linear regression analysis in each case and are plotted only for cases when correlation slopes were statistically significant ($P \leq 0.05$) (R^2 and P values are reported in Table 3.1). All currents are expressed in nA/nF.

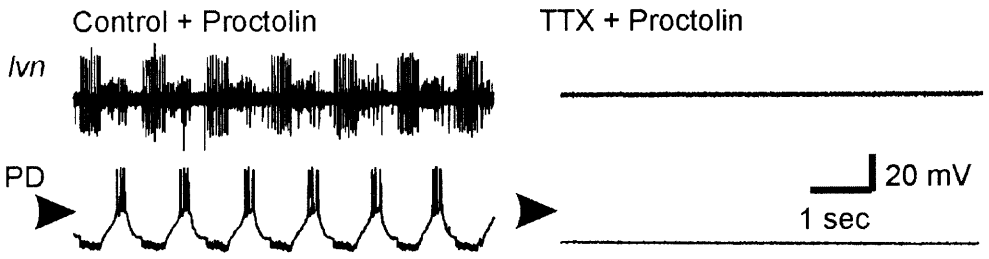

Figure 3.7 Effect of tetrodotoxin on proctolin-induced pyloric rhythm. Extracellular recordings were obtained from the lateral ventricular nerve *lvn* and intracellular recordings from a PD neuron. Left: decentralized preparation in normal saline + 1 μM proctolin (bath applied). Right: same preparation 15 min after addition of 0.1 μM TTX. Addition of TTX completely blocks all activity in the pyloric network as can be seen from the extracellular *lvn* and intracellular PD neuron recordings. Arrowheads point to –40 mV.

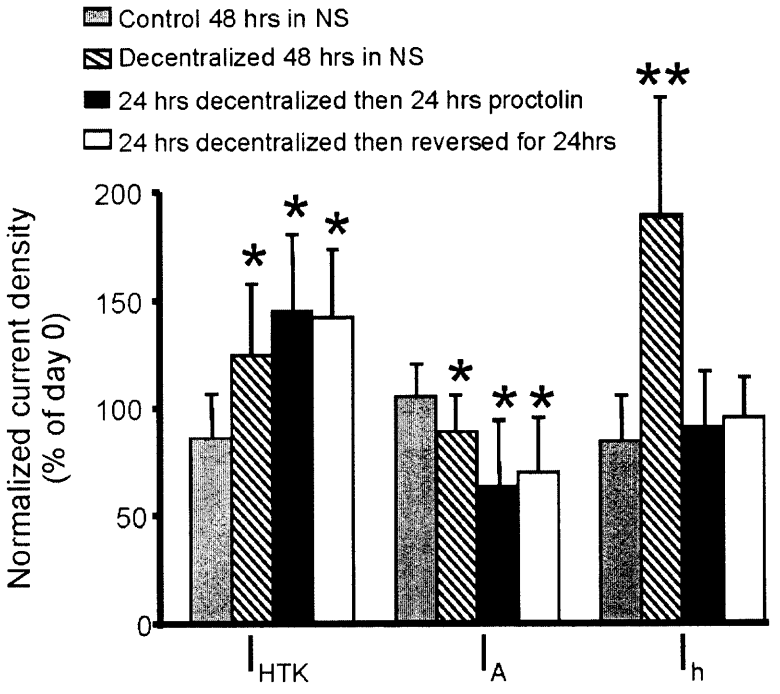

Figure 3.8 Neuromodulator applied past a critical window after decentralization does not restore control current densities. "Control 48 hrs in NS": non-decentralized preparations were kept in organ culture for 48 hours in normal saline (n = 5). "24 hrs decentralized then 24 hrs in NS": preparations were decentralized and the kept in organ culture for 24 hours in normal saline (n = 20). "24 hrs decentralized then 24 hrs proctolin": preparations were decentralized and placed in organ culture for ~24 hours. Current densities were then measured (day 1) and placed in bath applied 1 μM proctolin (n = 12). "24 hrs decentralized then reversed for 24 hrs": sucrose/TTX block of the input nerve *stn* was removed after 24 hr and the currents were measured. 18-24 hours later currents were measured again (n = 14). Bars represent current densities (± SD) normalized to day 0 using population averages. Currents were compared to levels on day 0 using a mixed design two-way ANOVA (* $P \leq 0.05$).

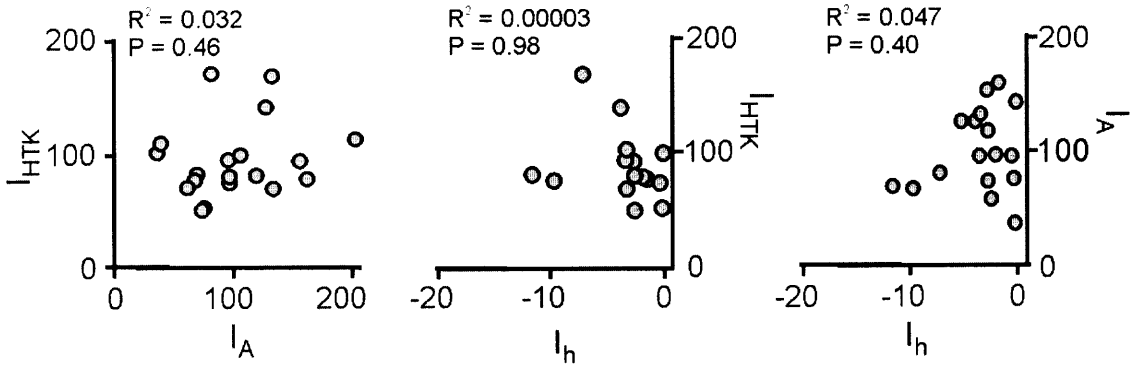

Figure 3.9 Effect of neuromodulators on the co-regulation of ionic currents after long-term decentralization. Each point corresponds to current density values of the two indicated currents measured in an individual PD neuron. Not all current pairs were always measured in each cell, which resulted in different sample sets for the different current pairs. Experiments were conducted as described in Figure 8. ANCOVA analysis of the data from the two sets of experiments showed no difference in the linear regressions and data were pooled together. Shown on each panel are coefficients of determination (R^2) and statistical significance (P) of the regression slopes. All currents are expressed in nA/nF

CHAPTER 4

COORDINATED EXPRESSION OF IONIC CURRENTS WITHIN NEURONS AND ACROSS NEURONAL TYPES IN A RHYTHM-GENERATING NETWORK

4.1 Abstract

How do rhythm-generating neuronal networks coordinate the activity of their neuronal components to produce a coherent output, especially when exposed to constantly changing environmental conditions? To address this question the pyloric network of the crab *Cancer borealis* was studied. It was found that the maximum amplitude levels of several ionic currents, namely I_{HTK}, I_A and I_h, were each coordinated (or co-regulated) between the two PD cells of the pyloric network. I_{HTK} and I_A, but not I_h, were also coordinated between two different neuronal types (PD and LP neurons) in the pyloric network. The INTER-cellular PD to LP neuron co-regulations of I_{HTK} and I_A, were disrupted if the preparations were treated with picrotoxin (PTX), a chloride channel blocker that abolishes cell to cell communication through glutamatergic synapses. Experimental blockade of the central neuromodulatory input (decentralization), which normally includes GABA, and treatment with 3MPA, an inhibitor of GABA synthesis, did not significantly affect the INTER-cellular I_{HTK} and I_A co-regulation. However, both of these treatments reversed the I_h co-regulation between the two PD neurons, which became disrupted or reversed, and between the PD and LP neurons, which became established. Neither PTX, nor 3MPA treatment affected the intracellular co-regulation of I_{HTK}/I_A, I_{HTK}/I_h and I_A/I_h current pairs, while decentralization abolished co-regulation of distinct current pairs in different cell types. These results indicate that the glutamatergic

feedback synapses from the LP neuron to the two PD cells were necessary to maintain the coordinated expression of HTK and I_A currents both between LP and PD and, either the glutamatergic feedback synapse from the LP neuron to the two PD cells and/or strong gap junction connections between the two PD neurons were required to maintain co-regulation of I_{HTK} and I_A between the two PD neurons. Coordination in I_h between the neurons was determined by GABA signaling and was not as crucial for the maintenance of regular pyloric output as the coordination in I_A or I_{HTK}. These results indicate that INTER- and intracellular current coordinations are maintained by different mechanisms.

4.2 Introduction

Rhythmic pattern-generating neuronal networks are widely represented in the animal kingdom, controlling the function of many vital organs, such as heart, lungs, digestive system, etc. The rhythmic output of these networks depends on the coordinated activity of the multiple neurons comprising the networks. Does interneuronal coordination in the network extend to the level of ionic currents that determine the neuronal activity and thus the network output?

Multiple pieces of evidence suggested that interneuronal current coordination might exist. It has been shown extensively in biological and model neuronal networks that the expression of ionic channels is regulated by a feedback loop in which neuronal activity regulates synaptic strength and expression of ionic currents. Changes in synaptic strength and ionic current levels can, in turn, affect neuronal activity levels (Turrigiano et al. 1995, LeMasson et al. 1993, Franklin et al. 1992, Fengler and Lnenicka 2001, Haedo and Golowasch 2006, Ueda and Wu 2006, Wierenga et al. 2005). Modification of cellular

or synaptic properties of any of the network neurons, not only of the pacemakers, has been shown to disrupt the output of the whole network (DiCaprio and Fourtner 1984, Ramirez and Pearson 1990, Marder et al. 2005a, Weaver and Hooper 2003). Given such highly developed cross-neuronal regulation in rhythm generating networks, and given the existence of co-regulation between ionic currents within one neuron, it is reasonable to expect that ionic current levels might be coordinated between the network neurons.

In fact, it has been shown that copy numbers of mRNAs for two ionic channels (IH, the channel carrying hyperpolarization-activated current (I_h) and shal, the channel carrying the fast transient potassium current, I_A) are closely correlated between the two PD neurons in the *C. borealis* pyloric network of an animal despite the high variability of copy numbers of these mRNAs between animals (Schulz et al 2006). In several instances it has also been shown that mRNA levels could correlate with the expressed channel conductance (Schulz et al. 2006, Baro et al. 1997, MacLean et al. 2005, Zhang et al 2003). However, coordination of ionic currents between different neurons, particularly between different cell types, has not been directly shown before.

If interneuronal current coordination exists, what does it depend on? I_h levels were significantly different between the two PD neurons when one of them did and the other did not receive *PAIH* RNA microinjection even after 5 days in culture (Zhang et al 2003). This brings up the possibility that current expression levels in each neuron could be pre-set in the course of development and do not respond to the dynamics of the environment and cell to cell communications in the network. On the other hand, modeling studies of the pyloric circuit indicate that establishing or destroying synaptic connections ultimately leads to changes in ionic current levels (Golowasch et al. 1999b)

This question was addressed in this dissertation by determining the status of INTER-cellular current coordination before and after changes in cell to cell communication, and before and after changes in the neuromodulator environment of the neurons.

Previously it has been shown that I_A/I_h pair at the RNA level (Schulz et al. 2006) and I_A/I_h, I_{HTK}/I_A and I_{HTK}/I_h current pairs at the current level (Khorkova and Golowasch 2007) are co-regulated in individual identified PD cells. If current expression is also coordinated between cells, are these two types of coordination regulated by similar mechanisms?

Here it is shown that the densities of several currents in the pyloric network are coordinated, in particular I_{HTK}, I_A and I_h are all correlated between the two PD neurons, while I_{HTK} and I_A, but not I_h, are correlated between LP and PD neurons. At the same time I_{HTK}/I_A, I_{HTK}/I_h, and I_A/I_h pairs are correlated within LP neurons. To further investigate the molecular mechanisms underlying the INTER-cellular current coordination, the role of the glutamatergic synaptic connections between the network neurons was studied in preparations treated with picrotoxin (PTX). Since PTX is also known to inhibit GABA responses the effects of GABA were tested by pharmacologically depleting GABA-releasing neurons of their GABA content. To determine if the central neuromodulator supply that is normally essential for pyloric rhythm generation plays a role in the INTER-cellular current coordination currents were studied in a pyloric network with neuromodulator supply blocked. Intracellular current co-regulation during all these treatments were monitored to establish if intra- and INTER-cellular current coordination involved shared mechanisms.

4.3 Results

4.3.1 Pyloric Network of the Crustacean STNS as an Experimental Model

To study the INTER-cellular coordination of ionic currents in a rhythm generating network the PD and LP neurons of the pyloric network of the Jonah crab (*Cancer borealis*) were used. As shown in chapter 3, when the STG is dissected together with the commissural (CoG) and oesophageal ganglia (OG) as shown in Figure 1.1A, the pyloric network retains its normal activity (shown with intracellular recordings from the LP (left) and the PD neuron (right) in Figure 4.1 Control) for up to 10 days in organ culture. In the pyloric network the two PD neurons and the network's pacemaker anterior burster (AB) neuron are electrically coupled to form a pacemaker kernel (Figure 1.1B). The activity of the follower LP neuron is driven by the AB neuron of the pacemaker kernel through a glutamatergic inhibitory synapse, and the LP neuron is the only follower neuron that provides feedback to the pacemaker kernel, in particular to the kernel's PD neurons, also through a glutamatergic synapse. The cholinergic PD to LP synapse is not sufficient to induce rhythmic firing in LP neurons (Miller and Selverston 1982, Eisen and Marder 1982).

In the intact preparations pyloric activity is dependent on central neuromodulatory input comprising more than 20 known components (Kushner and Maynard 1977, Belz et al. 1984, Nusbaum and Marder 1989a, b, Li et al. 2003). GABA was found to be one of them (Nusbaum et al. 1989, Swensen et al. 2000, Cournil et al. 1990). STG neurons do not produce GABA on their own (Ducret et al. 2007, Swensen et al. 2000).

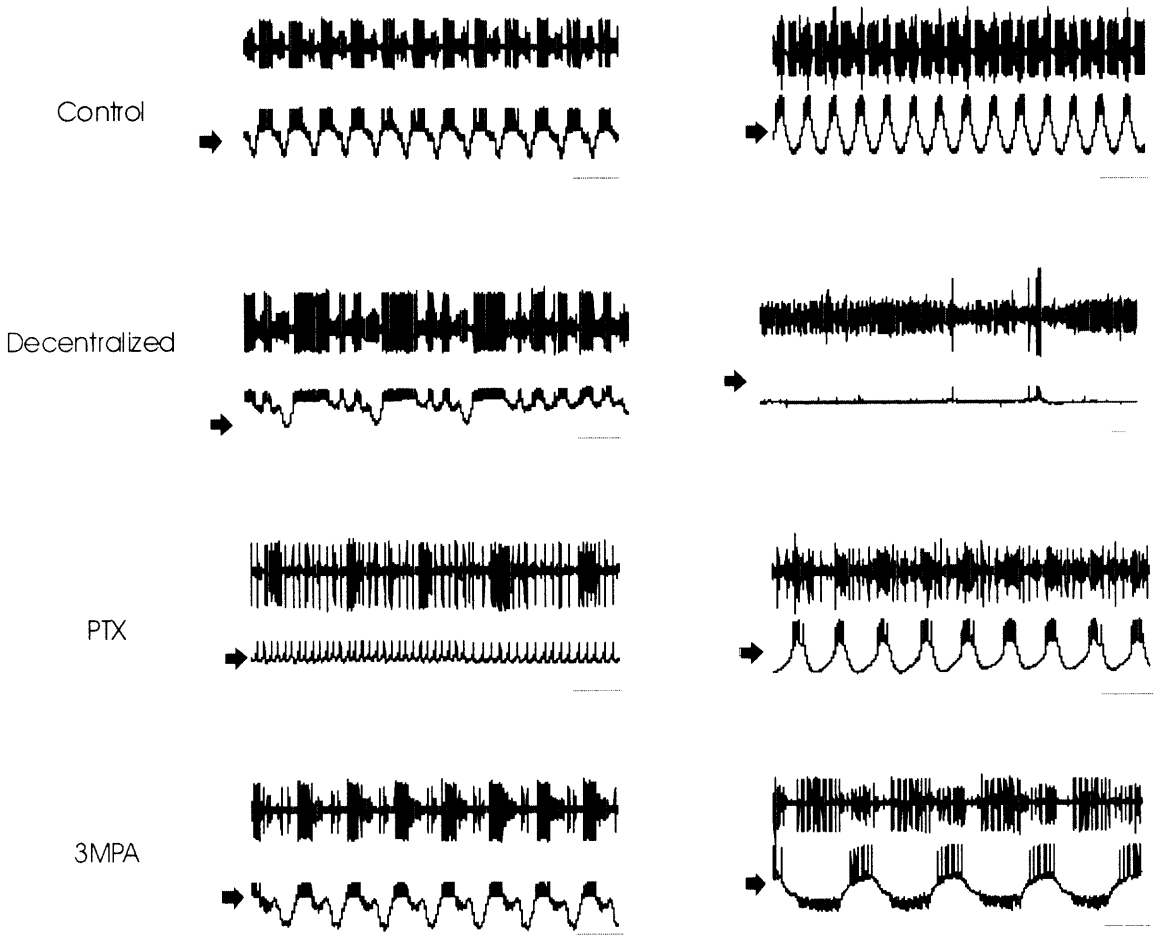

Figure 4.1 Changes in pyloric activity observed in decentralized, PTX-treated and 3MPA-treated preparations after 24 h in culture. Top traces for each condition represent lvn recordings, bottom traces represent intracellular LP recordings in the left column, and PD recordings in the right column. In control extracellular traces, action potentials with the largest amplitude are generated by LP, with medium amplitude by PD, and the smallest amplitude by pyloric constrictor neurons (PY). Twenty four hours after decentralization pyloric activity was unstable, with periods of complete silence, irregular pyloric rhythm (shown here in Decentralized) and bouts of regular pyloric activity of different duration. PTX treatment evoked tonic firing in LP and eliminated inhibitory postsynaptic potentials in PDs, but the rhythmic bursting of PDs was not affected. 3MPA did not cause significant qualitative changes in pyloric activity. Scale bars: horizontal 1 s, vertical 40 mV. Black arrows correspond to -40 mV.

This study concentrated on the currents that were previously shown to be expressed in pairwise coordination in PD neurons, namely I_{HTK}, I_A and I_h (Chapter 3). These currents can be measured in normal saline, thus excluding the possibility that the chemicals used to isolate the currents are affecting the coordination process. Examples of raw traces and current/voltage (I-V) plots for the ionic currents in LP cells are shown in Figure 4.2 (see Chapter 3, Figure 3.2, for examples of raw traces and I-V plots for PD cells).

As a first step the INTER-cellular current coordinations between the two PD and between PD and LP cells of the pyloric network were investigated.

4.3.2 Current Levels in the Two PD Neurons Are Closely Coordinated

In this dissertation it was found that in the intact STG preparations I_{HTK}, I_A and I_h were closely correlated between the two PD neurons (Figure 4.3, Table 4.1). The overall current levels were very similar between these two neurons (currents in PD_2 neurons, as % of currents in PD_1 neurons, both on day 0 in culture, were: $I_{HTK} = 109 \pm 45$, $I_A = 114 \pm 36$, $I_h = 134 \pm 110$, or in absolute levels (nA/nF), $I_{HTK\text{-}PD1} = 89 \pm 43$, $I_{HTK\text{-}PD2} = 88 \pm 39$, $I_{A\text{-}PD1} = 94 \pm 42$, $I_{A\text{-}PD2} = 101 \pm 43$, $I_{h\text{-}PD1} = -9 \pm 7$, $I_{h\text{-}PD2} = -9 \pm 6.6$, all paired t-test $p > 0.05$, $n = 57$). The first cell impaled during the experiment was referred to as PD_1 neuron, and the second as PD_2 neuron. Similar results were seen if each PD cell was randomly distributed between groups 1 and 2. To achieve this, each PD cell pair (two PD neurons from one ganglion) was assigned a random number. The list of all pairs was then sorted in ascending order and divided in half, then the order of PD cells in the second half was inverted. The results obtained from randomized pairs were as follows: currents in PD

neurons from group 2, as % of currents in PD neurons from group 1 were: I_{HTK} = 107 ± 40, I_A = 109 ± 36, I_h = 158 ± 260, or in absolute levels (nA/nF), $I_{HTK\text{-}PD1}$ = 88 ± 41, $I_{HTK\text{-}PD2}$ = 89 ± 40, $I_{A\text{-}PD1}$ = 97 ± 45, I_{APD2} = 98 ± 40, $I_{h\text{-}PD1}$ = −9 ± 7.6, $I_{h\text{-}PD2}$ = −8 ± 5.8, all paired t-test $p > 0.05$. Randomization did not significantly affect the INTER-cellular current correlations reported in Table 4.1.

Current density correlations for the two PD cells were completely preserved in control preparations after 24 hr in culture (Table 4.1), and current levels between PD_1 neurons and PD_2 neurons at that time remained close (currents in PD_2 neurons, as % of currents in PD_1 neurons after 24 h in culture, were: I_{HTK} = 102 ± 24, I_A = 92 ± 55, I_h = 150 ± 124, or in absolute levels (nA/nF), $I_{HTK\text{-}PD1}$ = 86 ± 28, $I_{HTK\text{-}PD2}$ = 85 ± 27, $I_{A\text{-}PD1}$ = 144 ± 83, $I_{A\text{-}PD2}$ = 99 ± 24, $I_{h\text{-}PD1}$ = −10 ± 8, $I_{h\text{-}PD2}$ = −14 ± 10, all paired t-test $p > 0.05$, n = 11).

Figure 4.2 (next page) Decentralization evokes complementary changes in PD and LP current densities. Currents are (from top to bottom) I_h, I_A, I_{Ba}, I_{HTK}(steady state) and I_{Kd}. *First column*, Examples of raw current traces from LP neurons. *Second column*, Examples of current-voltage plots in LP neurons (see Figure 3.2 for raw data and I-V plots of PD neurons). I_{HTK} measured at steady state. Open symbols/dotted lines are currents measured before decentralization. Solid symbols/lines are currents measured in the same cell 24 h after decentralizaton. *Third column*, Time course of current density changes in non-decentralized preparations. LP, solid symbols/lines; PD, open symbols/dotted lines. *Fourth column*, Time course of current density changes in decentralized preparations. LP, solid symbols/lines; PD, open symbols/dotted lines. Current densities are normalized to values measured in the same cell on day 0; no cell was impaled more than twice. Stars indicate results of the comparison of current densities between decentralized and non-decentralized preparations at the same day in the same cell type using two-way mixed design ANOVA and post-hoc Tukey tests (*$p<0.05$, **$p<0.01$, ***$p<0.001$). Comparisons for non-decentralized preparations at different times to the same cell type at day 0 are discussed in Results. The number of experiments is shown next to each point.

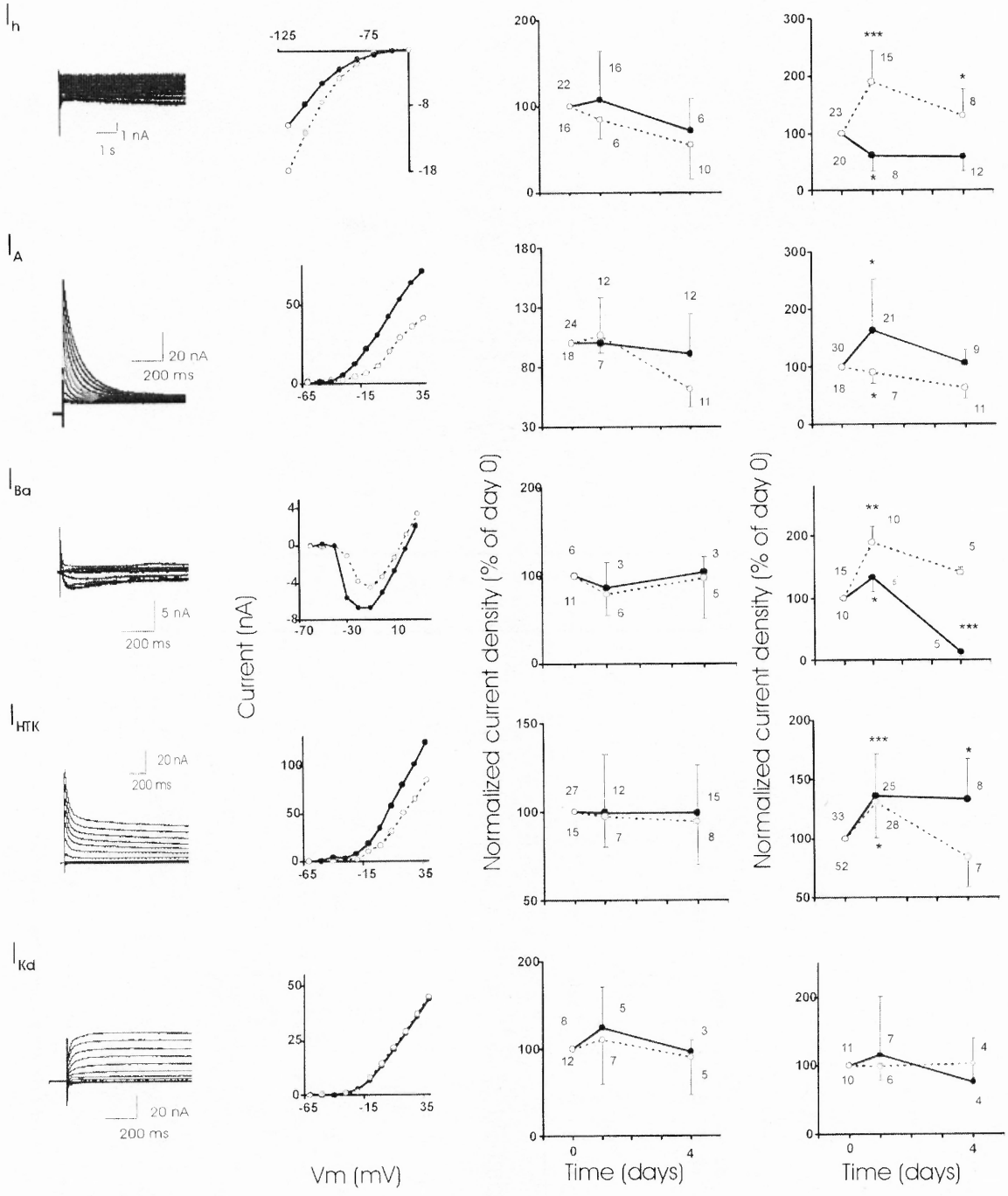

Figure 4.2 (continued)

4.3.3 I_A and I_{HTK}, but not I_h Levels Are Coordinated between LP and PD Neurons

Under normal physiological conditions I_A densities in LP and PD cells from the same ganglion were correlated, and I_{HTK} densities showed a linear correlation after a log/log transformation, which indicates that I_{HTK} densities in these two cells are coordinately changing according to the relation $I_{HTK\text{-}PD}=10^{(0.6443*\log I_{HTK\_LP}+0.6052)}$ (Figure 4.4, Table 4.2). Although there was no discernible correlation between PD and LP neurons in I_h current, the shape of the distribution suggested that extremely high I_h levels in PD corresponded to low current density values in LP, and vice versa (Figure 4.4).

As shown in Figure 4.5, while I_{HTK} and I_A currents were coordinated between PD and LP neurons, the average current density levels in each cell type were significantly different (LP currents, as % of PD currents in the same ganglion on day 0 in culture were: I_{HTK} = 143 ± 78, n = 78, I_A = 77 ± 37, n = 62, I_h = 134 ± 244, n = 55; or in absolute levels (nA/nF), $I_{HTK\text{-}PD}$ = 88 ± 48, $I_{HTK\text{-}LP}$ = 110 ± 55, p = 0.001; $I_{A\text{-}PD}$ = 91 ± 46, $I_{A\text{-}LP}$ = 63 ± 30, p < 0.001; $I_{h\text{-}PD}$ = −10 ± 9, $I_{h\text{-}LP}$ = −6 ± 4, p = 0.005; if measurements from both PDs were available for a ganglion, they were averaged; all p are from paired t-tests).

An approximately 2:1 ratio between I_{KCa} (the major component of I_{HTK}) and I_A conductances, close to the one observed in this dissertation, was reported in LP cells (Golowasch and Marder 1992a). mRNA levels for *Shal* (that codes for I_A) were also higher in PD neurons compared to LP neurons and correlated with I_A conductance levels in LP neurons in crab (Schulz et al. 2006) and lobster (Baro et al. 1997). Marder et al. (2005b) have shown significantly higher levels of the mRNA coding for I_{KCa} (*BK-KCa*; approximately 400% higher) and lower levels of *Shal* (about 50% lower) in LP cells compared to PD cells, with a similar 3-4 fold animal to animal variation within the cell

types. *Shab* mRNA levels (that codes for I_{Kd}), in contrast, did not correlate with I_{Kd} levels (Schulz et al. 2006). While Schulz et al. (2006) show that in crab shab mRNA levels were higher in LP neurons compared to PD neurons, in our experiments there was no significant difference between the two cells in I_{Kd} levels. These data indicate that differences in current levels between PD and LP cells are very stable and reproducible in preparations of different origin and that the current ratios between cells may be coordinated at the RNA level.

In single neurons of each type (PD and LP neurons) I_{HTK}/I_A, I_{HTK}/I_h and I_A/I_h current pairs were correlated at day 0 in culture and 24 h later (Figure 4.6 and Table 4.3 for the LP neuron and Figure 4.7 , Table 4.4 for the PD neuron).

4.3.4 LP and PD Exhibit Complementary Current Level Changes after Decentralization

Previously in this dissertation it was shown that neuromodulatory input plays a significant role in maintaining intracellular current correlations (Chapter 3). To study the effects of neuromodulators on the INTER-cellular current coordination, and to determine the relationship between current coordination and pyloric activity, current coordination in decentralized preparations were studied.

In decentralization experiments STG was disconnected from the CoGs and OG by stn transection (decentralized), which caused the normal activity of the pyloric network to temporarily stop. This interruption was caused by the cessation of neuromodulator release from the axonal termini of the CoG and OG neurons. After 24 to 50 h of irregular and/or intermittent pyloric activity (so called 'bouting period', Figure 5.1), the regular pyloric activity resumed.

It was shown previously in this dissertation that in PD neurons density levels of several currents dramatically changed 24 h after decentralization, the timeframe that corresponded to the significant interruptions and bouting activity in the pyloric activity (Chapter 3). By day 4 in culture when the regular pyloric activity had resumed, most PD neuron current levels had returned to control.

Current density changes in LP neurons followed the same overall temporal pattern, but the direction of change in each current was different and somewhat complementary to the alterations observed in PD neurons (Figure 4.2). In particular, in PD neurons 24 h after decentralization, the I_h levels were increased, while I_A levels were decreased ($p<0.001$ for I_h, $p<0.05$ for I_A; two-way mixed design ANOVA with post-hoc Tukey tests was used in all LP and PD current level comparisons shown below). In LP cells at 24 h after decentralization, I_h current density was decreased, while I_A density was elevated relative to control levels ($p<0.05$ for I_h and $I_{A)}$. By day 4 after decentralization I_h levels in PD neurons remained elevated ($p<0.05$, Figure 4.2), while in LP neurons they increased back to control levels ($p>0.05$, Figure 4.2). I_A levels returned to control by day 4 in both cell types ($p>0.05$ for both). I_{HTK} and I_{Ba} levels were elevated in both cell types at 24 h after decentralization (for PD, $p<0.05$ and $p<0.01$ respectively; for LP, $p<0.001$ and $p<0.05$ respectively). However, by day 4, I_{Ba} level in PD neurons returned to control ($p>0.05$, Figure 4.2) and in LP neurons it dropped below control levels ($p<0.001$, Figure 4.2). I_{HTK} levels in PD neurons by day 4, in contrast, were indistinguishable from controls ($p>0.05$), while in LP neurons I_{HTK} levels remained elevated at that time ($p<0.05$, Figure 4.2). There was no change in I_{Kd} levels in either cell type at any time studied ($p>0.05$ for both cell types, Figure 4.2).

There were also complementary differences in the changes of intracellular current correlation status in LP and PD neurons 24 h after decentralization (Figure 4.6 and Table 4.3 for LP neurons, Figure 4.7 and Table 4.4 for PD neurons). While in PD neurons correlation between I_{HTK}/I_A and I_{HTK}/I_h current pairs disappeared after decentralization, and the I_A/I_h pair correlation was preserved, in LP cells the opposite took place: I_{HTK}/I_A correlation was preserved, while I_{HTK}/I_h and I_A/I_h correlations disappeared.

In the non-decentralized (control) preparations kept in culture for 4 days there were no statistically significant differences in the levels of any of the LP neuron currents when compared to day 0 in the same cell (all $p>0.05$), while in PD neurons, I_h and I_A levels significantly decreased by day 4 ($p<0.05$ for both currents, Figure 4.2).

This data indicate that significant and complementary changes in current levels and intracellular current coordinations occur in both PD and LP cells after decentralization and at the time of irregular pyloric activity (bouting). Does decentralization lead to changes in the INTER-cellular coordination of current levels reported in 4.3.2 and 4.3.3?

4.3.5 Disruption of Neuromodulator Supply Correlates with Changes in INTER-Cellular Coordination of I_h

The INTER-cellular coordination of currents 24 h after cessation of the neuromodulator supply caused by decentralization was examined (Figure 4.3, 4.4, Table 4.1, 4.2). At that time coordination in I_h between the two PD cells had disappeared, while I_{HTK} and I_A correlations were unchanged (Figure 4.3, Table 4.1). Overall current levels however remained similar in both PDs (currents in PD_2 cells, as % of currents in PD_1 cells, both measured 24 h after decentralization, were: $I_{HTK} = 98 \pm 30$, $I_A = 120 \pm 48$, $I_h = 97 \pm 123$,

or in absolute levels (nA/nF), $I_{HTK\text{-}PD1} = 92 \pm 36$, $I_{HTK\text{-}PD2} = 89 \pm 37$, $I_{A\text{-}PD1} = 90 \pm 43$, $I_{A\text{-}PD2} = 93 \pm 36$, $I_{h\text{-}PD1} = -9 \pm 11$, $I_{h\text{-}PD2} = -7 \pm 10$, all paired t-test $p > 0.05$, n = 15). Similar effects on PD/PD current coordinations were observed when preparations were treated with TTX for 24 h (Table 4.1).

I_h coordination status between PD and LP cells was also altered 24 h after cessation of the neuromodulator supply (Figure 4.4, Table 4.2). While I_h was not coordinated in control preparations, after decentralization its coordination status was changed and showed a strong correlation. Decentralization did not affect I_{HTK} and I_A current correlations between LP and PD neurons (Figure 4.4, Table 4.2).

The differences in I_A and I_{HTK} levels between the two cell types were maintained, but the significant difference in I_h current levels between PD and LP neurons disappeared after decentralization (LP neuron currents, as % of PD neuron currents in the same ganglion, 24 h after decentralization: $I_{HTK} = 145 \pm 52$, n = 23, $I_A = 84 \pm 57$, n = 22, $I_h = 168 \pm 196$, n = 20; or in absolute levels (nA/nF), $I_{HTK\text{-}PD} = 90 \pm 45$, $I_{HTK\text{-}LP} = 118 \pm 46$, $p = 0.0003$, $I_{A\text{-}PD} = 100 \pm 50$, $I_{A\text{-}LP} = 71 \pm 31$, $p = 0.0007$, $I_{h\text{-}PD} = -5 \pm 5$, $I_{h\text{-}LP} = -3.7 \pm 3.7$, $p = 0.5$; if measurements from both PD neurons were available for a ganglion, they were averaged; all p are from paired t-tests).

4.3.6 I_{HTK} and I_A, but not I_h, Coordination between Neurons is PTX-Sensitive

To determine if INTER-cellular communications are important in maintaining current coordination between cells, non-decentralized STG preparations were treated with picrotoxin (PTX) for 24 h. PTX blocks the conduction of a glutamate-activated chloride channel, thus effectively stopping glutamate-driven inhibitory connections between the pacemaker AB neuron and the follower LP neuron, and preventing the feedback from the

LP cell to the PD neurons of the pacemaker kernel. Due to the loss of the rhythm-generating input from AB neurons, after PTX treatment, LP neurons exhibited a 'decentralized'-type, irregular activity, while the pacemaker PD neurons continued their rhythmic bursting, although at a slower pace (Figure 4.1). Current levels in LP and the two PD cells in each ganglion before and 24 h after the beginning of PTX application were measured.

INTER-cellular correlations of currents were significantly affected after the 24 h incubation in PTX (Figure 4.3, 4.4, Table 4.1, 4.2). I_{HTK} and I_A correlations between the two PD cells disappeared, while I_h correlations were preserved (Figure 4.3, Table 4.1). Overall current levels in the two PD cells however remained similar (currents in PD_2 neurons, as % of currents in PD_1 neurons, after 24 in PTX, were: I_{HTK} = 111 ± 72, I_A = 115 ± 55, I_h = 90 ± 53, or in absolute levels (nA/nF), $I_{HTK\text{-}PD1}$ = 128 ± 77, $I_{HTK\text{-}PD2}$ = 112 ± 56, $I_{A\text{-}PD1}$ = 104 ± 80, $I_{A\text{-}PD2}$ = 89 ± 37, $I_{h\text{-}PD1}$ = −12 ± 10, $I_{h\text{-}PD2}$ = −7 ± 5, all paired t-test $p > 0.05$, n = 15).

Figure 4.3 (next page) Current densities are coordinated between the two PD neurons. Control preparations. Density levels of the three currents were closely correlated in control preparations. Decentralized preparations. Decentralization disturbed coordination of Ih between the two PDs, leaving I_{HTK} and I_A coordinations intact. PTX-treated preparations. Treatment with PTX eliminated coordination between I_{HTK} and I_A currents, leaving I_h coordination intact. 3MPA-treated preparations. Treatment with 3MPA disturbed coordination of I_h, leaving I_{HTK} and I_A coordinations intact. Each point corresponds to current density (in nA/nF) measured separately in each of the PD cells from the same ganglion on day 0 in culture for control preparations and 24 h after the beginning of each treatment for the treated preparations. Current coordinations in control preparations after 24 h in culture did not differ from those seen on day 0 (Table 4.1). Not all currents were always measured in each ganglion, which resulted in different sample sets for each current. Left panels, I_{HTK}. Center panels, I_A. Right panels, I_h. *R*, R^2, and *p* values for the regressions and the numbers of experiments for each treatment condition are listed in Table 4.1

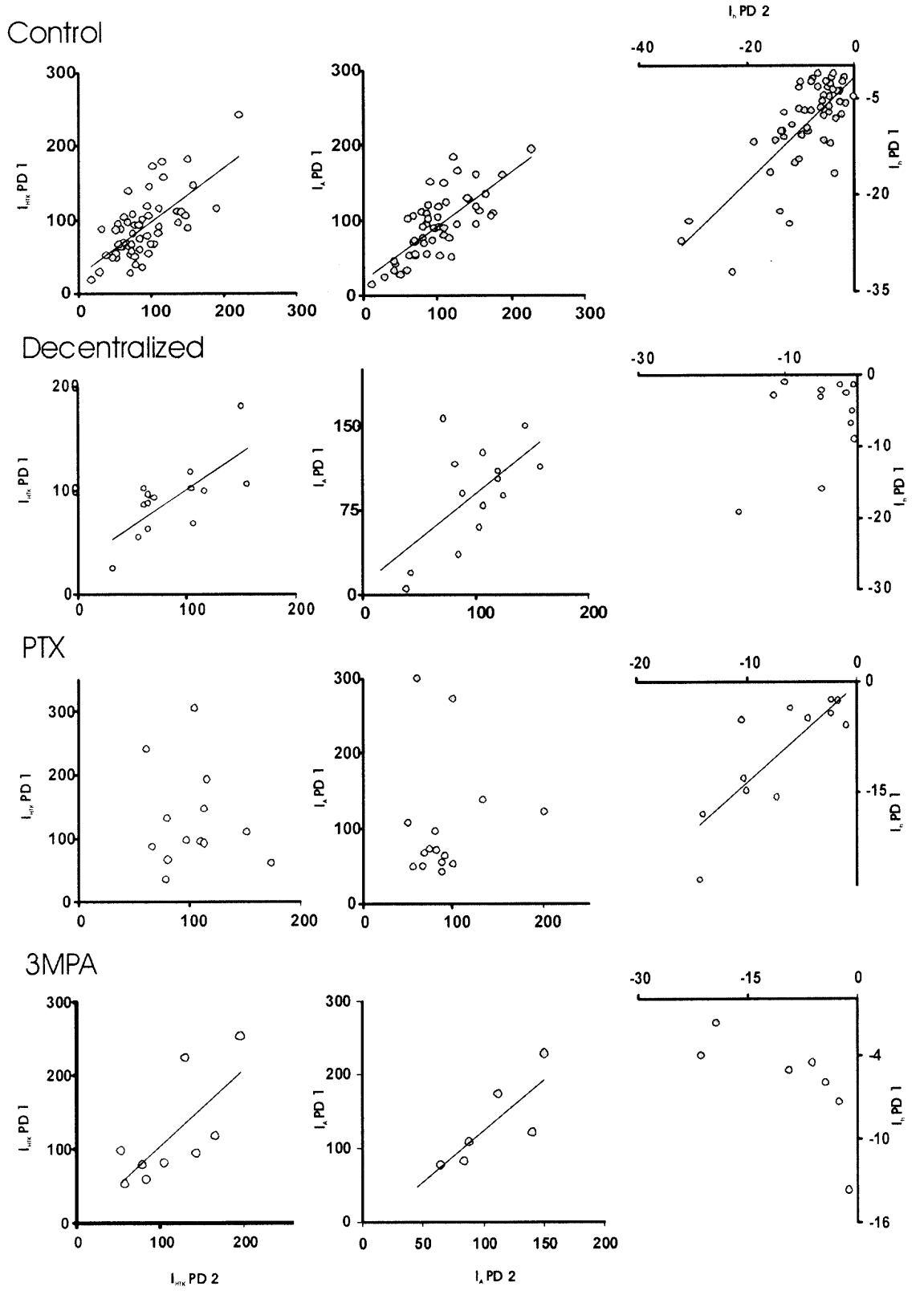

Figure 4.7 (continued)

I_{HTK} and I_A correlations between PD and LP cells also disappeared after PTX treatment (Figure 4.4, Table 4.2) and the normally pronounced differences in current levels of the two neuronal types (Figure 4.4) became statistically not significant (LP neuron currents, as % of PD neuron currents in the same ganglion after 24 h incubation in PTX: I_{HTK} = 143 ± 97, n = 15, I_A = 80 ± 52, n = 15, I_h = 184 ± 178, n = 15; or in absolute levels (nA/nF), $I_{HTK\text{-}PD}$ = 141 ± 82, $I_{HTK\text{-}LP}$ = 154 ± 96, p = 0.65, $I_{A\text{-}PD}$ = 116 ± 86, $I_{A\ LP}$ = 65 ± 27, p = 0.06, $I_{h\text{-}PD}$ = −12 ± 19, $I_{h\text{-}LP}$ = −15 ± 16, p = 0.63; if measurements from both PD neurons were available for a ganglion, they were averaged; all p are from paired t-tests).

Figure 4.4 (next page) Current densities are coordinated between PD and LP neurons. Control preparations. Density levels of I_A and logI_{HTK}, but not I_h were correlated in control preparations. Decentralized preparations. Decentralization reversed the coordination status of I_h, inducing coordination of this current between PD and LP neurons, while leaving i_{HTK} and I_A coordinations intact. PTX-treated preparations. Treatment with PTX eliminated coordination between I_{HTK} and I_A currents, leaving I_h coordination status unchanged. 3MPA-treated preparations. Treatment with 3MPA reversed the coordination status of I_h, inducing coordination of this current between PD and LP neurons, while leaving I_{HTK} and I_A coordinations intact. Each point corresponds to current density (in nA/nF) measured in PD and LP cells from the same ganglion on day 0 in culture for control preparations and 24 h after the beginning of each treatment for the treated preparations. Current coordinations in control preparations after 24 h in culture did not differ from those seen on day 0 (Table 4.2). If measurements for the two PD cells were available for a given ganglion they were averaged. Not all currents were always measured in each ganglion, which resulted in different sample sets for each current. Left panel, I_{HTK}. Center panel, I_A. Right panel, I_h. R, R^2, and p values for the regressions and the numbers of experiments for each treatment condition are listed in Table 4.2.

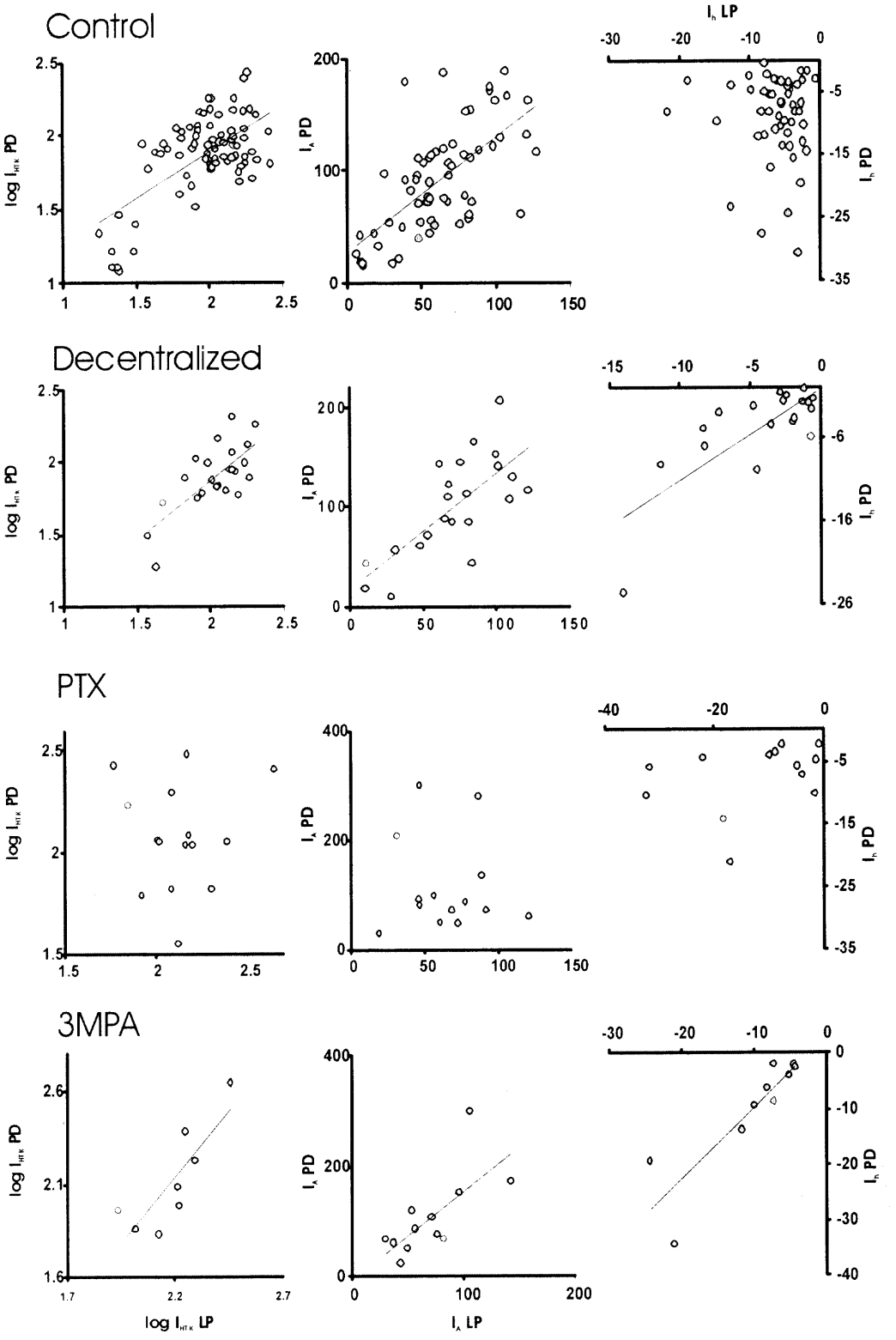

Figure 4.4 (continued)

4.3.7 PTX-Sensitive Chloride Channel Is Involved in Setting Current Levels of STG Neurons

In addition to the effects of glutamate synaptic block on the INTER-cellular coordination of ionic currents, a 24 h incubation in PTX caused significant changes in the current density levels of both LP and PD cell types compared to day 0 levels (currents after 24 h in PTX, as % of currents in the same cell on day 0, were, in PD neurons: I_{HTK} = 128 ± 41, p = 0.005, I_A = 87 ± 30, p = 0.02, I_h = 209 ± 214, p = 0.02, n = 28 and in LP: I_{HTK} = 127 ± 30, p = 0.05, I_A = 131 ± 43, p = 0.04, I_h = 54 ± 37, p = 0.05, n = 28; all p are from paired t-tests). The changes in current levels after incubation in PTX resembled changes observed 24 h after decentralization in both PD and LP (Figure 4.3 and Chapter 3).

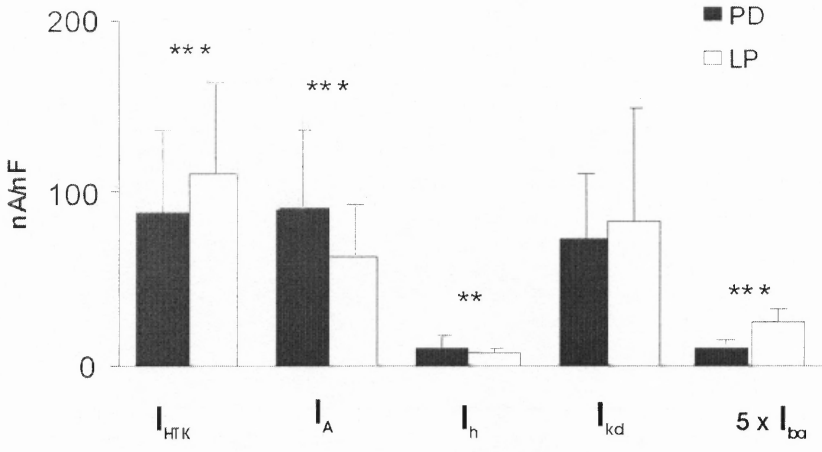

Figure 4.5 Average current density levels in LP and PD neurons from the same ganglion in control conditions. Black bars, PD currents. Open bars, LP currents. Error bars represent standard deviation. Stars represent the results of paired t-tests comparisons of the two cell types, **p<0.01, ***p<0.001.

In contrast to decentralization, PTX incubation did not affect intracellular current correlations in either cell (Figure 4.6, 4.7, Table 4.3, 4.4). This indicates that, as opposed to the current levels, the intracellular current correlations do not depend on the activity of

the PTX-sensitive channel, but are likely maintained by central neuromodulators and thus disappear only after decentralization, but not after PTX treatment.

PTX did not regulate the current levels acutely (currents after 15 min in PTX, as % of currents in normal saline in the same cell, were: I_{HTK} = 101 ± 29, I_A = 94 ± 14, I_h = 121 ± 70, all paired t-test $p > 0.05$, n = 8). Short incubations in PTX did not affect intracellular current correlations (Table 4.3, 4.4).

Effects of PTX completely disappeared after 24 h wash in NS (after-wash currents, as % of currents in the same cell on day 0, were: I_{HTK} = 123 ± 73, I_A = 111 ± 38, I_h = 96 ± 81, all paired t-test $p > 0.05$, n = 9). Intracellular current correlations were preserved after the wash (Table 4.4).

Figure 4.6 (next page) Intracellular current density correlations in LP neurons are altered by decentralization, but not by PTX or 3MPA treatments. Left column, I_{HTK} to I_A correlations. Center column, I_{HTK} to I_h correlations. Right column, I_A to I_h correlations. Control preparations. Density levels were correlated in all three current pairs in control preparations. Decentralized preparations. Decentralization eliminated the coordination of the I_A/ I_h pair, while leaving I_{HTK}/I_A and I_{HTK}/I_h coordinations intact. PTX-treated preparations. Treatment with PTX did not affect any of the three coordinated currents pairs. 3MPA-treated preparations. Treatment with 3MPA did not affect any of the three coordinated current pairs. Each point corresponds to current density (in nA/nF) measured in the same LP cell on day 0 in culture for control preparations and 24 h after the beginning of each treatment for the treated preparations. Current coordinations in control preparations after 24 h in culture did not differ from those seen on day 0 (Table 4.3). Not all currents were always measured in each ganglion, which resulted in different sample sets for each current. R, R^2, and p values for the regressions and the numbers of experiments for each treatment condition are listed in Table 4.3.

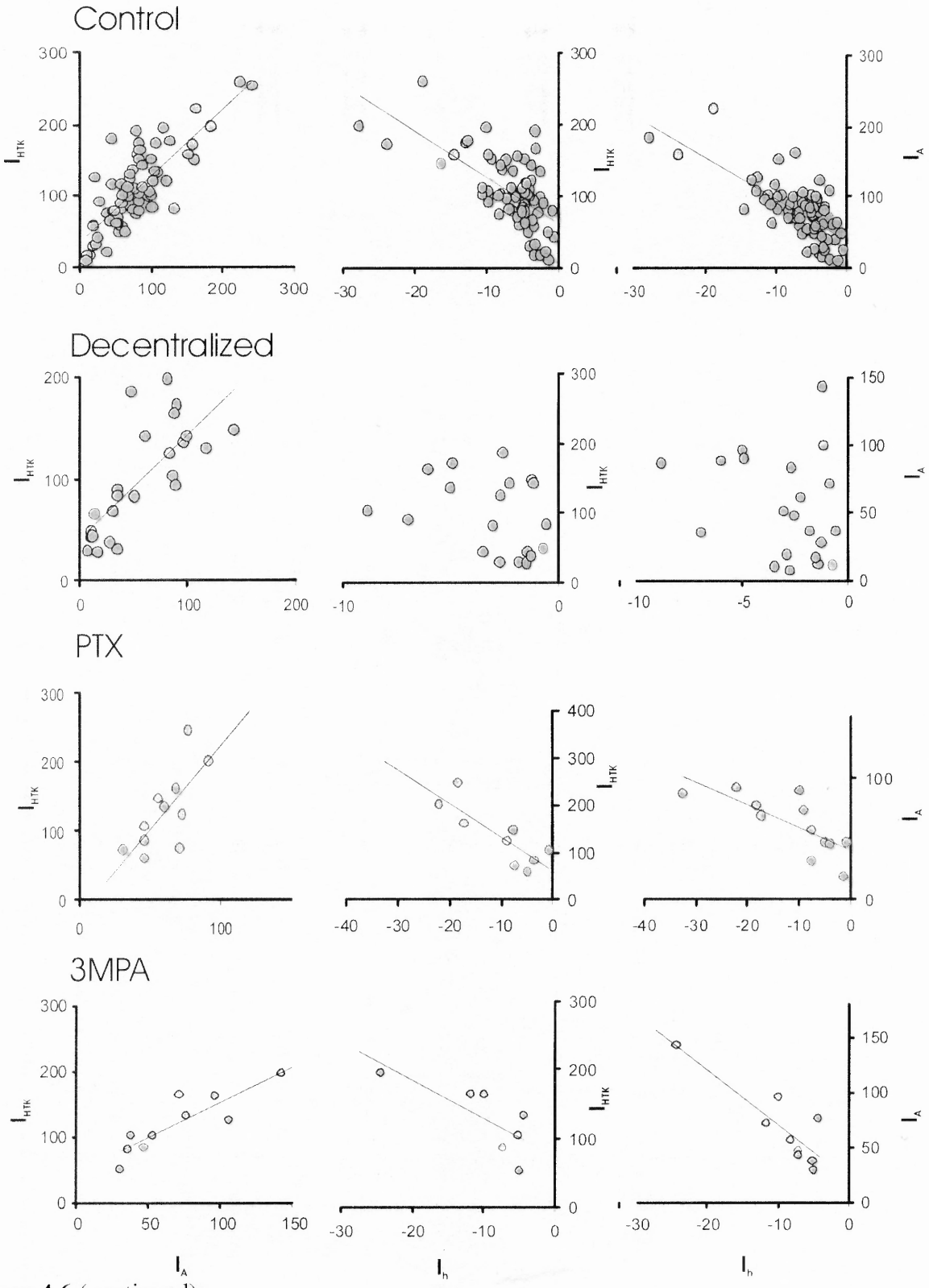

Figure 4.6 (continued)

These results indicate that setting of current levels and INTER-cellular coordination of the HTK and A currents in PD and LP neurons involves activation of a PTX-sensitive chloride channel, possibly through the glutamatergic interaction between the cells. However, since PTX is also known to affect GABA signaling in the STG neurons, an additional experiment was needed in which the effects of GABA and glutamate could be separated.

4.3.8 GABA Participates in Coordinating I_h Levels between the Cells

It has been shown previously that PTX in crab STG neurons not only abolishes the effects of glutamate, but also partially inhibits the effects of GABA (Swensen et al. 2000). Bath applications of glutamate or GABA, however, are not equivalent to their targeted release at specialized axonal terminals (Ducret et al. 2007). To circumvent this problem, 3-mercaptoprorionic acid (3MPA), a competitive inhibitor of glutamate decarboxylase, one of the GABA synthesis enzymes, was used to establish which of the two neurotransmitters plays a role in maintaining INTER-cellular current coordination through the PTX-sensitive chloride channel. 3MPA has been shown to abolish GABA synthesis in the STG without affecting glutamate or acetylcholine signaling (Ducret et al. 2007; M. Nusbaum, personal communication).

Twenty four-hour 3MPA treatment of the CoG and OG ganglia did not significantly interfere with the pyloric activity except for some decrease in cycle length (1.42±0.59 sec in control after 24 h in culture vs 2.61±1.51 sec after 24 h 3MPA treatment, t-test $p=0.02$, Figure 4.1). Preparations treated with 3MPA for 15 min (data not shown) or 24 h did not exhibit any significant changes in current levels compared to same

cell values before treatment (currents after 24 h in 3MPA, as % of currents in the same cell on day 0, were, in PD neurons: I_{HTK} = 92 ± 16, I_A = 91 ± 40, I_h = 105 ± 137, n = 15 and in LP neurons: I_{HTK} = 119 ± 28, I_A = 111 ± 51, I_h = 125 ± 157, paired t-test $p > 0.05$ in all cases, n = 10). Intracellular current correlations were also not affected by 3MPA treatment (Figs. 4.6, 4.7 and Tables 4.3, 4.4).

PD to PD and PD to LP neuron current correlations however, changed to resemble the situation seen in decentralized preparations After both decentralization and 3MPA treatment, I_{HTK} and I_A correlations remained intact between the PD neurons, but the I_h correlation changed to an inverse correlation from that observed in control preparations (Figure 4.3, Table 4.1). As for the PD to LP neuron correlations, I_{HTK} and I_A coordination was also unaffected, but correlation in I_h, normally absent, resembled the effect seen in the decentralized preparations (Figure 4.5, Table 4.2). The similarity of effects produced by decentralization and 3MPA treatment, and the differences between these two treatments and PTX, indicate that INTER-cellular coordination of I_h is determined by GABA and not PTX, while INTER-cellular coordination of I_{HTK} and I_A depends on the glutamatergic signaling via the PTX-sensitive chloride channel, and not GABA.

Figure 4.7 (next page) Intracellular current density correlations in PD neurons are not affected by PTX or 3MPA treatments. Left column, HTK to I_A correlations. Center column, HTK to I_h correlations. Right column, I_A to I_h correlations. Control preparations. Density levels were correlated in all three current pairs in control preparations. Decentralized preparations. Decentralization eliminated the coordination of the I_{HTK}/I_A and I_{HTK}/I_h pairs, while leaving I_A/ I_h pair coordination intact. PTX-treated preparations. Treatment with PTX did not affect any of the three coordinated current pairs. 3MPA-treated preparations. Treatment with 3MPA did not affect any of the three coordinated current pairs. Each point corresponds to the density of indicated currents (in nA/nF) measured in the same PD cell on 24 h after the beginning of each treatment. Current coordinations in control and decentralized preparations are replicated from Chapter 3. Not all currents were always measured in each ganglion, which resulted in different sample sets for each current. R, R^2, and p values for the regressions and the numbers of experiments for each treatment condition are listed in Table 4.4.

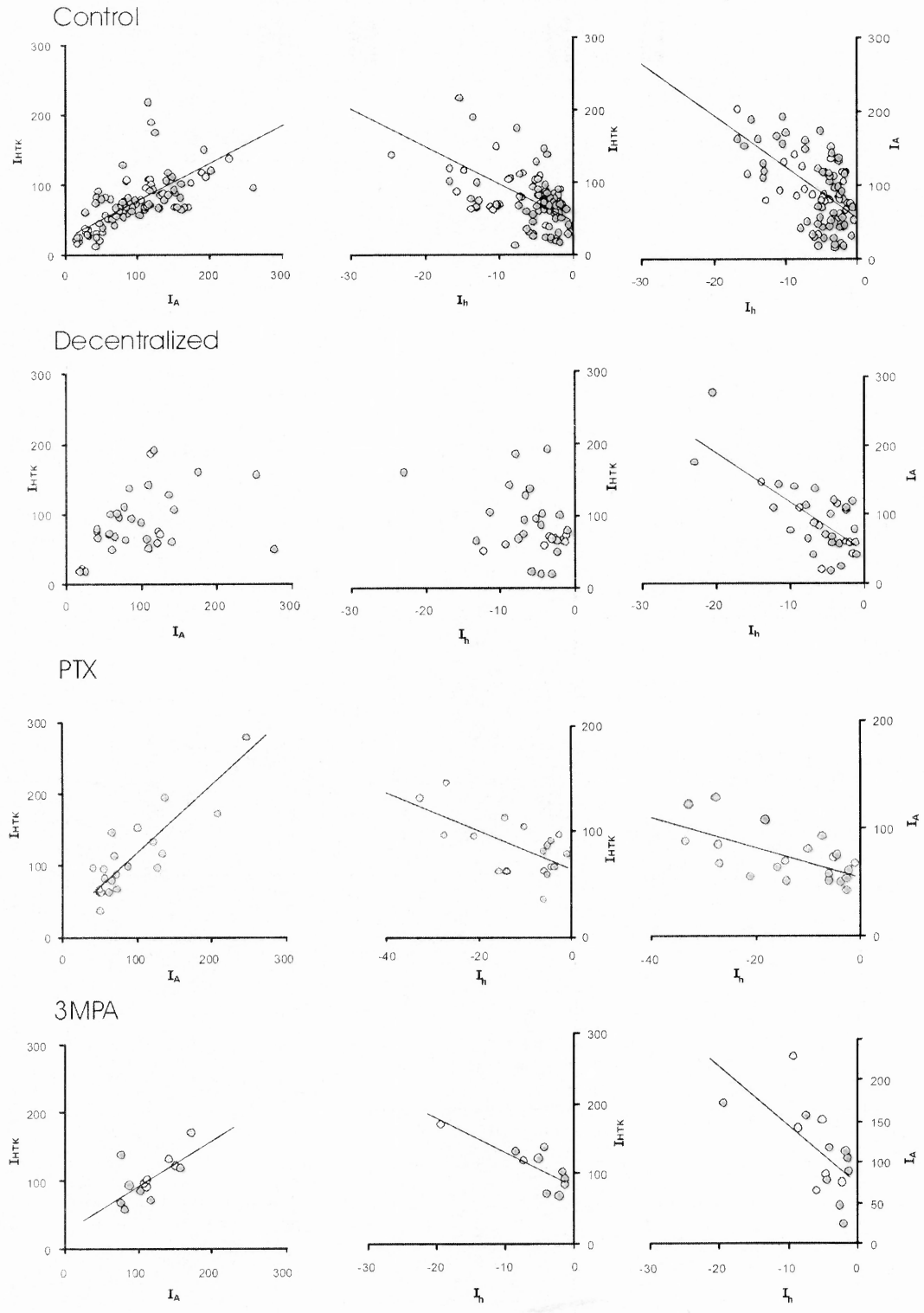

Figure 4.7 (continued)

4.4 Discussion

4.4.1 INTER-cellular Correlations

The possible existence of INTER-cellular current correlations could have been implied from previous modeling work (Turrigiano et al. 1995, LeMasson et al. 1993, Turrigiano et al. 1995, Franklin et al. 1992, Fengler and Lnenicka 2001, Haedo and Golowasch 2006, Ueda and Wu 2006, Wierenga et al. 2005) especially from experiments showing that the abundances of both *IH* and *Shal* mRNAs strongly correlated between the two PD neurons (Schulz et al. 2006). However, INTER-cellular coordination at the current level has not been studied directly before. Here it was shown that there was, indeed, significant coordination of I_A, I_{HTK} and I_h currents between the two PD cells of the network, and I_A and $\log(I_{HTK})$ coordination between the LP and PD cells. The non-linear coordination of I_{HTK} between PD and LP neurons is such that at lower levels HTK currents are closely coordinated, while at higher levels a wider range of $I_{HTK\text{-}PD}/I_{HTK\text{-}LP}$ combinations is observed. This could be due to the existence of threshold setting mechanisms the molecular nature of which is not clear at this time. The initial hypothesis about the nature and role of switching the correlation mode between high and low current values could be gained through computer modeling of the interaction between the two cells. I_h was not clearly coordinated between LP and PD neurons under control conditions.

The apparent INTER-cellular current coordination could simply be the function of pre-set stable current levels determined at the speciation of each neuronal type, and not the result of an active maintenance process. Some of the facts indeed seem to point in the direction of a passive pre-set coordination hypothesis. For example, in this dissertation

stable ratios of current levels within cell types and stable ratios of the levels of the same current between PD and LP neurons were observed (Fig 4.5). Other authors have reported similar results which indicates that current level ratios are stable across different preparations, labs and culture conditions (Golowasch and Marder 1992a, Schulz et al. 2006, Baro et al. 1997, Marder et al. 2005b). Additionally *PAIH* cRNA microinjection experiments demonstrated that I_h levels in the control (uninjected) PD cell did not rise to the same levels as in the microinjected PD cell in the same preparation over several days in culture, in spite of the fact that gap junction and chemical synapse connections remain intact between the cells in the network (Zhang et al. 2003).

However, the experiments reported here have demonstrated that the INTER-cellular current coordination status can change in an adult network in response to changes in the cell to cell communications and neuromodulator supply to the network, and thus is dynamically set and maintained according to the network activity status. The tables summarizing changes in INTER- and intracellular coordination status are shown in Figures 4.8 and 4.9 respectively.

4.4.2 Mechanisms of INTER-cellular Coordinations

INTER-cellular PD-to-PD and PD-to-LP neuron current coordinations could be based on either glutamatergic LP to PD neuron communication, gap junction communications between the two PDs (through transport of small regulatory molecules such as IP3, or Ca^{2+} (Saez et al. 1989), glutamate, K^+, Na^+, or NO_3^- (Beblo and Veenstra 1997)) and/or the action of central neuromodulators. All three mechanisms could be interrelated since neuromodulators are known to affect the permeability of gap junctions (Ducret et al.,

2007) and the efficiency of chemical synapses (reviewed in Engelman and MacDermott 2004), synaptic communication in turn is known to affect the release of neuromodulators and neurotransmitters (reviewed in Nusbaum et al. 2001), and the selectivity of gap junctions is known to be voltage-gated (Qu and Dahl 2002).

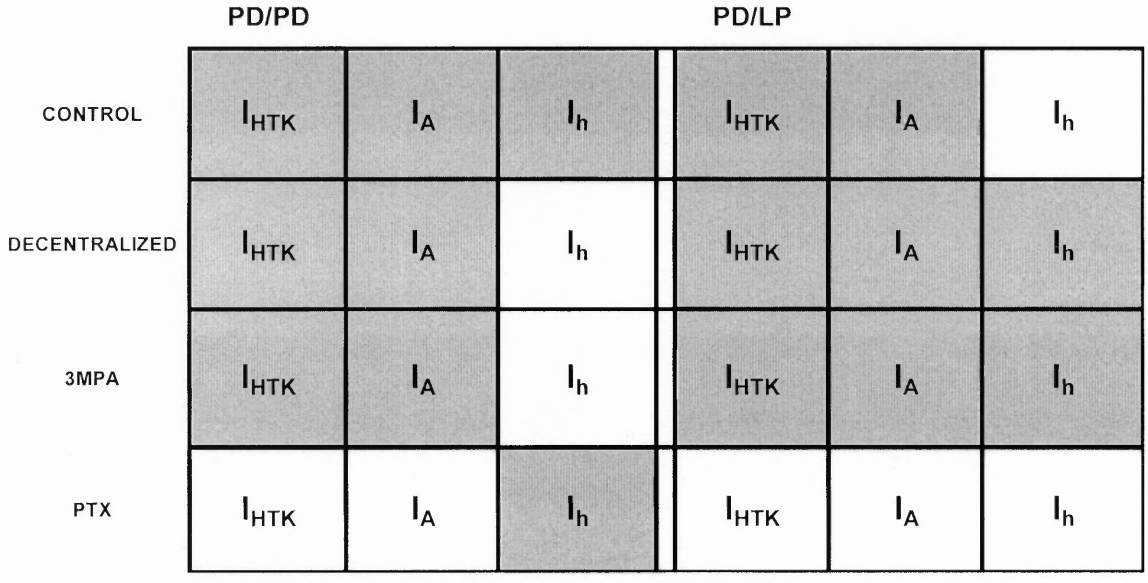

Figure 4.8 INTERcellular current density correlations between PD and LP neurons. Dark squares correspond to cases where current correlations are present, empty squares correspond to cases where correlations are absent. *R*, R^2, and *p* values for the regressions and the numbers of experiments for each treatment condition are listed in Table 4.1 and 4.2.

In this dissertation the initial hypothesis that the glutamatergic communication between cells plays the primary role in the maintenance of INTER-cellular coordinations was based on the previously published modeling results showing the importance of synaptic communications in establishing the ionic current levels via activity-dependent mechanism (LeMasson et al. 1993, Golowasch et al. 1999). Experimentally this hypothesis had to be verified in two steps because bath applications of glutamate or

GABA are not equivalent to their targeted release at specialized terminals (Ducret et al 2007). To circumvent this problem a set of two experiments was conducted, one including incubation in PTX, which blocks both glutamate and $GABA_A$-type activated channels, and the other including incubation in 3MPA, an inhibitor of GABA synthesis, to establish which of the neurotransmitters plays what role in maintaining PTX-sensitive INTER-cellular current coordination. The results demonstrate that INTER-cellular I_A and I_{HTK} coordinations depend on a PTX-sensitive mechanism, most likely through glutamatergic signaling between cells, since these correlations were abolished by PTX, but not 3MPA treatment. Interestingly, the I_{HTK} and I_A INTER-cellular coordinations destroyed by the loss of synaptic communication after PTX treatment, are unaffected by decentralization or, at least in case of PD/PD coordinations, TTX treatment, both of which also affect synaptic communication. One possible explanation could be that a component of the central neuromodulator supply (which is lost both after decentralization and during TTX, but not PTX, treatment) is necessary to make I_{HTK} and I_A INTER-cellular coordinations sensitive to the loss of synaptic communications. Possible experiments aimed at identifying such neuromodulator may include application of TTX (to remove endogenous neuromodulators and to exclude the effects of activity) together with known neuromodulators, for example proctolin, and determining if the INTER-cellular I_{HTK} and I_A coordinations are affected in this case.

The fact that in our experiments PTX disturbed the coordination of I_{HTK} and I_A currents between the two PD neurons, indicates that a glutamatergic synapse from the LP neuron, and not the gap junction coupling between the PD cells, as suggested by Schultz et al. (2006), may be important in maintaining the PD/PD neuron current coordination.

Glutamate from the presynaptic cell (LP) activates an ionic channel in the postsynaptic cell (PD), and the resulting current may affect the ionic current balance in the postsynaptic cell. Since little is known about the pharmacology of gap juctions in Crustacea, experimental photoinactivation of LP cell might provide some insight into this question. The ablation of the LP neuron would specifically remove the glutamate input that PD neurons receive from LP without affecting the GABA input from descending axonal terminals. Significant role of LP in current coordination between the two PD neurons will be confirmed if after LP ablation coordination of currents between PDs is lost. If the LP ablation does not mimic the effects of PTX, a gap junction blocker active in Crustacea, β-glycyrrhetinic acid (Rabbah, personal communication), which blocks gap junctions between PD neurons well, but also has other mild effects, can be used. During this treatment the status of intracellular coordinations can serve as control.

Here it is shown that intracellular coordination of I_h is likely to be governed by a different mechanism than coordinations of I_{HTK} and I_A, since I_h coordination status both between PD neurons and between PD and LP neurons was not affected by PTX, which completely inhibits the glutamate effects, but only partially weakens GABA signaling (Duan and Cooke 2000). The I_h coordination status however was reversed by the two conditions that eliminated the GABA supply to the pyloric network: decentralization and 3MPA treatment. Interestingly, the presence of GABA appeared to maintain the PD/PD neuron I_h coordination, but destroy PD/LP neuron I_h coordination. The direct involvement of GABA in maintaining INTRA-cellular coordination would gain additional support if GABA staining were present in descending axonal termini in control and PTX-treated preparations, and absent in decentralized and 3MPA-treated

preparations. Besides direct participation in I_h coordination, GABA could be altering the strength of gap junction connections, at least in the case of coordination between the two PD neurons. The strength and number of gap junction connections of the PD neurons has been shown to increase in the absence of GABA (Ducret et al. 2007), thus both decentralization and 3MPA treatment could have increased the number of cells electrically coupled to the PD neurons affecting the I_h balance between them. This could be further investigated by using the dye permeability technique described by Ducret et al. (2007), or by blocking the gap junction connections using β-glycyrrhetinic acid (Rabbah, personal communication).

4.4.3 Mechanisms of Intracellular Coordinations

The possibility of intracellular cross-current correlations at both RNA and current levels in one of the pacemaker kernel neurons (PD) was shown by MacLean et al. (2003, 2005) and Schulz et al. (2006). Our previous results have directly shown that I_{HTK}/I_A, I_{HTK}/I_h and I_A/I_h current pairs are correlated in PD (Chapter 3). It was of interest in this case to establish if such intracellular correlations at the current level are specific to the pacemaker neurons or present in the follower cells too and if INTER- and intracellular current correlations are maintained by similar mechanisms.

Here it is shown that intracellular current coordinations are maintained not only in the pacemaker kernel neuron (PD), but also in a follower neuron (LP). However, intracellular current coordinations in the pacemaker and follower neurons change differently in response to decentralization. While in PD neurons the coordination of I_{HTK}/I_A and I_{HTK}/I_h pairs is destroyed and of I_A/I_h pair is preserved after decentralizaton, in

LP the opposite happens: coordinations of I_{HTK}/I_A and I_{HTK}/I_h pairs is preserved and of I_A/I_h pair is destroyed. This implies not only that mechanisms maintaining coordinations of each of these ionic current pairs are different, but that they are also different in PD and LP neurons.

Intracellular current coordinations were not affected by PTX or 3MPA treatment, but were altered after decentralization, which supports the conclusion that INTER- and intracellular coordination processes are maintained by different mechanisms. It is likely that while the INTER-cellular coordinations of I_{HTK}, I_A and I_h are maintained through cell to cell glutamatergic communication and GABA signaling, the intracellular co-regulation of the current pairs depends on neuromodulators other than GABA, which is in agreement with our previous results (Chapter 3).

4.4.4 Mechanisms Controlling the Process of Recovery after Decentralization

Taken together, the findings reported here demonstrate that decentralization-induced changes occur as a complex process governed by both the loss of neuromodulator supply (see also Chapter 3) and the type of synaptic signals exchanged by the follower neurons and the pacemaker kernel. The disappearance of intracellular current coordination after decentralization could be attributed to the loss of one (proctolin) or more central neuromodulators (see also Chapter 3). Decentralization-induced changes in current levels are possibly mediated by altered synaptic signals received by LP and PD cells, possibly in an activity-dependent manner, as indicated by the fact that PTX treatment sets LP and PD currents to resemble 'decentralized' levels without affecting intracellular current co-regulation. The loss of another central neuromodulator, GABA, induces the reversal of Ih

coordination status between the two PD neurons and between LP and PD neurons, while the activity-dependent mechanism may play a role in the initiation of the recovery process (Zhang et al. 2007). Several lines of evidence suggest that decentralization–induced changes require participation of transcriptional events. It has been shown that recovery after decentralization requires RNA synthesis within a two hour window immediately after decentralization (Thoby-Brisson and Simmers 2000a). I_A and I_h currents in the two PD cells are coordinated at the RNA level (Schulz et al. 2006). In the experiments described here none of the agents affecting current levels or coordinations, e.g. proctolin (Chapter 3), TTX, PTX, 3MPA, affected these currents acutely, which implies participation of a slower, possibly transcription-based event. Modeling studies indicate that de-coregulation of ionic currents could be initiated by the loss of neuromodulators in a separate event, not mediated through the alterations in ionic current levels. Further investigation of the process of recovery after decentralization may include the experiments studying the effect of transcription inhibition on the levels and coordinations of ionic currents, and measurements of mRNA levels of these ion channels as a function of neuromodulatory input, using single cell RT-PCR. Cytoplasmic Ca^{2+} oscillations are known to mediate the effects of different factors on transcription (reviewed in Surmeier and Foehring 2004). One possible future research direction may be studying the effect of altering Ca^{2+} oscillations on the recovery after decentralization using the Ca^{2+} clamp technique described by Dolmetsch et al. (1998).

4.4.5 Functional Implications

What could be the function of the elaborate current coordination patterns in the rhythm generating networks? It is reasonable to suggest that current coordination is needed to restrict the degree to which currents in a neuron could be changed by the environmental influences. In fact, the variability of currents observed in biological neurons producing similar output is much smaller than would be expected based on modeling studies (Golowasch et al. 2002, Prinz et al 2004).

	PD			LP		
CONTROL	I_{HTK}/I_A	I_{HTK}/I_h	I_A/I_h	I_{HTK}/I_A	I_{HTK}/I_h	I_A/I_h
DECENTRALIZED	I_{HTK}/I_A	I_{HTK}/I_h	I_A/I_h	I_{HTK}/I_A	I_{HTK}/I_h	I_A/I_h
DECENTRALIZED IN PROCTOLIN	I_{HTK}/I_A	I_{HTK}/I_h	I_A/I_h	I_{HTK}/I_A	I_{HTK}/I_h	I_A/I_h
DECENTRALIZED IN PROCTOLIN + TTX	I_{HTK}/I_A	I_{HTK}/I_h	I_A/I_h	I_{HTK}/I_A	I_{HTK}/I_h	I_A/I_h
3MPA	I_{HTK}/I_A	I_{HTK}/I_h	I_A/I_h	I_{HTK}/I_A	I_{HTK}/I_h	I_A/I_h
PTX	I_{HTK}/I_A	I_{HTK}/I_h	I_A/I_h	I_{HTK}/I_A	I_{HTK}/I_h	I_A/I_h

Figure 4.8 Intracellular current density correlations in PD and LP neurons. Dark squares correspond to cases where current correlations are present, empty squares correspond to cases where correlations are absent. R, R^2, and p values for the regressions and the numbers of experiments for each treatment condition are listed in Table 4.3 and 4.4.

In the experiments described here there was no clear association between the presence of normal pyloric activity and the presence of inter- and intracellular current coordinations of all currents. This diversity in the relationships between the coordinations of different ionic currents and the rhythmicity of pyloric output could be explained by the differences in characteristics of these currents and the roles they play in producing the pyloric output, and by the overall complexity of coordination mechanisms implemented in the pyloric network. For example, less stringent coordination of I_h levels between cells and the smaller effect of I_h coordination on pyloric activity could be attributed to the slower kinetics of I_h compared to I_A and I_{HTK} (Golowasch and Marder 1992a). The oscillation in a two cell theoretical model was much less sensitive to increases in I_A compared to increases in I_h (Zhang et al. 2003). Relaxation of the tight current coordinations could be a necessary step in acquiring the new stable current configuration after a change in the network environment alters the existing current levels. In fact modeling studies (Zhang and Golowasch 2007) show that the absence of current correlations facilitates the recovery of model neuron after decentralization. On the other hand, current coordination increased the stability of activity in model neurons (Soto-Trevino, personal communication).

The presence of coordination between ionic currents indicates the necessity of a "higher level " approach to treatment of conditions caused by deafferentation of central pattern generators: apparently, increasing or decreasing the levels of just one current may not be enough to achieve the balance between the network cells necessary for the recovery of the network function.

Only coordinations between PD and LP cells of the network were studied here while more neurons are known to contribute directly (e.g. PY) or indirectly (e.g. neurons in gastric and oesophageal networks) to the generation of pyloric rhythm (Marder 2000, Blitz et al. 1999, Nusbaum and Marder 1989a,b). Studying current coordinations in all relevant neurons will help better understand the role of coordinations in pyloric rhythm maintenance. Full understanding of the current coordinations between neurons in the pyloric network will be an important step in understanding how the immense diversity of ionic current levels observed in the individual neurons is translated in a rhythmic output remarkably stable under changing environmental conditions.

Table 4.1 Parameters of the Linear Regression Analysis of Current Coordinations between the Two PD Cells of the Pyloric Network

	HTK				*I_A*				*I_h*			
	R^2	*R*	*p*	*N*	*R^2*	*R*	*p*	*N*	*R^2*	*R*	*p*	*N*
Control day 0[a]	0.46	0.68	<0.001	57	0.54	0.74	<0.001	52	0.56	0.75	<0.001	52
Control day 0 (randomized)	0.46	0.67	<0.001	57	0.54	0.73	<0.001	52	0.61	0.78	<0.001	52
Control 24 h	0.61	0.78	0.004	11	0.56	0.75	0.01	10	0.5	0.7	0.02	10
24 h after decentralization	0.53	0.72	0.003	14	0.36	0.6	0.02	14	0.02	0.14	0.6	15
24 h in PTX	0.02	0.14	0.6	12	0.007	0.08	0.8	15	0.66	0.81	0.001	12
24 h in 3MPA	0.72	0.52	0.02	9	0.8	0.64	0.05	6	0.53	0.72[b]	0.06	7
24 h in TTX	0.85	0.92	0.02	5	0.91	0.95	0.04	4	0.05	0.24	0.7	5

[a] Day 0 corresponds to pooled data from all preparations measured on day 0. Similar correlation parameters and statistical significance values were obtained for each subset of day 0 measurements corresponding to experimental set listed above

[b] negative slope

Table 4.2 Parameters of the Linear Regression Analysis of Current Coordinations between the PD and LP Cells of the Pyloric Network

	Log HTK				I_A				I_h			
	R^2	R	p	N	R^2	R	p	N	R^2	R	p	N
Control day 0 [a]	0.41	0.64	<0.001	78	0.43	0.65	<0.001	62	0.003	0.05	0.7	55
Control 24 h in culture	0.56	0.75	0.01	10	0.52	0.72	0.01	11	0.07	0.23	0.5	10
24 h after decentralization	0.52	0.72	0.0001	23	0.52	0.72	0.0001	22	0.58	0.77	<0.001	20
24 h in PTX	0.0024	0.04	0.9	15	0.005	0.07	0.8	14	0.01	0.12	0.6	15
24 h in 3MPA	0.69	0.83	0.01	8	0.49	0.7	0.01	12	0.76	0.87	0.0009	10

[a] Day 0 corresponds to pooled data from all preparations measured on day 0. Similar correlation parameters and statistical significance values were obtained for subsets of day 0 measurements corresponding to experimental set listed above

Table 4.3 Parameters of the Linear Regression Analysis of Intracellular Pairwise Current Coordinations in the LP Cells of the Pyloric Network

	HTK/I_A				HTK/I_h				I_A/I_h			
	R^2	R	p	N	R^2	R	p	N	R^2	R	p	N
Control day 0 [a]	0.63	0.79	<0.001	75	0.4	0.63	<0.001	69	0.51	0.71	<0.001	70
Control 24 h	0.58	0.76	0.002	12	0.45	0.67	0.01	12	0.6	0.77	0.001	14
24 h after decentralization	0.56	0.75	<0.001	24	0.09	0.3	0.2	19	0.05	0.24	0.28	21
24 h in PTX	0.52	0.72	0.01	11	0.69	0.83	0.005	9	0.57	0.75	0.004	12
24 h in 3MPA	0.76	0.87	0.0008	10	0.58	0.76	0.04	7	0.75	0.86	0.002	9
15 min in PTX	0.37	0.61	0.03	12	0.69	0.83	0.02	7	0.55	0.79	0.02	9

[a] Day 0 corresponds to pooled data from all preparations measured on day 0. Similar correlation parameters and statistical significance values were obtained for each subset of day 0 measurements corresponding to experimental set listed above

Table 4.4 Parameters of the Linear Regression Analysis of Intracellular Pairwise Current Coordinations in the PD Cells of the Pyloric Network

	HTK/I_A				HTK/I_h				I_A/I_h			
	R^2	R	p	N	R^2	R	p	N	R^2	R	p	N
Control day 0 [a]	0.48	0.69	<0.001	95	0.37	0.61	<0.001	94	0.4	0.63	<0.001	89
Control 24 h	0.49	0.7	0.007	12	0.81	0.9	0.002	8	0.54	0.73	0.009	11
24 h after decentralization	0.06	0.24	0.14	36	0.02	0.14	0.34	34	0.51	0.71	<0.001	32
24 h in PTX	0.81	0.9	<0.001	22	0.4	0.63	0.005	18	0.4	0.63	0.001	22
24 h in 3MPA	0.44	0.66	0.01	12	0.65	0.8	0.004	10	0.4	0.63	0.01	15
15 min in PTX	0.66	0.81	0.004	10	0.6	0.77	0.02	8	0.7	0.84	0.03	6
PTX washed	0.8	0.89	0.0009	9	0.67	0.82	0.01	8	0.89	0.94	0.001	8

[a] Day 0 corresponds to pooled data from all preparations measured on day 0. Similar correlation parameters and statistical significance values were obtained for each subset of day 0 measurements corresponding to experimental set listed above

CHAPTER 5

ACTIVITY AND NEUROMODULATORS CONTROL THE RECOVERY OF RHYTHMIC OUTPUT IN A RHYTHM-GENERATING NEURONAL NETWORK

This chapter is the result of collaboration with Rutgers University PhD student Yili Zhang and a former Rutgers University PhD student Rosa Rodriguez. Parts of the experiments reported here were performed by Y. Zhang and R. Rodriguez. However, in general, this was a joint effort and the parts are not easy to separate without losing the general perspective of these results. Therefore the results are presented as a whole while acknowledging that not all of them were exclusively obtained by the author.

5.1 Abstract

Rhythm-generating neuronal networks control vitally important rhythmic behaviors, including breathing, heartbeat and digestion. Understanding how these networks recover from perturbations has important theoretical and practical implications. Both experimental and modeling studies indicate that rhythm recovery after the loss of central neuromodulatory input (decentralization) could be driven entirely by activity-dependent mechanisms. This hypothesis was tested by examining the effects of altering the network activity patterns for several hours prior to decentralization on rhythm recovery in the pyloric network of the crab *Cancer borealis*. It was found that pretreatments that alter the network activity through shifting the ionic balance and membrane potential of the cells, such as hyperpolarization of the pacemaker neurons, and incubations with $GABA_A$-specific agonists or in low Na^+ saline, advanced the time of rhythm recovery. This is consistent with recovery process being triggered in advance of decentralization at the

beginning of the pretreatment period through a strictly activity-dependent mechanism. However, pretreatment with GABA, which also interrupted the pyloric activity, not only accelerated rhythm recovery, but additionally delayed the time of activity turnoff. Pretreatment with a metabotropic $GABA_B$ receptor agonist delayed the activity turnoff, but did not affect the time of recovery. These results demonstrate that the recovery process cannot be explained solely by activity-dependent mechanisms. Here an activity- and modulator dependent model of the recovery process proposed. Further, it is shown that the effect of proctolin pretreatment on the process of recovery after decentralization is consistent with the assumptions of such model.

5.2 Introduction

Studies in both vertebrates and invertebrates have shown that neuronal networks that control rhythmic behaviors such as breathing, heartbeat, swimming, feeding, walking, and flying, remain functional even when they are isolated from the organism and receive no rhythmic neuronal input from the environment (Marder and Bucher 2001, Luther et al. 2003). It has previously been shown that the pyloric network, located in the stomatogastric ganglion (STG) of decapod crustaceans, shows this type of recovery of rhythmic activity after a severe perturbation, namely the removal of central neuromodulatory input (decentralization), to the pyloric network (Golowasch et al. 1999, Luther et al. 2003, Thoby-Brisson and Simmers 1998). The recovery of activity occurs within several hours to days of decentralization and achieves levels and characteristics similar to those observed in control preparations (Golowasch et al. 1999b, Luther et al. 2003, Thoby-Brisson and Simmers 1998). Previous experimental work showing that

neurons of the pyloric network respond to changes in activity with changes in their intrinsic properties (Turrigiano et al. 1994, Haedo and Golowasch 2006) and in their ionic currents (Golowasch et al. 1999b, Haedo and Golowasch 2006) and modeling work showing that recovery of activity could be based entirely on activity-dependent mechanisms (Golowasch et al. 1999b, Zhang and Golowasch 2007) suggest that recovery could be strictly an activity-dependent process. However, other data exist that show that once initiated, recovery process is activity-independent (Thoby-Brisson and Simmers 1998, 2000) and that if the supply of one of the central neuromodulators, proctolin, is maintained after decentralization, the recovery process may not be initiated (Khorkova and Golowasch 2007).

In this chapter the activity-only vs neuromodulator-only hypotheses of pyloric rhythm recovery are tested by examining the effects of modifying the preparation's activity before decentralization on the recovery of pyloric rhythm after decentralization. The results presented in this chapter show that the recovery process is not governed solely by activity-dependent mechanisms. It is reported here that some aspects of the recovery process are regulated by neuromodulators. Based on these results, a neuromodulator- and activity-dependent recovery hypothesis is proposed and further confirmed by showing that the results of a proctolin-pretreatment experiment can be predicted based on the assumptions of this hypothesis.

5.3 Results

As described in Chapter 1, if the STG is isolated from the rest of the STNS by blocking action potential transmission along the *stn*, neuromodulator release is abolished and the

activity of the pyloric network decreases considerably or stops (Figure 3.1, 4.1, 5.1). Over time the pyloric rhythm resumes and stabilizes (Figure 3.1, 5.1) after a period characterized by the repeated turning on and off of the rhythm, henceforth called 'bouting' (Figure 5.1, 3.1, Luther et al. 2003). The recovered pyloric network activity is independent of the central neuromodulatory input.

In this study the hypothesis that the process of recovery of the pyloric network activity can be altered by the type of network activity that precedes decentralization was examined. Activity changes were induced experimentally using GABA, hyperpolarizing current injections into pacemaker neurons and low Na^+ saline solutions.

5.3.1 Experimental Protocols

All experiments described below followed the same protocol: after recording the normal pyloric network activity for at least 30 min, a pharmacological agent or a manipulation of the membrane potential of pyloric neurons was applied. The pharmacological agents were then washed rapidly with normal saline (or external current injection discontinued) until pyloric network activity was recovered (typically within 5-10 min). Only then was the STG decentralized by blocking the input stomatogastric nerve (*stn*).

Although decentralization using the protocol described here most often resulted in complete cessation of rhythmic pyloric activity, sometimes after *stn* blockade the pyloric rhythm frequency simply decreased to a much lower but stable level. Thus, bouting activity was defined as the activity characterized by the transient activation or acceleration of pyloric rhythmic activity after decentralization. We call each activation or acceleration event a "bout" (Figure 5.1, 3.1).

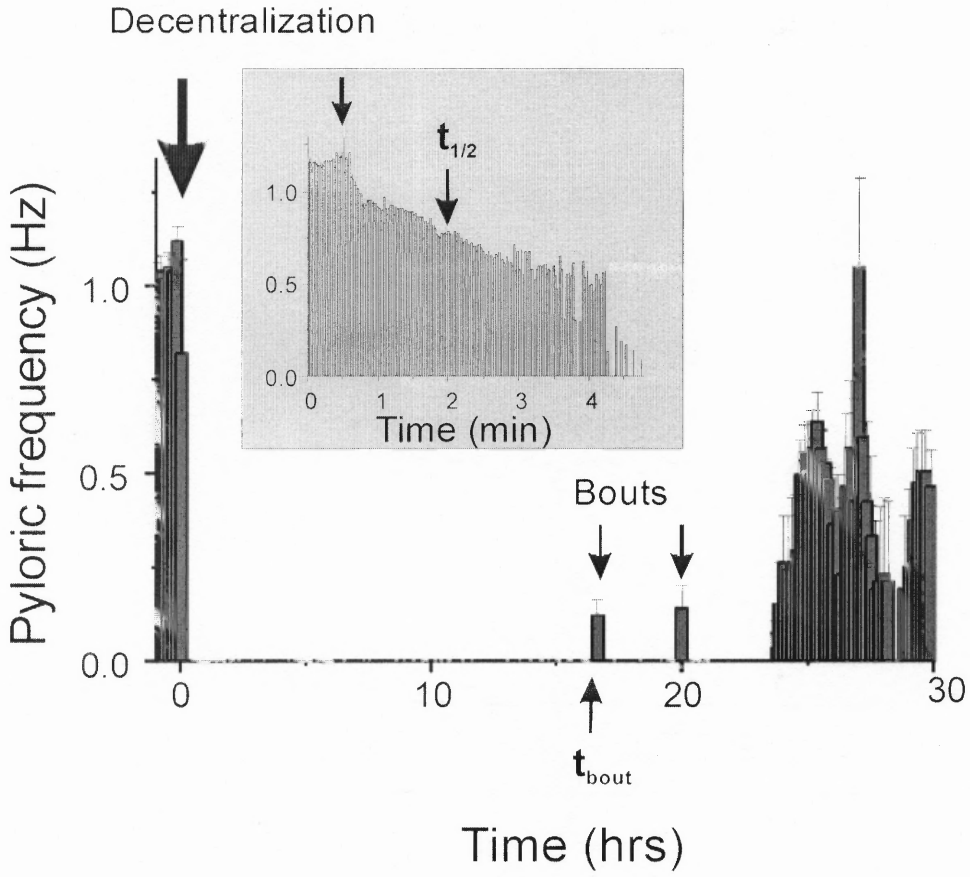

Figure 5.1 Pyloric rhythm frequency changes recorded via *lvn* after decentralization. The frequency before decentralization in this preparation was ~1.1Hz. The pyloric rhythm stopped immediately after decentralization. Bouting began ~17 hrs after decentralization with two short bouts followed by two much longer ones. The inset shows frequency changes immediately after decentralization (note different time scale).

Two parameters to characterize the recovery process were used: the rate of rhythmic activity turnoff (Figure 5.1, inset) and time to the first bout (Figure 5.1). The rate of activity turnoff was defined as the time needed for reduction in pyloric rhythm frequency to half of the pre-decentralization level ($t_{½}$). Time to the first bout (t_{bout}) after decentralization was chosen as a readout of the recovery rate because it is significantly shorter than time to stable recovery, and thus reduces the possibility of contribution by

random factors affecting the viability of the preparation, to the experimental outcome (Luther et al. 2003).

5.3.2 Activity Suppression by Hyperpolarization or Low Sodium Advances Recovery after Decentralization

To determine if the activation of pyloric rhythm recovery is a purely activity-dependent process, an attempt was made to reduce or eliminate pyloric activity during several hours preceding decentralization. The reasoning behind this was that the reduced pyloric activity before decentralization should advance the activation of the activity-dependent recovery mechanisms and thus accelerate the recovery after decentralization.

Hyperpolarization of the two PD neurons in the network, which are strongly electrically coupled to the pacemaker AB neuron, or reduction in the extracellular Na^+ concentration, were used to inhibit pyloric activity prior to decentralization (Figure 5.2, Table 5.1).

In preparations in which both PD neurons were hyperpolarized to -70 mV with current injection for 5 h prior to decentralization, the average time to half-maximal pyloric frequency was not different from control values (control $t_{½}$ = 0.25±0.26 h, hyperpolarized $t_{½}$ = 0.21±0.18 h, $p > 0.05$, n = 12, Tukey post-hoc test; Table 5.1, Figure 5.2A). However, the average time to first bout in hyperpolarized preparations was significantly shorter than that of the controls (control t_{bout} = 6.19±4.76 h , hyperpolarized t_{bout} = 1.60±1.72 h, $p < 0.05$, n=12, Tukey post-hoc test, Table 5.1, Figure 5.2A).

When preparations were incubated in *Cancer* saline containing 40% Na^+ for 5 h prior to decentralization, results similar to those observed in preparations hyperpolarized before decentralization were obtained (Figure 5.2B, Table 5.1). The time to half maximal

frequency $t_{½}$ was 0.29±0.34 h, which was not significantly different from the control or hyperpolarized PD preparations (p>0.05 in both cases, n=11, Tukey post-hoc test, Table 5.1). However, the average time required to produce the first bout in these low Na^+-treated preparations was 1.20±0.96 h, which was significantly shorter than in controls (p < 0.01, n=7, Tukey post-hoc test, Table 5.1, Figure 5.2B).

Table 5.1 Parameters of the Recovery Process in Controls and Preparations with Different Pretreatments before Decentralization

Treatment prior to decentralization	Time required to reduce the frequency by half (hours)	Time to first bout (hours)	Number of experiments
Control	0.25±0.26	6.19±4.76	18
GABA for 18 h	2.27±3.21*	3.91±4.60	10
GABA for 5 h	1.08±1.05	1.98±1.30*	10
GABA for 1 h	0.72±0.85	1.9±0.84*	9
Baclofen	5.89±8.64**	6.74±8.18	7
Muscimol	0.38±0.27	2.05±1.60*	6
Hyperpolarized	0.21±0.18	1.60±1.72*	12
Low sodium saline	0.29±0.34	1.20±0.96*	11
Proctolin	0.16±0.14	2.34±1.88*	7

Values represent average ± SD

* significantly different from control P<0.05;

** significantly different from control P<0.01

5.3.3 Pretreatment with GABA Affects Both Time to First Bout and Time of Activity Turnoff

Treatment of non-decentralized pyloric network with 1 mM GABA stops the pyloric rhythm completely and reversibly (Figure 5.3A), similar to hyperpolarization or low Na^+ saline treatment.

However, when preparations were treated with 1mM GABA for 1-18 h prior to decentralization, the half maximal time of pyloric rhythm cessation showed a time-dependent and statistically significant increase compared to control preparations ($p < 0.05$, one-way ANOVA, Table 5.1), while in hyperpolarization and low Na^+ saline pretreated preparations no effect on time to activity turnoff was observed. The decentralization of untreated (control) pyloric networks resulted in the rapid cessation of the pyloric rhythm ($t_{½}$ = 0.25±0.26 h, n = 18). Short term (<18 h) pretreatment with GABA did not significantly increase $t_{1/2}$ (0.72±0.85 h for 1 h pre-treatment, 1.08±1.05 h for the 5 h pretreatment, $p > 0.05$ for both, Tukey post-hoc test, n = 9 and n=10 respectively). After approximately 18 h of GABA incubation, $t_{½}$ increased to 2.27±3.21 h ($p < 0.02$, post-hoc Tukey test, n = 10) (Table 5.1). Furthermore, in preparations pre-treated with 1 mM GABA overnight, decentralization sometimes never completely interrupted the rhythmic activity, but only reduced its frequency (Figure 5.3A).

After decentralization in control preparations, t_{bout} was 6.19±4.76 h (n = 18), while in preparations treated with 1 mM GABA for 1, 5 or 18 hours, t_{bout} decreased to 1.9±0.84 h, 1.98±1.30 h, and 3.91±4.60 h, respectively. These effects were statistically significant ($p < 0.05$, one-way ANOVA, post-hoc Tukey test results comparing each pretreatment with control are shown in Table 5.1). It is important to note that when activity never completely stopped after GABA pretreatment, bouts were discernible as transient frequency increases of more than two fold over the background frequency, easily distinguishable from random frequency variation or transient artifacts (see Figure 5.3).

If the recovery process were solely activity-dependent, in GABA-pretreated preparations only the advanced recovery time would be observed, as in hyperpolarized or low sodium saline treated preparations, with no effect on the rhythm turnoff time. However, the experimental results also showed a significant increase in the time to pyloric activity turnoff after decentralization, which indicated a possible involvement of a different, activity-independent mechanism. Additionally, short term (<18 h) pretreatment with GABA only reduced the time to first bout, while time to half frequency was not significantly affected. The difference in the time of onset of these two effects also supported the possibility that they may be mediated by two different mechanisms.

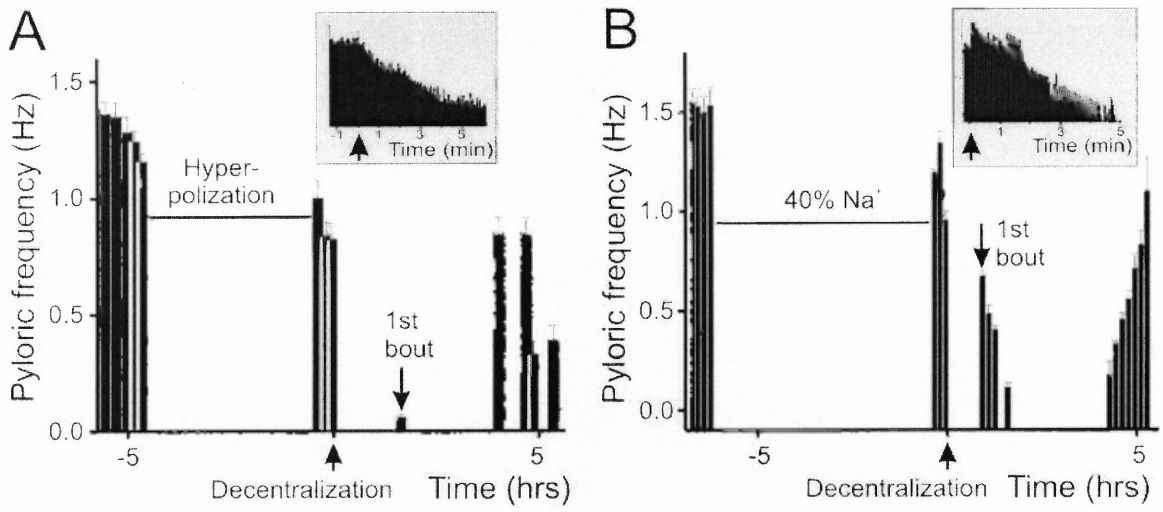

Figure 5.2 Examples of post-decentralization changes in pyloric rhythm frequency in different pre-inhibited preparations. A. Preparation was hyperpolarized for ~5 hours before decentralization. B. Preparation was incubated with 40% Na^+ solution for ~5 hours before decentralization. Insets in both panels show $t_{1/2}$ at a finer time scale.

Pyloric network neurons express at least two types of GABA receptors, an ionotropic type $GABA_A$ and a metabotropic type $GABA_B$ (Swensen et al. 2000).

Therefore, the contribution of the two different receptor types to the two observed effects was investigated using specific GABA receptor agonists.

5.3.4 Metabotropic $GABA_B$ Receptor Agonist only Increases Time to Rhythm Turnoff

Pretreatment of the STG with the $GABA_B$ receptor agonist baclofen (0.5 mM) for 5 h before decentralization never resulted in the complete cessation of pyloric rhythmic activity (Figure 5.3, n = 7) and $t_{½}$ in these preparations was significantly increased compared to controls ($t_{½}$ = 5.89±8.64 h, p <0.01, t- test) (Figure 5.3B, C, Table 5.1). In contrast, the average time required to produce the first bout was not significantly different from control preparations (t_{bout} = 6.74±8.18 h; p >0.05, t-test, Figure 5.3C, Table 5.1). Therefore, the baclofen pretreatment affects the time course of pyloric activity turnoff after decentralization but not the rate of pyloric rhythm recovery as estimated by the time to generate the first bout of activity (Figure 5.3C). Participation of the slower metabotropic process in controlling the time course of activity cessation is also supported by the slower onset of this effect after GABA pretreatment (Table 5.1).

5.3.5 Ionotropic $GABA_A$ Receptor Agonist only Reduces Time to First Bout

Pretreatment of the STG with the $GABA_A$ receptor agonist muscimol (0.5 mM) for 5 h before decentralization almost always resulted in the complete termination of rhythmic activity after decentralization (Figure 5.3D). After decentralization, $t_{½}$ was 0.38±0.27 hours, with no significant difference from control (p > 0.05, n = 6, Tukey post-hoc test, Table 5.1).

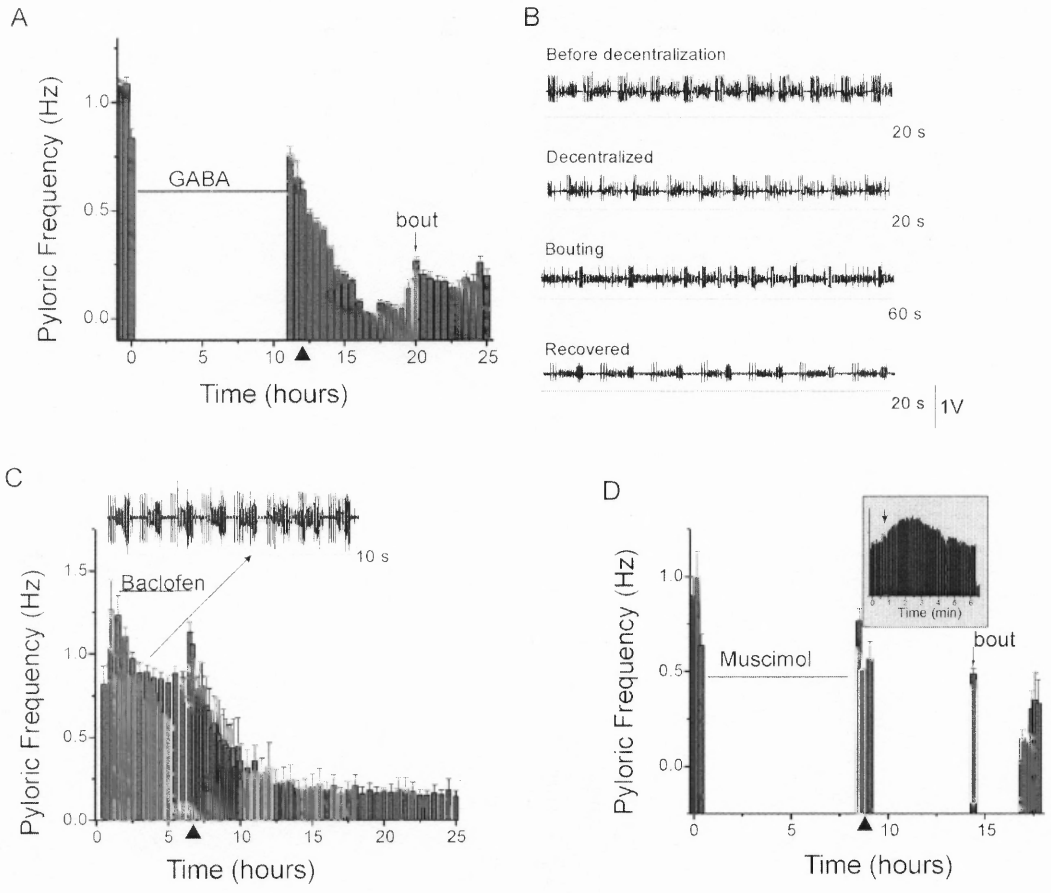

Figure 5.3 Examples of post-decentralization changes in pyloric rhythm frequency in different neuromodulator pre-treated preparations. Black triangle ▲indicates the time of decentralization. A. Preparation was incubated with 1mM GABA for 18 h before decentralization. After decentralization, there was a significant delay in rhythmic activity turnoff and the first bout appeared significantly faster than in control. B. Extracellular *lvn* recording (for 20 or 60 seconds) of pyloric network activity recovery in GABA pretreated preparation. C, Top trace, lvn recording in 0.5 mM baclofen. Preparation was incubated with 0.5mM baclofen for ~5 hours before decentralization. After decentralization, there was a significant delay in rhythmic activity turnoff but no decrease in time to first bout compared to control. D. Preparation was incubated with 0.5mM muscimol for ~8 hours before decentralization. After decentralization, there was no delay in rhythmic activity turnoff but the first bout appeared significantly faster than in control.

However, the average time to first bout was significantly shorter than in control preparations (t_{bout} = 2.05±1.60 h, p = 0.05, n = 6, Tukey post-hoc test, Table 5.1), similar to low Na^+ and hyperpolarization treatments, which indicates activity-dependent

regulation. Participation of the faster ionotropic signaling process in controlling the time course of activity recovery is also supported by the faster, already after 1 h, onset of this effect after GABA pretreatment (Table 5.1).

5.3.6 An Activity- and Neuromodulator-Dependent Hypothesis of the Recovery Process Regulation is Supported by Proctolin-Pretreatment Experiments

The experimental results reported above led to the formulation of an activity- and neuromodulator-dependent hypothesis of the recovery process regulation (Zhang, personal communication). This hypothesis postulates the existence of two cooperating sensor mechanisms controlling the process of recovery after decentralization, one activity-dependent and the other neuromodulator-dependent. Based on the assumptions of this model, proctolin pretreatment should have resulted in a time of activity turnoff not different from control, but shortened time to first bout (see Discussion and Figure 5.4 for the more detailed description of the model-based predictions).

The results of biological experiments agreed with the predictions made using the activity- and neuromodulator-dependent hypothesis. In the proctolin pretreatment experiments crab STNS preparations were incubated in 1μM proctolin for 1-18 hours before decentralization. After proctolin pretreatment all preparations turned off their rhythmic activity immediately after decentralization with no significant difference from control ($t_{½}$=0.16±0.14 h, $p > 0.05$, t-test, n= 7, Figure 5.5, Table 5.1), and their time to first bout was reduced compared to control (t_{bout}=2.34±1.88 h, $p < 0.05$, t-test, n= 7, Figure 5.5, Table 5.1).

5.4 Discussion

Both experimental and modeling work suggested that the recovery after decentralization might be mediated solely through the activity dependent mechanism that triggers the readjustment of intrinsic properties of pyloric neurons (Luther et al. 2003; Golowasch et al. 1999b). If the bursting activity was perturbed in a model neuron, the function of ionic channels that underlie the generation of neuronal activity was altered to favor the recovery of activity (Liu et al., 1998). Modeling studies have shown that an activity-dependent feedback mechanism, which detects the intracellular calcium concentration changes and then regulates calcium and potassium channels, is sufficient to generate a recovery of neuronal activity after decentralization, including the intermittent bouts of activity that precede the stable activity recovery in biological experiments (Zhang and Golowasch 2007). However, other data indicate that the process of recovery maybe activity independent and that neuromodulators may be involved in its regulation (Thoby-Brisson and Simmers, 1998, 2000, Khorkova and Golowasch, 2007)

In this study the possibility that the process of pyloric activity recovery after decentralization is determined by a strictly activity-dependent mechanism was examined. For this purpose the type of network activity that precedes decentralization was experimentally altered using GABA, proctolin, hyperpolarizing current injections into pacemaker neurons and low external Na^+ solutions.

These experiments demonstrated that when only ionotropic $GABA_A$ receptors were activated during pretreatment, only the time to first bout was changed, and not the time to half-maximal frequency after decentralization. On the other hand, if during pretreatment only $GABA_B$ metabotropic receptors were activated by baclofen, only the

rate of activity termination after decentralization was significantly affected, but not the rate of activity recovery. It appears therefore that two separate and in principle independent signaling pathways control the effects of GABA pretreatment on the recovery after decentralization, one activated via $GABA_A$, and another via $GABA_B$ receptors. $GABA_A$ signaling is mediated by an ionotropic effect and consequent changes in the ionic balance of the cell, pre-activated the recovery mechanisms which lead to decreased time to first bout, similar to the effects of other activity-altering treatments (hyperpolarization and incubation in low Na^+ saline). $GABA_B$ signaling, probably acting through a G-protein pathway (Swensen et al. 2000, Duan and Cooke 2000) controls the rate of activity termination, possibly by increasing the stability of the network activity under conditions in which the neuromodulatory input is present (Zhang, personal communication).

These experimental results provided the basis for a hypothesis of the recovery process as a complex event, different aspects of which governed by different mechanisms. These are an activity-dependent mechanism that regulates the onset of the rhythm recovery process, and a G-protein mediated mechanism responsible for the rate with which preparations decrease their activity after decentralization (Zhang, personal communication). A schematic diagram of this hypothesis is shown in Figure 5.4. The hypothesis postulates the presence of two sensors that regulate calcium conductance, S_A and S_{NM}, with different time constants. S_A detects the activity-dependent changes of a cell via $[Ca]_{cyt}$ changes, that depend on four components: Ca^{++} influx through calcium channel located in the cytoplasmic membrane, Ca^{++} diffusion and buffering through the cytoplasm, Ca^{++} release from ER through the IP_3-sensitive calcium channel on the ER

membrane, and Ca^{++} reuptake by a calcium pump on the ER membrane (Figure 5.4). S_{NM} is a neuromodulator-dependent sensor. Neuromodulators, e.g., GABA or $GABA_B$ receptor agonists, bind to the G protein-coupled $GABA_B$ receptors. The activated G proteins regulate S_{NM}, which triggers a signaling pathway that in turn increases calcium conductance.

At the moment of decentralization, the inward current normally activated by neuromodulators (I_{NM}) is abolished, which hyperpolarizes the neuron and stops its activity. However, the loss of neuromodulator-evoked current could be compensated for by one of the inward currents, if such current could be sufficiently elevated prior to decentralization. Calcium current can be one such current since it does not lose it's activity after neuromodulator turnoff. In case of sufficient upregulation of the calcium current the neuronal activity will be sustained after decentralization. However, if the levels of calcium current are not sufficient to depolarize the cell beyond the threshold required for the generation of activity, neuronal activity will stop. The loss of rhythmic activity after decentralization would activate the S_A sensor, that in turn would initiate the slow increase in G_{Ca}. G_{Ca} increase gradually depolarizes the neuron and eventually leads to bursting activity recovery.

Following this model, when neuronal bursting is inhibited without decentralization, the activity-dependent feedback system will detect the loss of neuronal activity through the drop in cytoplasmic calcium concentration and readjust the neuronal conductances, namely G_{Ca}. S_A-dependent upregulation of G_{Ca} prior to decentralization will shorten the time needed to reach the depolarization level needed for bursting and thus will accelerate the appearance of the first bout. The hypothesis further assumes that

the elevation of G_{Ca} caused by the activity-dependent regulation is not sufficient by itself to reach depolarization level needed to maintain bursting in the absence of the neuromodulatory input.

However, if during pretreatment G-protein-coupled $GABA_B$ receptors are also activated, as in baclofen- or GABA-pretreated preparations, the second sensor, S_{NM}, is engaged, forcing G_{Ca} to increase even further so as to be able to maintain activity in the absence of neuromodulators. When exogenous GABA is washed off before decentralization, S_{NM} activation will begin to slowly decrease, eventually leading to the hyperpolarization of the neuron and the loss of activity, but with a significant delay relative to the control condition in which S_{NM} is not as strongly activated.

The activity and neuromodulator-dependent recovery hypothesis was implemented in a model neuron (Zhang, personal communication). The process of activity recovery, as well as the effects of hyperpolarizing and neuromodulatory pretreatments in this model neuron closely resembled the recovery and pretreatment results seen in biological experiments (Zhang, personal communication).

The biological relevance of the activity- and neuromodulator-dependent hypothesis of recovery was tested by using it to predict the results of a biological experiment, in which pre-incubation with the neuromodulator proctolin is followed by decentralization after proctolin wash off. Recall that the neuromodulator proctolin activates an inward current (Golowasch and Marder 1992b), probably via a G-protein coupled pathway (Swensen et al. 2000) which depolarizes pyloric neurons and activates the pyloric rhythm (Nusbaum and Marder 1989a, b). According to the activity- and neuromodulator-dependent hypothesis (Zhang, personal communication), pretreatment

with proctolin should have the following effects. During proctolin pretreatment, the activity-dependent feedback system will detect the upregulated status of neuronal activity through S_A and downregulate G_{Ca}. Meanwhile exogenous proctolin, acting through a G-protein-coupled receptor activates S_{NM}, but the increase of G_{Ca} through S_{NM} is offset by its decrease through S_A. As a result, at the time of decentralization G_{Ca} will likely not be high enough to maintain the pyloric activity in the absence of neuromodulator input. However, G_{Ca} will be higher than in control conditions. This will lead to proctolin-pretreated preparations having shorter time to first bout, but no extra delay in activity turnoff after decentralization. The experimental results matched the outcome predicted on the basis of the activity- and neuromodulator-dependent hypothesis, which supports the existence of the two independent feedback systems controlling the recovery after decentralization.

Interestingly, according to the activity- and neuromodulator-dependent hypothesis, although the effects of hyperpolarization and low Na^+ saline pretreatment were similar, they were brought on by the activation of different mechanisms. While hyperpolarization of PD neurons only activated S_A through activity-dependent changes in intracellular calcium concentration, low Na^+ saline treatment also decreased the activity of S_{NM} due to the fact that the endogenous neuromodulator supply is interrupted when action potential transmission along the *stn* is blocked by low Na^+ concentration. Decreased activity of S_{NM} was not able to offset the increased activity of S_A because normal physiological levels of neuromodulators provide only minor contributions into modulating G_{Ca}.

In this study it was only possible to provide a rough outline of both activity- and neuromodulator-dependent mechanisms controlling the process of recovery after decentralization. The choice of calcium-mediated regulation to be the core of the activity- and neuromodulator-dependent mechanism was prompted by vast number of studies placing calcium at the intersection of activity and neuromodulator-dependent regulatory mechanisms (reviewed in Adams and Dudek 2005). However, a number of alternative mechanisms, including the ones not involving calcium signaling could be responsible for the postdecentralization events. Further experiments are needed to confirm the activity- and neuromodulator-dependent hypothesis and identify the exact signaling pathways involved in the activity- and neuromodulator-dependent feedback systems. Some of the experiments directed at this goal could include experimentally determining the kinetics of the calcium conductance changes at different times during specific GABA receptor agonists pretreatments, and after decentralization. Establishing the molecular identities of activity- and neuromodulator-dependent sensors will also require further investigation. It is likely that the roles of S_A and S_{NM} are not played by single proteins but by signaling pathways including multiple proteins. Some of the potential candidates to participate in the S_A signaling pathway could be synaptotagmin I, known to participate in fast effects of the changes in conductance of the calcium channels (reviewed in Koch and Bellen 2003). Frequenin could be a possible player in the S_{NM} pathway. It is known to participate in the regulation of calcium channel activity by the GPCRs and is involved in the regulation of potassium channels (reviewed in Burgoyne et al. 2004). Lobster frequenin has been cloned, which would facilitate the initiation of the RNAi experiments. It has been shown that frequenin RNA microinjection modifies the properties of the transient A current in

lobster STG neurons (Zang et al. 2003b). Another protein family of interest is potassium channel interacting proteins (KChIPs) that are known to modulate the properties of the transient potassium current in response to calcium signaling and thus affect the stability of rhythmic neuronal output. One of these proteins, KChIP3 is known to be downregulated in epilepsy, while a KChIP2 null mouse is highly susceptible to cardiac arrythmias, both diseases involving disregulation of the rhythmic output of the neuronal networks (reviewed in Burgoyne et al. 2004).

The results described in this dissertation demonstrate that the process of recovery after decentralization is governed by a complex regulatory mechanism, integrating both activity- and neuromodulator-based inputs. Multiple and redundant regulatory mechanisms are very common in biological systems, and could be an evolutionary way to ensure the uninterrupted function of the vitally important organs in the face of the constantly changing environmental conditions.

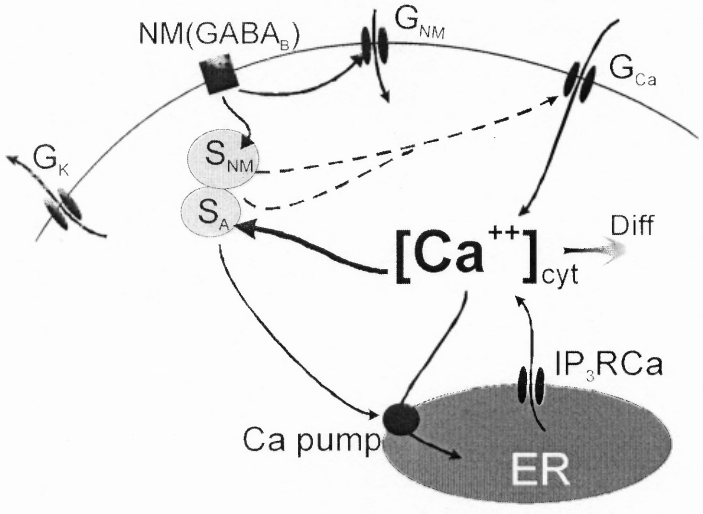

Figure 5.4 Schematic diagram of intracellular activity- and neuromodulator-dependent regulation. G_K, G_{Ca} and G_{NM} are the conductances of I_K, I_{Ca} and I_{NM}, respectively. ER here represents a generic intracellular Ca^{++} store. IP_3RCa is the activated status of IP_3 sensitive Ca^{++} receptor/channel on ER membrane, and Ca^{++} pump on ER membrane represents the intracellular Ca^{++} uptake process. The shaded arrow labeled Diff stands for the Ca^{++} diffusion.S_A is the activity-dependent Ca^{++} sensor. S_A detects changes of $[Ca]_{cyt}$, and in turn regulates G_{Ca} and Ca^{++} pump. S_{NM} is the neuromodulator sensor triggered by neuromodulators that also regulates G_{Ca}. Diagram courtesy of Y. Zhang.

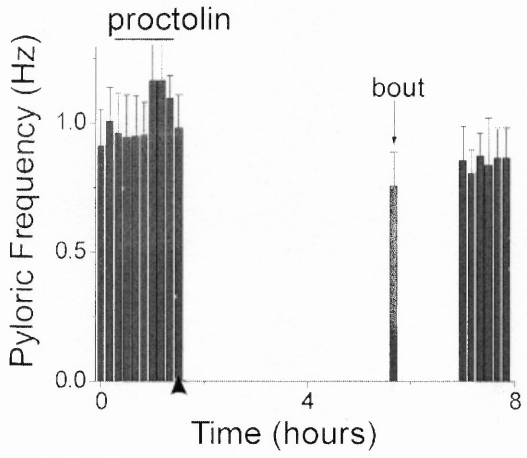

Figure 5.5 The recovery process after decentralization in the proctolin pre-treated preparation. Black triangle ▲ indicates the time of decentralization. Before decentralization, 1uM proctolin was added to the preparation for ~1 hour. After decentralization, there was no significant delay in rhythmic activity turnoff, but the first bout appeared faster than in controls (Table 5.1).

CHAPTER 6

CONCLUSION

6.1 Summary of Results

The goal of this dissertation was to investigate the mechanisms that ensure stability and adaptation of a rhythm-generating neuronal network under changing environmental conditions. Since the activity of a rhythm generating network depends on the coordinated activity of the neurons comprising this network, and neuronal activity in turn is generated by the coordinated action of ionic currents expressed by the neurons, the regulation of ionic current expression was the primary focus of this investigation.

To achieve the goal of this dissertation, changes in neuronal ionic currents were studied at the time of significant perturbations in the activity of the pyloric rhythm-generating neuronal network. In the process of this investigation, coordination in expression of currents within and between network neurons under normal physiological conditions was demonstrated. Alterations in current levels and current coordinations in the process of pyloric network recovery after decentralization and in response to treatments with neuromodulators provided insights into molecular mechanisms underlying the observed current level and coordination dynamics. Next, it was shown that synaptic communication plays an important role in maintaining ionic current levels and their coordination within the network. Finally, an experimental characterization of the dual role of activity and neuromodulators in the process of recovery was carried out. Part of this work, carried out in collaboration with Yili Zhang and Rosa Rodriguez, has been used by Y.Zhang to develop a computer model that captures this phenomenon. Y.Zhang's

computer model was based on a conceptual model incorporating the assumption of two independent mechanisms working in parallel. This dissertation presents additional experimental that support this model.

The contribution of this dissertation to the understanding of the mechanisms employed by the nervous system to ensure stability and adaptation of the rhythm-generating networks is outlined below in more detail.

6.1.1 Discovery of Ionic Current Coordination within and between Cells

In this dissertation it was shown for the first time that ionic current pairs within one neuron and same name ionic currents in different neurons are expressed in coordinated fashion in a rhythm-generating network.

In particular, HTK/I_A, HTK/I_h and I_A/I_h current pairs were coregulated in both pacemaker PD and follower LP neurons. I_{Kd} and I_{Ca} on the contrary did not correlate with any other current or to each other in either neuronal type (Chapter 3). Between the two PD neurons I_{HTK}, I_A and I_h were coordinated, while between PD and LP neurons only $logI_{HTK}$ and I_A, but not I_h were coordinated under normal physiological conditions (Chapter 4). Decentralization and treatment with glutamate and GABA signaling inhibitors caused significant alterations in the status of both intra- and intercellular ionic current coordination (Chapter 3, 4). Changes in the current coordination status in response to the modifications of neuronal environment proved that the observed current coordination is not a passive function of pre-setting of current levels in each neuronal type during development, but an actively maintained and regulated process.

6.1.2 Novel Functions of Neuromodulators in Rhythm Generating Networks

In this dissertation a novel role of central neuromodulators in a rhythm generating network was demonstrated for the first time, namely that of controlling intra- and INTER-cellular current coordinations in the network (Chapter 3, 4). Results reported in Chapter 3 demonstrate that proctolin maintains the coregulation of I_{HTK} /I_A and I_{HTK} /I_h pairs in PD cells and I_A/I_h pair in LP cells. GABA regulated the intracellular coordination of I_h between the two PD and PD and LP neurons (Chapter 4).

6.1.3 Novel Function of Glutamatergic Synaptic Communications in Rhythm Generating Networks

The results reported in this dissertation identify a new function of the glutamatergic synapses present in a rhythm generating network: they were involved in maintaining the coordination of I_{HTK} and I_A currents between the two PD neurons and PD and LP neurons (Chapter 4). The silencing of synaptic communications between AB and LP and LP and PD neurons using PTX treatment completely abolished coordination in I_{HTK} and I_A in both PD/PD and PD/LP neuronal pairs (Chapter 4).

6.1.4 Mechanisms Involved in INTRA-cellular Current Coregulation

The results reported in this dissertation show that coordinations of different current pairs within neurons of different types are controlled by independent mechanisms and that at least some of these coordinations are maintained by centrally released neuromodulators, in particular proctolin, in an activity-independent manner (Chapter 3).

When central neuromodulatory supply to the pyloric network was interrupted

after decentralization, correlation between I_{HTK} and I_h and I_{HTK} and I_A in PD cells and I_h and I_A in LP neurons was eliminated. However, correlation of I_{HTK} /I_A, I_{HTK} /I_h and I_A/I_h current pairs in either cell was not affected by decentralization if one of the neuromodulators normally released from descending axonal terminals (proctolin) was continuously bath applied (Chapter 3). Continuous bath-application of proctolin together with TTX, which completely eliminated pyloric activity, produced the same results as application of proctolin alone, indicating that the effect of proctolin was not activity-dependent. The intracellular current coordination status was not affected by treatments with the glutamate and $GABA_A$-type ionic current blocker PTX and by the GABA synthesis inhibitor 3MPA (Chapter 4). These results indicate that intracellular coordinations of I_{HTK} /I_h and I_{HTK} /I_A current pairs in PD and I_H/I_A pair in LP are maintained by neuromodulators such as proctolin, while I_A/I_h coordination in PD cells, and I_{HTK} /I_h and I_{HTK} /I_A in LP cells are regulated by different mechanisms. None of the studied intracellular coordinations depended on glutamatergic cell to cell communication or GABA signaling.

6.1.5 Mechanisms Involved in Intercellular Current Coordination

This dissertation provides evidence that coordination of currents between neurons is maintained by independent mechanisms for each current and between each pair of neurons. Some of the coordinations were determined by GABA while others were driven by glutamate-mediated mechanisms. Inter- and intracellular current coregulations were controlled by non-overlapping mechanisms.

In particular, I_{HTK} and I_A INTER-cellular coordinations depended on

glutamatergic synaptic communications, while I_h coregulation status was determined by GABA (Chapter 4). Decentralization and 3MPA treatment affected only the coordination of I_h, but not I_{HTK} and I_A between the two PD cells and PD and LP cells. Treatment with PTX abolished I_{HTK} and I_A coordinations in both neuronal pairs without affecting the I_h coordination status. Additionally while I_A, I_{HTK} and I_h showed linear correlation between the two PD neurons, the type of coordination was different for each of the three currents between LP and PD neurons (linear for I_A, log/log for I_{HTK} and absent for I_h). GABA regulated I_h coordination between both PD/PD and PD/LP neuronal pairs, establishing coordination between the two PD cells and eliminating it between PD and LP cells. Glutamatergic synaptic and possibly gap junction communication between cells was important for the maintenance on I_{HTK} and I_A coordinations in both cell pairs (Chapter 4).

6.1.6 Mechanisms Involved in Setting Ionic Current Levels

Results reported in this dissertation demonstrate that modification of the ionic current levels induced by changes in the network environment was driven primarily by altered synaptic and possibly gap junction communication between the cells in the network (Chapter 3, 4).

Decentralization, which affects both neuromodulator supply to the pyloric network and the type of synaptic communication exchanged by the cells in the network, induced significant and complementary changes in current levels and intracellular current coordinations in both LP and PD neurons (Chapter 3, 4). PTX treatment affects the activity at the glutamatergic synapses in the network, but leaves the neuromodulatory supply intact. PTX treatment did not change the intracellular current coordinations, but

led to ionic current level changes that closely resembled changes induced by decentralization (Chapter 4). Taken together, these results indicate that intracellular current coordinations were maintained by the central neuromodulatory supply, and the current levels in both the LP and PD cells were set through activity-dependent effects induced by glutamatergic synapses. In seeming contradiction, continuous application of proctolin+TTX after decentralization, which theoretically creates a situation similar to PTX treatment (silent glutamatergic synapses together with uninterrupted neuromodulator (proctolin) supply), did not induce changes in current levels or their coordinations. This could be explained by the failure to initiate post-decentralization recovery process in the presence of proctolin (Chapter 3). This possibility is supported by the fact that PTX effects on currents and their INTER-cellular coregulations were completely reversed after PTX wash off, as opposed to the effects of decentralization (Chapter 4).

6.1.7 Post-decentralization Changes Occur during a Critical Window

Results reported in this dissertation demonstrate that modification of the ionic current levels and their coregulations induced by the complete removal of neuromodulator input (decentralization) and glutamatergic and GABAergic blockade is a process that occurs within a relatively short time window (Chapter 3) that coincides with the critical window for post-decentraliztion RNA synthesis described by Thoby-Brisson and Simmers (2000a). While continuous presence of neuromodulator after decentralization protected the preparations from decentralization-induced changes, application of proctolin or restoration of the full central neuromodulator supply 24 h after decentralization, the time

past the critical window, did not restore pre-decentralization current levels or coregulation status (Chapter 3).

6.1.8 Decentralization Leads to Restructuring of Signaling Pathways

The data presented in this dissertation shows that neuromodulators, such as proctolin, produce different long term effects on current levels and their coordinations depending on the state (non-decentralized or undergoing recovery) of the preparation. Long term bath application of proctolin did not induce any changes in current levels in control preparations, but produced significant changes in current levels when applied to the recovered preparations (I_{HTK} remained at 'decentralized' level, I_A levels were significantly decreased compared to 'decentralized' and control levels, and I_h levels were reduced compared to 'decentralized' and equal to control levels, Chapter 3). This indicates that signaling pathways that link proctolin receptors to their effector ionic channels were restructured in the process of recovery after decentralization

6.1.9 Recovery after Decentralization is Controlled by Activity- and Neuromodulator-Dependent Mechanisms

Experiments described in this dissertation have shown that the process of recovery after decentralization was initiated by an activity-dependent mechanism, while activity turnoff process was neuromodulator controlled (Chapter 5). When activity of the pyloric network was interrupted for several hours prior to decentralization by hyperpolarizing the pacemaker kernel neurons or by incubating the preparations in low sodium saline or in GABA or $GABA_A$ agonist solutions, the recovery of the preparations was advanced. GABA or $GABA_B$ receptor agonist preincubation did not affect the onset of recovery

process but delayed the activity turnoff after decentralization (Chapter 5). Thus, it appears that the rather drastic perturbations used reveal two processes, that regulate the pyloric network activity on two different time scales (one slow and neuromodulator-dependent mechanism, and one relatively fast and activity-dependent). Previous work shows that in fact activity dependent changes occur in a relatively fast time scale of several hours (Golowasch et al. 1999, Haedo and Golowasch 2006, Turrigiano et al. 1994, 1995). As for effects of neuromodulators, only their acute effects have been previously studied (Golowasch et al. 1992b, Swensen and Marder 2000). Here we show a heretofore unknown mechanism of action of neuromodulators that operates on a much slower scale (up to 18 h) than previously known.

6.1.10 Current Coregulations Contribute to both Stability and Plasticity of the Network

Results reported in this dissertation indicate that both gain and loss of current coordinations may be associated with stabilization of network output (Chapter 3, 4). For example, after decentralization, some of the intracellular current correlations were lost at the time of the maximal pyloric rhythm disturbance (about 24 h after decentralization, Chapter 3). However, intracellular ionic current correlations were not regained at the time of stable activity recovery after decentralization (approximately 100 h after decentralization, Chapter 3). Coordination of I_h current between LP and PD cells was absent under normal physiological conditions. However, during 3MPA treatment that did not significantly affect the pyloric activity (except for reduction of its frequency), coordination of I_h current between LP and PD cells was established. Additionally, perturbations in pyloric activity after decentralization or PTX treatment corresponded to

disturbances in only some of the inter- and intra-cellular current coordinations (Chapter 3, 4).

These results indicate that while maintenance of strict ionic current correlations could play a role in restricting the range of current fluctuations both within and between the cells in the network and thus stabilize the patterned activity (see Bucher and Marder 2006), the relaxation of such correlation could facilitate the process of finding a new current equilibrium after a significant perturbation, that will re-enable the network to produce the lost patterned activity with a different set of ionic currents, and different ionic current levels (Chapter 3, 4).

6.2 Implications of the Results in the Context of Rhythm Generating Network Biology

In the history of neuroscience many of the insights gained from studying simple model systems were invaluable in understanding more complex organisms. For over 35 years the pyloric network of crustaceans was one of such model systems (Marder and Calabrese 1996, Selverston 2005).

One of the mammalian systems closely resembling the pyloric network is respiratory system, especially in such aspects as the presence of pacemaker neurons, modification of intrinsic neuronal properties by neuromodulators and reconfiguration of network architecture in response to changes in environment (Marder 2000, Ramirez et al. 2004).

In this dissertation novel aspects of network architecture, namely coordination of current expression within and between cells, have been described. The phenomenon of current coordination would have been extremely difficult to observe in a more complex

mammalian system due to significantly larger numbers of participating neurons and difficulties in their identification. This dissertation also elucidated the complexity of molecular processes that govern intra- and inter-cellular current coordination, identifying two types of mechanisms: one involving neuromodulators such as proctolin and GABA, and the other involving activity-dependent mechanisms and glutamatergic cell to cell communications. Even such initial survey of current coregulation mechanisms would have been extremely difficult in a more complex system.

Important features of the process of recovery after decentralization, relevant to many pathological events involving trauma or neurodegeneration in mammals, were established in this dissertation. These features included decentralization-induced changes in the levels and coordination of ionic currents, critical time window of recovery initiation, restructuring of the neuromodulator-activated signaling pathways during the recovery process, control of recovery by both activity- and neuromodulator-dependent mechanisms, etc. These results have expanded and deepened the existing knowledge of the recovery process (Rezer and Moulins 1993, Thoby-Brisson and Simmers 1998, 2000, 2001, Mizrahi et al. 2001, Luther et al. 2003).

One of the long term goals in biology is the construction of the exact computer model of the living organism that would allow predicting the effect a given event or treatment would have without actually administering them to a living organism. The significance of simple model systems like the pyloric rhythm generating network of the crustaceans, in the process of developing the whole organism model cannot be overestimated. Many computer models of this system capable of reproducing different aspects of experimentally observed behaviors have been built (Abbott and LeMasson

1993, LeMasson et al. 1993, Siegel et al. 1994, Liu et al. 1998, Soto-Trevino et al. 2006, Zhang and Golowasch 2007). Besides serving as building blocks in the whole organism computer model, these 'local' models provide deeper understanding of the biological mechanisms involved in experimentally observed behaviors and provide a blueprint for the new directions in experimental work. The results obtained in this dissertation will potentially assist in building a model neuronal network that will be used to further understand the mechanism of activity recovery. The results described in this dissertation will also be used to plan further biological experiments aimed at uncovering the details of molecular mechanisms involved in the process of recovery after decentralization and identifying the biological molecules involved in this process.

REFERENCES

Abbott LF and Marder E (1998) Model small networks. Chap.10 in: *Methods in neuronal modeling: from ions to networks*. Koch C & Segev (eds). 2nd ed. MIT Press, Cambridge.

Adams JP and Dudek SM (2005) Late-phase long-term potentiation: getting to the nucleus. Nat Rev Neurosci. 6:737-43.

Baines RA, Walther C, Hinton JM, Osborne RH, Konopinska D (1996) Selective activity of a proctolin analogue reveals the existence of two receptor subtypes. J Neurophysiol 75:2647-50.

Baro DJ, Cole CL, Harris-Warrick RM (1996) The lobster shaw gene: cloning, sequence analysis and comparison to fly shaw. Gene 170:267-70.

Baro DJ, Levini RM, Kim MT, Willms AR, Lanning CC et al. (1997) Quantitative single cell reverse transcription PCR demonstrates that A-current magnitude varies as a linear function of shal gene expression in identified stomatogastric neurons. J Neurosci 17: 6597-10.

Beblo DA and Veenstra RD (1997) Monovalent cation permeation through the connexin40 gap junction channel. J Gen Physiol 109(4):509-22.

Belz B, Eisen JS, Flamm R, Harris-Warrick RM, Hooper S, Marder E (1984) Serotonergic innervation and modulation of the stomatogastric ganglion of three decapod crustaceans. J Exp Biol 109:35-54.

Blitz DM and Nusbaum MP (1999). Distinct functions for cotransmitters mediating motor pattern selection. J Neurosci. 19:6774-6783.

Blitz DM, Christie AE, Coleman MJ, Norris BJ, Marder E, Nusbaum MP (1999) Different proctolin neurons elicit distinct motor patterns from a multifunctional neuronal network. J Neurosci 19:5449-5463.

Bucher D, Prinz AA, Marder E (2005) Animal-to-animal variability in motor pattern production in adults and during growth. J Neurosci 25:1611-1619.

Burdakov D (2005) Gain control by concerted changes in IA and Ih conductances. Neural Computation 17:991-995.

Burgoyne R, O'Callaghan DW, Hasdemir B, Haynes LP, Tepikin A (2004) Neuronal Ca2+-sensor proteins: multitalented regulators of neuronal function. Trends Neurosci 27:203-209.

Cai SQ, Hernandez L, Wang Y, Park KH, Sesti F (2005) MPS-1 is a K+ channel beta-subunit and a serine/threonine kinase. Nat Neurosci 8:1503-1509.

Catterall WA, Hulme JT, Jiang X, Few WP (2006) Regulation of sodium and calcium channels by signaling complexes. J Recept Signal Transduct Res 26:577-598.

Calabrese RL (1998) Cellular, synaptic, network, and modulatory mechanisms involved in rhythm generation. Curr Opin Neurobiol 1998 8:710-7.

Cleland TA and Selverston AI (1995) Glutamate-gated inhibitory currents of central pattern generator neurons in the lobster stomatogastric ganglion. J Neurosci 15:6631-6639.

Cleland TA and Selverston AI (1998) Inhibitory glutamate receptor channels in cultured lobster stomatogastric neurons. J Neurophys 77:3189-3196.

Clemens S, Combes D, Meyrand P, Simmers J (1998) Long-term expression of two interacting motor pattern-generating networks in the stomatogastric system of freely behaving lobster. J Neurophysiol 79:1396-1408.

Coleman MJ, Nusbaum MP, Cournil I, Claiborne BJ (1992) Distribution of modulatory inputs to the stomatogastric ganglion of the crab, *Cancer borealis*. J Comp Neurol 325:581-594.

Coleman MJ, Meyrand P, Nusbaum MP (1995) A switch between two modes of synaptic transmission mediated by presynaptic inhibition. Nature 378:502-505.

Cournil I, Meyrand P, Moulins M (1990) Identification of all GABA-immunoreactive neurons projecting to the lobster stomatogastric ganglion. J Neurocytol 19(4):478-93

Darlington CL, Dutia MB, Smith PF (2002) The contribution of the intrinsic excitability of vestibular nucleus neurons to recovery from vestibular damage. Eur J Neurosci 15:1719-27.

Davis GW (2006) Homeostatic control of neural activity: from phenomenology to molecular design. Annu Rev Neurosci 29:307-323.

Desai NS, Rutherford LC, Turrigiano GG (1999) Plasticity in the intrinsic excitability of cortical pyramidal neurons. Nat Neurosci 2:515-520.

DiCaprio RA and Fourtner CR (1988) Neural control of ventilation in the shore crab, *Carcinus maenas*. II. Frequency-modulating interneurons. J Comp Physiol [A] 162(3):375-88.

Duan S and Cooke IM (2000) Glutamate and GABA activate different receptors and Cl^- conductances in crab peptide-secretory neurons. J Neurophys 81:31-37.

Dolmetsch RE, Xu K, Lewis RS (1998) Calcium oscillations increase the efficiency and specificity of gene expression. Nature 392:933-936.

Ducret E, Le Feuvre Y, Meyrand P, Fenelon V (2007) Removal of GABA within adult modulatory systems alters electrical coupling and allows expression of an embryonic-like network. J Neurosci 27:3626-3638.

Egerod K, Reynisson E, Hauser F, Cazzamali G, Grimmelikhuijzen CJ (2003) Molecular identification of the first insect proctolin receptor. Biochem Biophys Res Commun 306:437-42.

Eisen JS, Marder E (1982) Mechanisms underlying pattern generation in lobster stomatogastric ganglion as determined by selective inactivation of identified neurons. J Neurophysiol 48: 1392-415.

Engelman HS and MacDermott A (2004) Presynaptic ionotropic receptors and control of transmitter release. Nature Neurosci 5:135-145.

Fengler BT and Lnenicka GA (2001) Activity-dependent plasticity of calcium clearance from crayfish motor axons. J Neurophysiol 87:1625-1628.

Franklin JL, Fickbohm DJ, Willard AL (1992) Long-term regulation of neuronal calcium currents by prolonged changes of membrane potential. J Neurosci 12:1726-1735.

Galante M, Avossa D, Rosato-Siri M, Ballerini L (2001) Homeostatic plasticity induced by chronic block of AMPA/kainite receptors modulates the generation of rhythmic bursting in rat spinal cord organotypic cultures. Eur J Neurosci 14:903-917.

Gibson JR, Bartley AF, Huber KM (2006) Role for the subthreshold currents ILeak and IH in the homeostatic control of excitability in neocortical somatostatin-positive inhibitory neurons. J Neurophysiol 96:420-432.

Gisselmann G, Marx T, Bobkov Y, Wetzel CH, Neuhaus EM, Ache BW, Hatt H (2003) Molecular and functional characterization of an I(h)-channel from lobster olfactory receptor neurons. Eur J Neurosci 21:1635-47.

Goldman MS, Golowasch J, Marder E, Abbott LF (2001) Global structure, robustness, and modulation of neuronal models. J Neurosci 21:5229-5238.

Golowasch J and Marder E (1992a) Ionic currents of the lateral pyloric neuron of the stomatogastric ganglion of the crab. J Neurophysiol 67:318-331.

Golowasch J and Marder E (1992b) Proctolin activates an inward current whose voltage dependence is modified by extracellular Ca++. J Neurosci 12:810-817.

Golowasch J, Buchholtz F, et al. (1992) Contribution of individual ionic currents to activity of a model stomatogastric ganglion neuron. J Neurophysiol 67(2):341-9.

Golowasch J, Abbott LF, Marder E (1999a) Activity-dependent regulation of potassium currents in an identified neuron of the stomatogastric ganglion of the crab *Cancer borealis*. J Neurosci 19:RC33(1-5).

Golowasch J, Casey M, Abbott LF, Marder E (1999b) Network stability from activity-dependent regulation of neuronal conductances. Neural Comput 11:1079-1096.

Golowasch J, Goldman MS, Abbott LF, Marder E (2002) Failure of averaging in the construction of a conductance-based neuron model. J Neurophysiol 87:1129-1131.

Gonzalez-Islas C and Wenner P (2006) Spontaneous network activity in the embryonic spinal cord regulates AMPAergic and GABAergic synaptic strength. Neuron 49:563-575.

Graubard K and Hartline DK (1991) Voltage clamp analysis of intact stomatogastric neurons. Brain Res 557:241-254.

Gutovitz S, Birmingham JT, Luther J, Simon D, Marder E (2001) GABA enhances transmission at an excitatory glutamatergic synapse. J Neurosci 21:5935-5943.

Haedo RJ and Golowasch J (2006) Ionic mechanism underlying recovery of rhythmic activity in adult isolated neurons. J Neurophysiol 96:1860-1876.

Harris-Warrick RM (1992) *Dynamic biological networks: the stomatogastric nervous system*. Cambridge, Mass., MIT Press.

Harris-Warrick RM and Marder E (1991) Modulation of neural networs for behavior. Annu Rev Neurosci 14:39-57.

Harris-Warrick R, Marder E, Selverston A, Moulins M (1992) *Dynamic biological networks: the stomatogastric nervous system. Cambridge*, MA: MIT.

Harris-Warrick RM, Coniglio LM, Barazangi N, Guckenheimer J, Gueron S. (1995) Dopamine modulation of transient potassium current evokes phase shifts in a central pattern generator network. J Neurosci 15:342-358.

Heinzel HG, Weimann JM, Marder E (1993) The behavioral repertoire of the gastric mill in the crab, *Cancer pagurus*: an in situ endoscopic and electrophysiological

examination. J Neurosci 13(4):1793-803.

Hodgkin AL and Huxley AF (1952) A quantitative description of membrane current and its application to conduction and excitation in nerve. J Physiol 117:500-544.

Hollins B and McClintock T (2000) Lobster GABA receptor subunit expressed inneural tissues. J Neurosci Res 59:534-541.

Hong SJ and Lnenicka GA (1997) Characterization of a P-type calcium current in a crayfish motoneuron and its selective modulation by impulse activity. J Neurophysiol 77(1): 76-85.

Hooper SL (1997) Phase maintenance in the pyloric pattern of the lobster (Panulirus interruptus) stomatogastric ganglion. J Comput Neurosci 4:191-205.

Hooper SL and Marder E (1987) Modulation of the lobster pyloric rhythm by the peptide proctolin. J Neurosci 7, 2097-2112.

Hooper SL, O'Neil MB, Wagner R, Ewer J, Golowasch J, Marder E (1986) The innervation of the pyloric region of the crab *Cancer borealis*: homologous muscles in decapod species are differently innervated. J Comp Physiol A Sens Neural Behav Physiol 159:227-240.

Johnson BR and Harris-Warrick RM (1990) Aminergic modulation of graded synaptic transmission in the lobster stomatogastric ganglion. J Neurosci 10:2066-2076.

Johnson AE, Liminga U, Liden A, Lindefors N, Gunne LM, Wiesel FA (1994) Chronic treatment with a classical neuroleptic alters excitatory amino acid and GABAergic neurotransmission in specific regions of the rat brain. Neuroscience 63(4):1003-20.

Johnson EC, Garczynski SF, Park D, Crim JW, Nassel DR, Taghert PH (2003) Identification and characterization of a G protein-coupled receptor for the neuropeptide proctolin in Drosophila melanogaster. Proc Natl Acad Sci U SA, 100(10):6198-203.

Kaila K and Voipio J (1987) Postsynaptic fall in intracellular pH induced by GABA-activated bicarbonate conductance. Nature 330:163-165.

Katz PS (1995) Intrinsic and extrinsic neuromodulation of motor circuits. Curr Opin Neurobiol 5:799-808.

Khorkova OE and Golowasch J (2007) Neuromodulators, not activity, control coordinated expression of ionic currents. J Neurosci 27(32):8709-18.

Kiehn O and Harris-Warrick RM (1992) 5-HT modulation of hyperpolarization-activated inward current and calcium-dependent outward current in a crustacean motor neuron. J Neurophysiol 68(2):496-508.

Klimesch W (1999) EEG alpha and theta oscillations reflect cognitive and memory performance: a review and analysis. Brain Res Brain Res Rev 29:169-195.

Knapp AG and Dowling JE (1987) Dopamine enhances excitatory amino acid-gated conductances in cultured retinal horizontal cells. Nature 325(6103):437-9.

Koh TW and Bellen HJ (2003) Synaptotagmin I, a Ca^{2+} sensor for neurotransmitter release. Trends Neurosci 26:413-422.

Krenz W, Nguyen D, Perez-Acevedo NL, Selverston AI (2000) Group I, II and III mGluR compounds affect rhythm generation in the gastric circuit of the crustacean stomatogastric ganglion. J Neurophys 86:1188-1201.

Kushner PD and Maynard EA (1977) Localization of monoamine fluorescence in the stomatogastric nervous system of lobsters. Brain Res 129:13-28.

LeMasson G, Marder E, Abbott LF (1993) Activity-dependent regulation of conductances in model neurons. Science 259:1915-1917.

Levi R and Selverston A (2006) Mechanisms underlying type I mGlur-induced activation of lobster gastric mill neurons. J Neurophysiol 96:3378-3388.

Levitan IB (2006) Signaling protein complexes associated with neuronal ion channels. Nature Neurosci 9:305-310.

Linsdell P and Moody WJ (1994) Na^+ channel mis-expression accelerates K^+ channel development in embryonic Xenopus laevis skeletal muscle. J Physiol 480:405-410.

Lisman JE (1997) Bursts as a unit of neural information: making unreliable synapses reliable. Trends Neurosci 20:38-43.

Li L, Kelley WP, Billimoria CP, Christie AE, Pulver SR, Sweedler JV, Marder E (2003) Mass spectrometric investigation of the neuropeptide complement and release in the pericardial organs of the crab, *Cancer borealis*. J Neurochem 87:642-656.

Liu Z, Golowasch J, Marder E, Abbott LF (1998) A model neuron with activity-dependent conductances regulated by multiple calcium sensors. J Neurosci 18:2309-2320.

Luther JA, Robie AA, Yarotsky J, Reina C, Marder E, Golowasch J (2003) Episodic bouts of activity accompany recovery of rhythmic output by a neuromodulator- and activity-deprived adult neural network. J Neurophysiol 90:2720-2730.

MacLean JN, Zhang Y, Johnson BR, Harris-Warrick RM (2003) Activity-independent homeostasis in rhythmically active neurons. Neuron 37:109-120.

MacLean JN, Zhang Y, Goeritz ML, Casey R, Oliva R, et al. (2005) Activity-independent coregulation of IA and Ih in rhythmically active neurons. J Neurophysiol 94:3601-17.

Marder E (1985) Neurotransmitters and neuromodulators. In: *The Crustacean Stomatogastric System* (Selverston AI, Moulins M, eds) Berlin: Springer Verlag, 263-300.

Marder E (2000) Motor pattern generation. Curr Opin Neurobiol 10:691-698.

Marder E and Bucher D (2001) Central pattern generators and the control of rhythmic movements. Curr Biol 11:986-96.

Marder E and Bucher D (2007) Understanding circuit dynamics using the stomatogastric nervous system of lobsters and crabs. Annu Rev Physiol 69:13.1-13.26.

Marder E and Eisen JS (1984) Electrically coupled pacemaker neurons respond differently to same physiological inputs and neurotransmitters. J Neurophysiol 51:1345-1361.

Marder E and Paupardin-Tritsch D (1978) The pharmacological properties of some crustacean neuronal acetylcholine, gamma-aminobutyric acid and L-glutamate responses. J Physiol Lond. 280, 213-236.

Marder E, Hooper S, Siwicki K (1986) Modulatory action and distribution of the neuropeptide proctolin in the crustacean stomatogastric nervous system. J Comparative Neurobiol 243:454-467.

Marder E, Bucher D, Schulz DJ, Taylor AL (2005a) Invertebrate central pattern generation moves along. Curr Biol 15: R685-699.

Marder E, Goaillard J, Schulz DJ (2005b) Co-regulation of ion channel expression in identified electrically coupled neurons. Program No. 54.6. 2005 Abstract Viewer/Itinerary Planner. Washington, DC: Society for Neuroscience, online.

Maynard DM (1972) Simpler networks. Ann NY Acad Sci 193:59-72.

Maynard DM and Dando MR (1974) The structure of the stomatogastric neuromuscular system in *Callinectes sapidus, Homarus americanus* and *Panulirus argus* (*Decapoda Crustacea*). Philos Trans R Soc Lond B Biol Sci 268:161-220.

McAnelly ML and Zakon HH (2000) Coregulation of voltage-dependent kinetics of Na+ and K+ currents in electric organ. J Neurosci 20:3408-3414.

Miller JP and Selverston AI (1982) Mechanisms underlying pattern generation in lobster stomatogastric ganglion as determined by selective inactivation of identified neurons. II. Oscillatory properties of pyloric neurons. J Neurophysiol 48:1378-1391.

Miwa A, Ui M, Kawai N (1990) G protein is coupled to presynaptic glutamate and GABA receptors in lobster neuromuscular synapse. J Neurophysiol 63(1):173-80.

Mizrahi A, Dickinson PS, Kloppenburg P, Fenelon V, Baro DJ, Harris-Warrick RM, Meyrand P, Simmers J (2001) Long-term maintenance of channel distribution in a central pattern generator neuron by neuromodulatory inputs revealed by decentralization in organ culture. J Neurosci 21(18): 7331-9.

Nusbaum MP and Beenhakker MP (2002) A small-systems approach to motor pattern generation. Nature 417:343-350.

Nusbaum MP and Marder E (1989a) A modulatory proctolincontaining neuron (MPN). I. Identification and characterization. J Neurosci 9:1591-1599.

Nusbaum MP and Marder E (1989b) A modulatory proctolincontaining neuron (MPN). II. State-dependent modulation of rhythmic motor activity. J Neurosci 9:1600-1607.

Nusbaum MP, Cournil I, Golowasch J, Marder E (1989) Modulating rhythmic motor activity with a dual-transmitter neuron. In: *Neural Mechanisms of Behavior* (Erber J, Menzel R, Pfluger H-J, Todt D, eds), p 228. Stuttgart: Georg Thieme Verlag.

Nusbaum MP, Blitz DM, Swensen AM, Wood D, Marder E (2001) The roles of cotransmission in neural network modulation. Trends Neurosci 24:146-154.

Philipp B, Rogalla N, Kreissl S (2006) The neuropeptide proctolin potentiates contractions and reduces cGMP concentration via a PKC-dependent pathway. J Exp Biol 209:531-540.

Prinz AA, Bucher D, Marder E (2004) Similar network activity from disparate circuit parameters. Nat Neurosci 7:1345-1352.

Qu Y and Dahl G (2002) Function of the voltage gate of gap junction channels: selective exclusion of molecules. Proc Natl Acad Sci U S A 99(2):697-702.

Rabbah P, Golowasch J, Nadim F (2005) Effect of electrical coupling on ionic current and synaptic potential measurements. J Neurophysiol 94:519-30.

Ramirez JM and Pearson KG (1990) Chemical deafferentation of the locust flight system by phentolamine. J Comp Physiol [A] 167(4):485-94.

Ramirez JM, Tryba AK, Pena F (2004) Pacemaker neurons and neuronal networks: an integrative view. Curr Opin Neurobiol 14:665-74.

Raper JA (1979) Nonimpulse-mediated synaptic transmission during the generation of a cyclic motor program. Science 205:304-306.

Rathmayer W and Djokaj S (2000) Presynaptic inhibition and the participation of GABA(B) receptors at neuromuscular junctions of the crab *Eriphia spinifrons*. J Comp Physiol [A] 186(3):287-98.

Rezer E and Moulins M (1983) Expression of the crustacean pyloric pattern generator in the intact animal. J Comp Physiol [A] 153:17-28.

Rezer E and Moulins M (1992) Humoral induction of pyloric rhythmic output in lobster stomatogastric ganglion: in vivo and in vitro studies. J Exp Biol 163:209-230.

Runnels LW, Yue L, Clapham DE (2001) TRP-PLIK, a bifunctional protein with kinase and ion channel activities. Science 291:1043-1047.

Saez JC, Connor JA, Spray DC, Bennett MV (1989) Hepatocyte gap junctions are permeable to the second messenger, inositol 1,4,5-trisphosphate, and to calcium ions. Proc Natl Acad Sci U S A 86(8):2708-12.

Saghatelyan A, Roux P, Migliore M, Rochefort C, Desmaisons D, Charneau P, Shepherd GM, Lledo PM (2005) Activity-dependent adjustments of the inhibitory network in the olfactory bulb following early postnatal deprivation. Neuron 46:103-116.

Selverston AI and Moulins M, eds. (1987) The crustacean stomatogastric system. Springer-Verlag, Berlin.

Selverston AI, Russell DF, Miller JP, King DG (1976) The stomatogastric nervous system: structure and function of a small neural network. Prog Neurobiol 7:215-290.

Schulz DJ, Goaillard JM, Marder E (2006) Variable channel expression in identified single and electrically coupled neurons in different animals. Nat Neurosci 9:356-62.

Siegel M, Marder E, Abbott LF (1994) Activity-dependent current distributions in model neurons. Proc Natl Acad Sci USA 91:11308-11312.

Singer W (1993) Synchronization of cortical activity and its putative role in information processing and learning. Annu Rev Physiol 55:349-374.

Soto-Trevino C, Thoroughman KA, Marder E, Abbott LF (2001) Activity-dependent modification of inhibitory synapses in models of rhythmic neural networks. Nat Neurosci 4:297-303.

Soto-Trevino C, Rabbah P, Marder E, Nadim F (2005) Computational model of electrically coupled, intrinsically distinct pacemaker neurons. J Neurophysiol 67:599-609.

Spitzer NC (2006) Electrical activity in early neuronal development. Nature 444:707-712.

Starratt AN and Brown BE (1975) Structure of the pentapeptide proctolin, a proposed neurotransmitter in insects. Life Sci 17(8):1253-6

Stein P (1997) *Neurons, neworks and motor behavior*. Cambridge, MA: MIT press.

Surmeier DJ and Foehring R (2004) A mechanism for homeostatic plasticity. Nature Neurosci 7:691-692.

Swensen AM and Marder E (2000) Multiple peptides converge to activate the same voltage-dependent current in a central pattern-generating circuit. J Neurosci 20(18):6752-9.

Swensen AM and Marder E (2001) Modulators with distinct cellular actions elicit distinct circuit output. J Neurosci 21:4050-4058.

Swensen AM, Golowasch J, Christie A, Coleman M, Nusbaum M, Marder E (2000) GABA and responses to GABA in the stomatogastric ganglion of the crab *Cancer borealis*. J Exp Biol 203:2075-2092.

Szucs A, Pinto RD, Rabinovich MI, Abarbanel HD, Selverston AI (2003) Synaptic modulation of the interspike interval signatures of bursting pyloric neurons. J Neurophysiol 89:1363-77.

Szucs A, Vehovszky A, Molnar G, Pinto RD, Abarbanel HD (2004) Reliability and precision of neural spike timing: simulation of spectrally broadband synaptic inputs. Neuroscience 126:1063-1073.

Taylor A, Durbaba R, Ellaway PH (2004) Direct and indirect assessment of gamma-motor firing patterns.Can J Physiol Pharmacol 82(8-9):793-802.

Thoby-Brisson M and Simmers J (1998) Neuromodulatory inputs maintain expression of a lobster motor pattern-generating network in a modulationdependent state: evidence from long-term decentralization in vitro. J Neurosci 18:2212-2225.

Thoby-Brisson M and Simmers J (2000a) Transition to endogenous bursting after long-term decentralization requires de novo transcription in a critical time window. J Neurophysiol 84:596-599.

Thoby-Brisson M, Telgkamp P, Ramirez JM (2000b) The role of the hyperpolarization-activated current in modulating rhythmic activity in the isolated respiratory network of mice. J Neurosci 20:2994-3005.

Thoby-Brisson M and Simmers J (2002). Long-term neuromodulatory regulation of a motor pattern-generating network: maintenance of synaptic efficacy and oscillatory properties. J Neurophysiol 88(6):2942-53.

Tierney AJ and Harris-Warrick RM (1992) Physiological role of the transient potassium current in the pyloric circuit of the lobster stomatogastric ganglion. J Neurophysiol 67(3):599-609.

Turrigiano GG (1999) Homeostatic plasticity in neuronal networks: the more things change, the more they stay the same. Trends Neurosci 22:221-227.

Turrigiano GG and Nelson SB (2004) Homeostatic plasticity in the developing nervous system. Nat Rev Neurosci 5:97-107.

Turrigiano G, Abbott LF, Marder E (1994) Activity-dependent changes in the intrinsic properties of cultured neurons. Science 264:974-977.

Turrigiano G, LeMasson G, Marder E (1995) Selective regulation of current densities underlies spontaneous changes in the activity of cultured neurons. J Neurosci 15:3640-3652.

Ueda A and Wu CF (2006) Distinct frequency-dependent regulationof nerve terminal excitability and synaptic transmission by IA and IK potassium channels revealed by *Drosophila* shaker and shab mutations. J Neurosci 26:6238-6248.

Von Euler C (1983) On the origin and pattern control of breathing rhythmicity in mammals. Symp Soc Exp Biol 37:469-485

Weaver AL and Hooper S (2002) Follower neurons in lobster (*Panulirus interruptus*) pyloric network regulate pacemaker period in complementary ways. J Neurophysiol 89:1327-1338.

Wierenga CJ, Ibata K, Turrigiano G (2005) Postsynaptic expression of homeostatic plasticity at neocortical synapses. J Neurosci 25:2895-2905.

Wong RK, Traub RD, Miles R (1986) Cellular basis of neuronal synchrony in epilepsy. Adv Neurol 44:583-592.

Xu J, Kang N, Jiang L, Nedergaard M, Kang J (2005) Activity-dependent long term potentiation of intrinsic excitability in hippocampal CA1 pyramidal neurons. J Nerosci 25:1750-1760.

Zhainazarov AB, Wachowiak M, Boettcher A, Elenes S, Ache BW (1997) Ionotropic GABA receptor from lobster olfactory projection neurons. J. Neurophysiol. 77:2235-2251.

Zhang Y, Oliva R, Gisselmann G, Hatt H, Guckenheimer J, Harris-Warrick RM (2003a) Overexpression of hyperpolarization-activated cation current (Ih) channel gene modifies the firing activity of identified motor neurons in a small neural network. J Neurosci., 23(27):9059-9067.

Zhang Y, MacLean JN, An WF, Lanning CC, Harris-Warrick RM (2003b) KChIP1 and frequenin modify shal-evoked potassium currents in pyloric neurons in the lobster stomatogastric ganglion. J Neurophysiol 89:1902-1909.

Zhang Y and Golowasch J (2007) Modeling Recovery of Rhythmic Activity: Hypothesis for the role of a calcium pump. Neurocomputing 70:1657-1662